Copyright Statement

HOPF BIFURCATION AND CENTRE BIFURCATION IN THREE DIMENSIONAL LOTKA-VOLTERRA SYSTEMS

by

RIZGAR HAJI SALIH

A thesis submitted to Plymouth University in partial fulfilment for the degree of

DOCTOR OF PHILOSOPHY

School of Computing, Electronics and Mathematics

Faculty of Science and Environment

Plymouth University

May 2015

Abstract

This thesis presents a study of the centre bifurcation and chaotic behaviour of three dimensional Lotka-Volterra systems. In two dimensional systems, Christopher (2005) considered a simple computational approach to estimate the cyclicity bifurcating from the centre. We generalized the technique to estimate the cyclicity of the centre in three dimensional systems. A lower bounds is given for the cyclicity of a hopf point in the three dimensional Lotka-Volterra systems via centre bifurcations. Sufficient conditions for the existence of a centre are obtained via the Darboux method using inverse Jacobi multiplier functions. For a given centre, the cyclicity is bounded from below by considering the linear parts of the corresponding Liapunov quantities of the perturbed system. Although the number obtained is not new, the technique is fast and can easily be adapted to other systems. The same technique is applied to estimate the cyclicity of a three dimensional system with a plane of singularities. As a result, eight limit cycles are shown to bifurcate from the centre by considering the quadratic parts of the corresponding Liapunov quantities of the perturbed system.

This thesis also examines the chaotic behaviour of three dimensional Lotka-Volterra systems. For studying the chaotic behaviour, a geometric method is used. We construct an example of a three dimensional Lotka-Volterra system with a saddle-focus critical point of Shilnikov type as well as a loop. A construction of the heteroclinic cycle that joins the critical point with two other critical points of type

planar saddle and axial saddle is undertaken. Furthermore, the local behaviour of trajectories in a small neighbourhood of the critical points is investigated. The dynamics of the Poincare map around the heteroclinic cycle can exhibit chaos by demonstrating the existence of a horseshoe map. The proof uses a Shilnikov-type structure adapted to the geometry of these systems. For a good understanding of the global dynamics of the system, the behaviour at infinity is also examined. This helps us to draw the global phase portrait of the system.

The last part of this thesis is devoted to a study of the zero-Hopf bifurcation of the three dimensional Lotka-Volterra systems. Explicit conditions for the existence of two first integrals for the system and a line of singularity with zero eigenvalue are given. We characteristic the parameters for which a zero-Hopf equilibrium point takes place at any points on the line. We prove that there are three 3-parameter families exhibiting such equilibria. First order of averaging theory is also applied but we show that it gives no information about the possible periodic orbits bifurcating from the zero-Hopf equilibria.

Contents

Abstract **iii**

Acknowledgements **xiii**

Dedication **xv**

Author's Declaration **xvii**

List of Abbreviations **xxi**

1 Introduction **1**

2 Background **9**

2.1 Hopf Points in Three Dimensional Systems 9

2.2 The Centre-Focus Problem and Inverse Jacobi Multiplier 13

2.3 The Poincaré Return Map and the Liapunov Quantities 15

2.4 The Darboux Theory of Integrability in 3DS 21

3 The Existence of Centre in 3DLVS Via the Darboux Method Using Inverse Jacobi Multipliers **25**

3.1 The Inverse Jacobi Multiplier Function of Darboux Type 26

3.2 Centre Conditions of 3DLVS 28

4 Centre Bifurcations **35**

4.1 The Basic Technique for Estimating Cyclicity from Centre 35

4.2 Centre Bifurcation for the 3DLVS 37

4.3 Perturbing the 3DS Having a Plane of Singularities 44

5 Some Chaotic Behaviour in Three Dimensional Systems **55**

5.1 The Horseshoe Map 55

5.2 Symbolic Dynamics 60

5.3 The Shilnikov Phenomena 68

5.3.1 Saddle-Focus and Saddle Index 68

5.3.2 Poincaré Map 69

6 The Existence of Horseshoe Dynamics in 3DLVS **75**

6.1 A Heteroclinic Cycle 75

6.1.1 A Heteroclinic Orbit Between Two Different Planar Critical Points 76

6.1.2 A Planar Heteroclinic Orbit on the x_1x_2-plane 77

6.1.3 A Planar Heteroclinic Orbit on the x_1x_3-plane 79

6.2 The Local Study of Trajectories 80

6.2.1 Planar Saddle-Focus Critical Point 81

6.2.2 Planar Saddle Critical Point 87

6.2.3 Axial Saddle Critical Point 91

6.3 The Behaviour at Infinity 97

6.4 The Horseshoe Map of the 3D Lotka-Volterra System 102

7 The Integrability and the Zero-Hopf Bifurcation of the 3DLVS **109**

7.1 The Darboux Integrability of the 3DLVS 109

7.2 Zero-Hopf Bifurcation 112

7.2.1 The First Order Averaging Method for Periodic Orbits . . 113
7.2.2 Periodic Orbits in the Zero-Hopf Bifurcation of the 3DLVS 114

List of Figures

3.1 The zero set of the inverse Jacobi multiplier (3.3) where L is an invariant algebraic surface of conic type. The parameters satisfy the conditions of Proposition 3 and $a_{2,3} = 1$. 32

3.2 The zero set of the inverse Jacobi multiplier (3.3) where L is of type plane, the parameters satisfy the conditions of Proposition 4 with $a_{1,2} = 1,\ a_{2,2} = 1,\ a_{3,1} = -\dfrac{2}{\sqrt{3}},\ a_{3,3} = \sqrt{3},\ a_2 = 1$ and $k = 0$. 33

4.1 (a) The graph of function $h(x)$ in (4.9) has exactly two real roots. (b) The Jabian determinant function J(x) in (4.10) at these two real roots of function $h(x)$ is not equal zero. 53

5.1 The geometrical Horseshoe map. The solid curves depict the Horseshoe map $\mathbf{F}$ and the dotted curves depict inverse of the Horseshoe map $\mathbf{F}^{-1}$. 56

5.2 The second iteration of the Horseshoe map F: $V_{i,j} = F^2(H_{i,j}),\ i, j = 1, 2$. 60

5.3 The Shilnikov phenomena. 73

6.1 Isoclines and their analysis for system (6.1) on x_1x_2-plane with heteroclinic orbit that connects the two critical points A_2 and A_3 which is depicted by a dotted curve. 78

6.2 Isoclines and their analysis for system (6.1) on x_1x_3-plane with heteroclinic orbit that connects the two critical points A_3 and A_1 which is depicted by a dotted curve. 80
6.3 The Heteroclinic cycle connecting the three critical points. 81
6.4 The behaviour of trajectories near the planar saddle-focus critical point where the ratio of the eigenvalues around the point is equal to $\frac{-\mu}{\lambda}$. 86
6.5 The boundaries of the closed region R_k with their images under Ψ_1^1. 87
6.6 The behaviour of trajectories near the planar saddle critical point where the ratio of the eigenvalues around the point is equal to $\frac{\lambda}{\alpha_2}$. 92
6.7 The image of S_2 under Ψ_2, which shows the local behaviour of trajectories near the critical point A_2. On S_2, the solid curves depict the points that tend toward the cross section D_2 and the doted curves depict the points that tend toward infinity. Double arrows label the stable non-leading (strong stable). 93
6.8 The image of S_3 under Ψ_3, which shows the local behaviour of trajectories near the critical point A_3. Double arrows label the stable non-leading (strong stable). 95
6.9 The behaviour of trajectories near the axial saddle critical point where the ratio of the eigenvalues around the point is equal to $\frac{-\beta_2}{\beta_3}$. 96
6.10 Global phase portraits of Lotka-Volterra system (6.1) for $x_i \geq 0,\ i = 1, 2, 3$. 100
6.11 The eigenvalues at the origin, axial and infinity critical points for the three dimensional Lotka-Volterra system (6.1). 101
6.12 The Poincaré return map around the cycle. 105
6.13 The horizontal strip H_k on C_1. 106
6.14 The image of $\mathbf{F_t}(H_k)$ on C_2. 106

6.15 The image of the horizontal strip H_k and its image under $\mathbf{F}_t$ on the cross section C_1. 107

7.1 The red line depicts the line of singularities and blue cycles depict the periodic orbits a round one of the zero Hopf equilibrium points on the invariant plane $x_1 + x_2 + x_3 = 1$, where the parameters satisfy conditions (7.1), (7.3), condition (i) of Proposition 6, $r_1 = -2$, $r_3 = 1$ and $a_{3,1} = -\frac{10}{3}$. 120

Acknowledgements

This thesis would not have been possible without the help, support and patience of my principal supervisor Dr Colin Christopher. I would like to thank Colin for accepting me as a PhD student, for his support during the whole period of my study, for his insightful discussions, offering valuable advice and for introducing me to mathematical research, I hope to continue our collaboration in the future. Thanks also to my second supervisor Professor Roman Borisyuk whose valuable support, friendship and advice throughout the PhD has been very supportive.

I also appreciate the financial support of the Ministry of Higher Education and Scientific Research- Kurdistan Regional Government during my study. Thanks also to the organizers of the Human Capacity Development Program (HCDP). This higher education scholarship program was established in 2010 by the Kurdistan Regional Government and is an active program that aims to develop human capacities in the Kurdistan Region.

In addition, I would like to thank both Adriana Buică and Susanna Maza for giving me the opportunity to attend the 10*th* AIMS Conference on Dynamical Systems, Differential Equations and Applications and to meet so many interesting people. Special thanks also go to Professor Jaume Llibre (Universitat Autnoma de Barcelona - Spain), Professor Andrey Shilnikov (Georgia State University - USA) and Professor John Guckenheimer (Cornell University - USA) for guiding my research, answering my questions and my emails and also for providing journal articles. I gratefully thank my friend Robert Merrison (Plymouth University - UK) for providing the GPU dynamical systems program and his continuous help throughout my study.

Finally, I am thankful to my parents for their material and spiritual support in all aspects of my life. I also thank my brothers and sisters for providing assistance in numerous ways. Sincere thanks to my eldest son Zhiar, my younger daughter Zhewar and my youngest son Zhir for staying with me and providing love and kindness. Thanks also to my wife Chiman for her personal support, great patience at all times and for keeping me sane. Her love and support has been very important in helping the successful completion of my study. Last but not least, I would like to thank God for always giving me what I need.

Dedication

This dissertation is lovingly dedicated to these people:

- My parents, who emphasized the importance of education and helped me to continue my study, without your support I would not have obtained a degree.
- My wife, Chiman, who has always loved me unconditionally and supported me.
- My children, Zhiar, Zhewar and Zhir , who have been very proud of me.
- My brothers and sisters, who have been my emotional anchor.
- My friends, who have encouraged and supported me.

Author's Declaration

At no time during the registration for the degree of Doctor of Philosophy has the author been registered for any other University award without prior agreement of the Graduate Committee.

Work submitted for this research degree at the Plymouth University has not formed part of any other degree either at Plymouth University or at another establishment.

Relevant scientific seminars and conferences were regularly attended at which work was often presented. Two journal papers are in preparing for submission.

Word count of main body of thesis: 21,000

Signed ....

Date ....

Oral Presentations

- “ Chaos in Three Dimensional Lotka-Volterra Systems ”. *The 10th AIMS Conference on Dynamical Systems, Differential Equations and Applications*, 7th July, 2014 Madrid, Spain.

- “The Existence of Horseshoe Dynamics in Three Dimensional Lotka-Volterra Systems”. *SIAM Conference on Applications of Dynamical Systems*. May 18, 2015 Snowbird Ski and Summer Resort, Snowbird, Utah, USA.

Posters Presentations

- “ Centre Bifurcations of Limit Cycles for Three Dimensional Lotka-Volterra Systems ”. presented at: *International conference on Nonlinear Differential and Difference Equations: Recent Developments and Applications (ICNDDE-2014)*, May 27-30, 2014, Side, Antalya, Turkey.

Seminars

- " Horseshoe in Three Dimensional Lotka-Volterra Systems ". *School of Computing and Mathematics, Faculty of Science and Environment, Plymouth University*, 3rd July, 2014.

- " Averaging Methods for Finding Periodic Orbits ". *School of Computing and Mathematics, Faculty of Science and Environment, Plymouth University*, 9th December, 2014.

Papers

- Colin Christopher, Rizgar Salih. *A Simple Proof of Chaos in Three Dimensional Lotka-Volterra Systems.* Preprint, Plymouth University, 2015.

- Colin Christopher, Rizgar Salih. *Centre Bifurcations of Limit Cycles for Three Dimensional Lotka-Volterra Systems.* Preprint, Plymouth University, 2015 .

List of Abbreviations

W^c .... Centre Manifold

$Cl(V)$ .... Closure of V

D .... Determinant of the Jacobian Matrix

$\nabla V(u^*)$ .... Gradient of V at the Hopf point u^*

IJM .... Inverse Jacobi Multiplier

$\mathbb{N}$ .... Natural Numbers

$\mathbb{R}$ .... Real Numbers

W^s .... Stable Manifold

C^1 .... The space of continuously differentiable functions

3DLVS .... Three Dimensional Lotka-Volterra Systems

3DS .... Three Dimensional Systems

T .... Trace of the Jacobian Matrix

W^u .... Unstable Manifold

$\mathcal{X}$ .... Vector Field

Chapter 1

Introduction

We consider the N-dimensional Lotka-Volterra system:

$$\dot{u}_i = u_i(r_i + \sum_{j=1}^{N} a_{i,j} u_j), \qquad i = 1, 2, ..., N, \tag{1.1}$$

where r_i and $a_{i,j}$ $(i, j = 1, ..., N)$ are real parameters. For $r_i > 0$ and $a_{i,j} < 0$, the system described by equation (1.1) is called a *competitive system*, this is a subject of special investigation, but we consider all parameter values here. This system is a basic model of predator-prey interactions. Such systems were first considered by American biophysicist Lotka (1925), and Italian mathematician Volterra (1926). In this thesis, we are interested in studying the system in the case $N = 3$, *i.e.* the three dimensional case. The three dimensional Lotka-Volterra system has eight finite critical points, the origin, the three axial critical points, the three planar critical points and the interior critical point. We are interested in bifurcation from the interior point. Without loss of generality, we can scale the coordinates such that this point is at $(1, 1, 1)$, in which case $r_i = -\sum_{j=1}^{3} a_{i,j}$. The critical point $(1, 1, 1)$ can be transformed to the origin by setting $x_i = u_i - 1,\ i = 1, 2, 3$, then the system becomes:

$$\dot{x}_i = (x_i + 1)(\sum_{j=1}^{3} a_{i,j} x_j), \qquad i = 1, 2, 3. \tag{1.2}$$

Zeeman (1993) gave a full classification of the competitive three-dimensional Lotka-Volterra system and identified thirty-three stable equivalence classes. She showed that there are no periodic solutions for the first twenty-five classes and, together with van den Driessche, also eliminated classes thirty-two and thirty-three (Zeeman and van den Driessche, 1998). Then, the only classes that can have limit cycles are classes twenty-six to thirty one.

Zeeman's classification has opened the door to some questions about the occurrence of limit cycles with its maximum numbers and much research has been done on this. First of all, Hofbauer and So (1994) constructed an example with two limit cycles in class twenty-seven and they conjectured that two limit cycles was the maximum number. In addition, Xiao and Li (2000) have proved that if the competitive three-dimensional Lotka-Volterra system has no heteroclinic polycycles in $\mathbb{R}^3_+$, then the number of limit cycles of the system is finite. After that, in 2002, Lu and Luo (2002) built five examples for each of the classes twenty-six to twenty-nine and one non-competitive system where two limit cycles are created via Hopf bifurcation. In (Gyllenberg and Yan, 2009b), it has been proved that the classes thirty and thirty-one in the classification of Zeeman have two limit cycles without a heteroclinic cycle. Lu and Luo (2003) formed an example of the system of class twenty-seven and showed that it has three limit cycles with a heteroclinic cycle. By this pioneering work, the conjecture of Hofbauer and So has been refuted. In 2006, Gyllenberg et al. (2006) proved that the class twenty-nine of Zeeman's classification has three limit cycles without a heteroclinic polycycle, Gyllenberg and Yan (2009a) have shown that the class twenty-seven has four limit cycles with a heteroclinc cycle, and also in 2011, Wang et al. (2011b) found some singular point quantities for the corresponding Hopf bifurcation which are algebraic equivalent to Lyapunov quantities and which shows that the class twenty-nine has four limit cycles. Four limit cycles is the maximum number that has been found till now. However, the maximum number of limit cycles that can appear in Zeeman's classes twenty-six to thirty-one still remains as an open problem.

Work on the subject of limit cycles for the non-competitive Lotka-Volterra system has attracted less attention. Computing up to now has relied on full expression of the so-called Lyapunov quantities of the system. In general, it is very difficult to calculate due to growth of the complexity of the Liapunove quantities in these system. In (Wang et al., 2011a), the authors have constructed an example with four limit cycles. In their work, four singular point quantities which are equivalent to the Liapunov quantities corresponding to Hopf bifurcation equation are found.

In this thesis, we use a new technique examining centre bifurcations to estimate the cyclicity of system (1.2), which is explained in chapter four. Based on (Christopher, 2005) the technique can be applied to other differential systems in $\mathbb{R}^3$ and we hope that it will be useful for a wider audience. In two dimensional systems, such a technique was used by Christopher (2005) to show that at least eleven and seventeen limit cycles can bifurcate from a cubic centre and a quadratic non-degenerate centre, respectively, with at least twenty-two limit cycles for another quadratic system globally.

In addition to examining cyclicity, chaotic behaviour of the three dimensional Lotka-Volterra systems has also been investigated. Chaos is one of the more interesting and complex subjects in the dynamical system. Many authors had studied the chaotic behaviour of a non-linear system, but the use of the word chaos in dynamical systems was introduced by Li and Yorke in 1975 (Li and Yorke, 1975). Chaotic behaviour of Lotka-Volterra systems has been studied by many authors (see Coste et al. (1979); Gilpin (1979); Kuznetsov et al. (1992); Rinaldi et al. (1993); Sabin and Summers (1993); Schaffer (1985); Ushiki (1982)). According to the Poincare-Bendixan theory, $N \geq 3$ is the only case where chaotic motion may occur. Numerical evidence of the existence of chaotic motion for $N \geq 3$ is presented in Arneodo et al. (1982); Hofbauer and Sigmund (1998); Takeuchi (1996) and the references therein. However, attempting an analytical proof of the existence of chaotic behaviour of the Lotka-Volterra systems has received less attention.

Lotka-Volterra systems with N species and n resources have been studied in (Kozlov and Vakulenko, 2013). The existence of chaotic behaviour for the system with few resources and many species is shown. The method of realization of vector fields (RVF) proposed by Polácik (2002) is used to prove the existence of chaotic large time behaviour. These gives an example of a Lotka-Volterra system with Lorenz dynamics consisting of ten species and three resources.

In the case where $N = 3$, Gardini *et al.* in (Gardini et al., 1989) reported numerical evidence of transition to chaotic dynamics from the Hopf bifurcated limit cycle. It was expected that the subharmonic cascade is a common route to chaos in such systems. Furthermore, Christie et al. (2001) studied a slowly varying three-dimensional perturbed Lotka-Volterra equation and showed that the corresponding unperturbed system possesses a heteroclinic cycle. Melnikov's method was used to obtain sufficient conditions for the perturbed system to have a transverse heteroclinic cycle. According to the Smale-Birkhoff homoclinic theorem (Wiggins, 1992; Wiggins and Shaw, 1988), the existence of such a cycle implies the existence of chaotic behaviour for the system.

In the case where $N = 4$, the occurrence of chaos in Lotka-Volterra competitive system has been studied in (Vano et al., 2006). It was shown that chaos occurs in a narrow region of parameter space by finding some numerical conditions on the largest Lyapunov exponent. Symbolic dynamics were used to study the dynamic of the attractor for a maximally chaotic case. In this thesis, we study chaotic behaviour using a geometrical method. In the case where $N = 3$, an example of a Lotka-Volterra system is constructed, where we can show that the three dimensional Lotka-Volterra system can exhibit chaos by demonstrating the existence of a horseshoe map.

As well as the above two topics, the zero-Hopf bifurcation for 3DLVS is also studied. A zero-Hopf equilibrium point is an equilibrium point of a three dimensional autonomous differential system which has a zero eigenvalue and a pair of purely imaginary eigenvalues. When an infinitesimal periodic orbit bifurcates from the equilibrium point, such a kind of bifurcation is called *zero-Hopf bifurcation*. This type of bifurcation has been analysed by Guckenheimer (1981); Guckenheimer and Holmes (2013); Han (1998); Kuznetsov (2004); Scheurle and Marsden (1984). It has been shown that from the isolated zero-Hopf equilibrium point complicated invariant sets could be bifurcated under some conditions. In some cases, chaotic behaviour has been obtained as can be seen in the work of Baldoma and Seara, Baldom and Seara , Broer and Vegter, Champneys and Kirk and Scheurle and Marsden in (Baldomá and Seara, 2006, 2008; Broer and Vegter, 1984; Champneys and Kirk, 2004; Scheurle and Marsden, 1984) respectively.

The averaging method is a classical and a useful computational technique for analysing nonlinear oscillations. It has been used by many authors to study the bifurcating periodic orbits from a zero-Hopf equilibrium point. Using the first order of averaging theory, Castellanos et al. (2013) studied the tritrophic food chain model and proved that two periodic orbits can bifurcate simultaneously each one from one of the two zero-Hopf equilibrium of the model. García et al.

(2014) showed that one periodic orbit can bifurcate from the zero-Hopf equilibrium point of a slow-fast system with two slow variables and one fast variable. Llibre (2014) found two one-parameter families exhibiting a zero-Hopf equilibrium of the Rössler system. He proved that only one periodic orbit can bifurcate from one of the family and no periodic orbits from the other. In (Llibre et al., 2015), it has proved that two periodic orbits can bifurcate from the zero-Hopf equilibrium point of the Chen-Wang differential system.

The averaging theory of the second order has been applied to a quadratic polynomial differential system in $\mathbb{R}^3$ in (Llibre et al., 2009) to show that at most three limit cycles can bifurcate from a zero-Hopf equilibrium point. In addition, an example has been provided where exactly three limit cycles bifurcate from such an equilibrium point. Llibre and Prez-Chavela in (Llibre and Pérez-Chavela, 2014) applied the averaging theory to a class of three dimensional autonomous quadratic polynomial differential systems of Lorenz-type to show the existence of one periodic orbit from an equilibrium point of zero-Hopf type. Llibre and Xiao (2014) studied the periodic orbits bifurcating from a non-isolated zero-Hopf equilibrium point of a three differential system. In their work, the averaging theory of second order was used to find explicit conditions for the existence of one or two periodic orbits bifurcating from such a zero-Hopf type point. In (Euzébio et al., 2014), the first and second orders of averaging theory were used to study the bifurcating periodic orbits of the FitzHugh-Nagumo system. They found two two-parameter families for which the equilibrium point at the origin is a zero-Hopf and showed that only one periodic orbit can bifurcate from the origin in each case using the first order of averaging theory. Moreover, for the other two equilibrium points, three two-parameter families exhibiting a zero-Hopf equilibrium were found and it was proven that at most three periodic orbits can bifurcate from each equilibrium points. In (Llibre and Euzebio, 2014), the authors studied the Chua system and showed that it has three 4-parameter families for which the equilibrium points is a zero-Hopf. After perturbation, only one periodic orbit was obtained from one family using first order averaging theory and at most three periodic orbits were obtained from the other two families by using second order averaging theory. In this thesis, first order averaging theory is applied to 3DLVS to study the possible limit cycles bifurcating from a line of singularity of type zero-Hopf.

The format of the thesis is as follows. Chapter Two presents the general background on three dimensional systems that are used in this thesis. Some general background material on Hopf bifurcations, centre-focus problem and inverse Jacobi multiplier are given. There is also an explanation of the relation between the Poincaré return map and the Liapunov Quantities. Furthermore, some basic notions on the Darboux theory of integrability for three dimensional system are given. The third chapter is devoted to studying the centre of the three dimensional Lotka-Volterra system. In addition to the three invariant algebraic surfaces, a fourth invariant algebraic surface which passes through the interior critical point was found and this was used to construct an inverse Jacobi multiplier for the system. In Chapter Four, a new technique for bifurcating from centres was investigated and an examination of the cyclicity of the centres of the Lotka-Volterra system was undertaken by using centre bifurcation. More precisely, by using a centre bifurcation, it has been demonstrated that four limit cycles can be bifurcated from the centre. Furthermore, this technique is then applied to examine the cyclicity of the centre of a system that has a plane of singularities. In this case, we can show the existence of three dimensional quadratic system with eight limit cycles. Some aspects of chaotic behaviour, such as the Horseshoe map with its symbolic dynamics and the Shilnikov phenomena, are given in Chapter Five. In Chapter Six, the existence of the heteroclinic cycle for the three dimensional Lotka-Volterra systems connecting three critical points A_1, A_2 and A_3 is studied in the first section. The second section is devoted to a study of the local behaviour in a small neighbourhood of these critical points. In the next section, an investigation of the behaviour at infinity were conducted. In the final section, we show the existence of chaos via a horseshoe map for the three dimensional Lotka-Volterra system. The last chapter of this thesis consists of two sections, the first one presents some sufficient conditions for the existence of a line of singularities with two first integrals for the three dimensional Lotka-Volterra systems. The last section is devoted to studying the zero-Hopf conditions of the line of singularities and also to an investigation of the possible limit cycles bifurcating from such equilibria.

Chapter 2

Background

Understanding the results that are obtained in this thesis requires a basic background of certain fundamental concepts and tools. In this introductory chapter, we give an overview of three dimensional systems. We first make a short description of the Hopf bifurcation. Then we explain how the inverse Jacobi multiplier can solve the centre-focus problem. The relation between the Poincaré return map and the Liapunov quantities is shown in the next section. Furthermore, we explain the concept of the Darboux theory of integrability and also the relation between the invariant algebraic surfaces and first integral as a Darboux first integral was given. In general, this chapter provides definitions, notation and background information that will be used uniformly throughout the thesis.

2.1 Hopf Points in Three Dimensional Systems

The aim of this section is to present some basic background on Hopf bifurcation. A sufficient condition for a Hopf bifurcation in the three dimensional system (it possess two pure imaginary and one non-zero real eigenvalue) is illustrated below.

Consider the family of three dimensional systems

$$\dot{U} = AU + F(U;\mu), \tag{2.1}$$

with parameter $\mu \in \mathbb{R}^N$, variable $U \in \mathbb{R}^3$, the dot denotes derivation with respect to time t and F is an analytic function satisfying $F(0;\mu) = 0$ and $D_U(0;\mu) = 0$ for all μ, where $D_U(0;\mu)$ is the determinant of Jacobian matrix of $F(U;\mu)$ at $U = 0$. Let

$$\lambda^3 - T\lambda^2 - K\lambda - D = 0, \tag{2.2}$$

be the characteristic polynomial for system (2.1) where

$$\begin{aligned} T &= \text{Trace of the Jacobian matrix of system (2.1) at the origin and } T = \sum_{i=1}^{3} a_{i,i}\ ; \\ D &= \text{Determinant of the Jacobian matrix of system (2.1) at the origin;} \\ K &= -(A_1 + A_2 + A_3); \end{aligned}$$

where $A_1 = a_{2,2}a_{3,3} - a_{2,3}a_{3,2}$, $A_2 = a_{1,1}a_{3,3} - a_{1,3}a_{3,1}$ and $A_3 = a_{1,1}a_{2,2} - a_{1,2}a_{2,1}$ and $a_{i,j},\ i,j = 1,2,3$ are elements of the Jacobian matrix of system (1.2) at the origin. Then the Hopf bifurcation occurs at a point (which is called a Hopf point) where

$$TK + D = 0; \quad K < 0 \quad \text{and} \quad T \neq 0. \tag{2.3}$$

Moreover, the square matrix A in equation (2.1) has two complex eigenvalues $\alpha \pm i\beta,\ \beta \neq 0$, and a non-zero eigenvalue γ. By a non-singular linear change of coordinates and the time rescaling $\tau = \beta t$, such a system can be written in the form

$$
\begin{aligned}
\dot{x_1} &= \alpha_1 x_1 - x_2 + F_1(x_1, x_2, x_3; \mu), \\
\dot{x_2} &= \alpha_1 x_2 + x_1 + F_2(x_1, x_2, x_3; \mu), \\
\dot{x_3} &= \lambda x_3 + F_3(x_1, x_2, x_3; \mu),
\end{aligned}
\tag{2.4}
$$

where $\alpha_1 = \frac{\alpha}{\beta}$, $\lambda = \frac{\gamma}{\beta}$, $F_i(x_1, x_2, x_3; \mu) = \sum_{k=2}^{\infty} F_i^k(x_1, x_2, x_3; \mu)$, $i = 1, 2, 3$ and $F_i^k(x_1, x_2, x_3; \mu)$ are homogeneous polynomials of degree k. At $\alpha_1 = 0$, the critical point of equation (2.4) at the origin is a Hopf point, that is, it possesses two purely imaginary eigenvalues, $\pm i$, and a non-zero eigenvalue λ. A good source for background information on bifurcation from a Hopf point in $\mathbb{R}^n$ is (Marsden and McCracken, 1976). At the Hopf point system (2.4) can be written of the form

$$
\begin{aligned}
\dot{x_1} &= -x_2 + F_1(x_1, x_2, x_3; \mu), \\
\dot{x_2} &= x_1 + F_2(x_1, x_2, x_3; \mu), \\
\dot{x_3} &= \lambda x_3 + F_3(x_1, x_2, x_3; \mu),
\end{aligned}
\tag{2.5}
$$

and the associated vector field of family (2.5) is denoted by $\mathcal{X}$, that is

$$
\begin{aligned}
\mathcal{X} = (-x_2 + F_1(x_1, x_2, x_3; \mu))\frac{\partial}{\partial x_1} &+ (x_1 + F_2(x_1, x_2, x_3; \mu))\frac{\partial}{\partial x_2} \\
+ (\lambda x_3 + F_3(x_1, x_2, x_3; \mu))\frac{\partial}{\partial x_3}&.
\end{aligned}
\tag{2.6}
$$

The set of all parameters $\mu_1, \mu_2, ..., \mu_N$ of F_1, F_2 and F_3 is denoted by Λ and $\mathbf{K} \in \mathbb{R}^N$ is the corresponding parameter space. Since system (2.5) has two eigenvalues with zero real part at the origin Hopf point, then the Centre Manifold Theorem implies that system (2.5) has a local 2-dimensional centre manifold, $W^c(0)$ (Carr, 1981). This manifold is invariant in a small neighbourhood of the origin (for sufficiently small $\|x_1\|$ and $\|x_2\|$) and there exists a function h of class $C^k,\ k \geq 1$ in a small neighbourhood of the origin such that $h(0,0;\mu) = Dh(0,0;\mu) = 0$, where $Dh(0,0;\mu)$ is a Jacobian matrix of h at the origin. The 2-dimensional centre manifold, $W^c(0)$, is defined by

$$W^c(0) = \{(x_1, x_2, h(x_1, x_2; \mu); \mu) \in \mathbb{R}^3 : (x_1, x_2) \in \text{a small neighbourhood of the origin}\}$$

After substituting $x_3 = h(x_1, x_2; \mu)$ into the third component of equation (2.5) and using the chain rule the following quasilinear partial differential equation is obtained:

$$Dh(x_1, x_2; \mu) \begin{bmatrix} -x_2 + F_1(x_1, x_2, h(x_1, x_2; \mu); \mu) \\ x_1 + F_2(x_1, x_2, h(x_1, x_2; \mu); \mu) \end{bmatrix} = \lambda\ h(x_1, x_2; \mu) + F_3(x_1, x_2, h(x_1, x_2; \mu); \mu). \tag{2.7}$$

Substituting $x_3 = h(x_1, x_2; \mu)$ into the first two components of equation (2.5), we obtain the following two dimensional differential system with linear part of centre-focus type which is called the *reduced system* (bifurcation equation) to the centre manifold,

$$\begin{aligned} \dot{x}_1 &= -x_2 + F_1(x_1, x_2, h(x_1, x_2; \mu); \mu), \\ \dot{x}_2 &= x_1 + F_2(x_1, x_2, h(x_1, x_2; \mu); \mu). \end{aligned} \tag{2.8}$$

We note that the Hopf point at the origin of system (2.5) need not generally have a unique centre manifold. This can be illustrated by the following simple example below

$$\dot{x_1} = -x_2 - x_1(x_1^2 + x_2^2),$$
$$\dot{x_2} = x_1 - x_2(x_1^2 + x_2^2), \tag{2.9}$$
$$\dot{x_3} = -x_3.$$

Polar coordinates $x_1 = rcos(\theta)$ and $x_2 = rsin(\theta)$ bring system (2.9) to the following equations

$$\dot{r} = -r^3,$$
$$\dot{\theta} = 1,$$
$$\dot{x_3} = -x_3,$$

and its solution is given by $x_3 = x_3(0)\ e^{\frac{-1}{2(x_1^2+x_2^2)}}$ which is the centre manifold for system (2.9). Thus, the Hopf point at the origin for system (2.9) does not have a unique centre manifold. However, the centre manifold of system (2.5) at the Hopf point is unique if it has a centre at the origin, for more detail see (Sijbrand (1985); Burchard et al. (1992)).

2.2 The Centre-Focus Problem and Inverse Jacobi Multiplier

The centre-focus problem is one of central problems in the qualitative theory of planar differential equations and is known as Poincaré centre-focus problem. Aulbach (1985) has shown that the origin saddle centre/focus of (2.5) on the centre manifold is either a weak focus or a centre. If there exists a neighbourhood U of the origin on the local centre manifold such that all orbits are periodic on it, the origin is called *centre*, otherwise is a saddle *focus* that the orbits spiral around the origin critical point. The problem of distinguishing between centre and focus is called the *centre-focus problem*. The centre problem at the Hopf point can be solved by two main methods. The critical point at the origin is a centre for (2.5) if and only if (2.5) admits a real analytic local first integral of the form $F(x_1, x_2, x_3) = x_1^2 + x_2^2 + \cdots$ in a neighbourhood of the critical point in $\mathbb{R}^3$. This is the classical Lyapunov Centre Theorem, for more detail see (Bibikov, 1979). An alternative method is given by inverse Jacobi multiplier. The real valued function V which is defined in an open subset $U \subset \mathbb{R}^3$ and satisfies the linear first order partial differential equation

$$div(\mathcal{X}/V) = 0 \quad \text{or} \quad \mathcal{X}(V) = V div(\mathcal{X}), \qquad V \neq 0, \tag{2.10}$$

where $\mathcal{X}$ is a vector field associated to (2.5) and *div* refers the divergence operator, is called an *inverse Jacobi multiplier*. The reader interested in a detailed exposition of this subject should consult (Berrone and Giacomini, 2003). The inverse Jacobi multiplier solves the centre problem by the following theorem, which is proved by Buică *et al*. in (Buică et al., 2012).

Theorem 1. The analytic system (2.5) has a centre at the origin if and only if it admits a local analytic inverse Jacobi multiplier of the form $V(x_1, x_2, x_3) = x_3 + \ldots$ in a neighbourhood of the origin in $\mathbb{R}^3$. Moreover, when such V exists, the local analytic centre manifold, W^c, lies in $V^{-1}(0)$.

Remark 1. The origin is a centre of (1.2) if and only if it admits a local analytic inverse Jacobi multiplier V at the origin with $\nabla V(0) \neq 0$, where $0 \in \mathbb{R}^3$ is a Hopf point of (1.2). This follows directly from the above theorem.

2.3 The Poincaré Return Map and the Liapunov Quantities

To study the relation between the Poincaré return map and the Liapunov quantities on the centre manifold, we start from the bifurcation equation (2.8). Under the polar coordinates $x_1 = rcos(\theta),\ x_2 = rsin(\theta)$, the reduced system (2.8) can be transformed into

$$\begin{aligned}
\dot{r} &= r^2(F_1^{(2)}(cos(\theta), sin(\theta), h(cos(\theta), sin(\theta); \mu); \mu)cos(\theta) \\
&\quad + F_2^{(2)}(cos(\theta), sin(\theta), h(cos(\theta), sin(\theta); \mu); \mu)sin(\theta) + ...), \\
\dot{\theta} &= 1 - r(F_1^{(2)}(cos(\theta), sin(\theta), h(cos(\theta), sin(\theta); \mu); \mu)sin(\theta) \\
&\quad - F_2^{(2)}(cos(\theta), sin(\theta), h(cos(\theta), sin(\theta); \mu); \mu)cos(\theta) + ...).
\end{aligned}$$

We can rewrite above equation as follows

$$\frac{dr}{d\theta} = \frac{r^2 F(r, cos(\theta), sin(\theta); \mu)}{1 + rG(r, cos(\theta), sin(\theta); \mu)} = R(r, \theta; \mu), \tag{2.11}$$

where $R(r, \theta; \mu)$ is a smooth function over the cylinder $\{(r, \theta; \mu) \in R \times S^1 : |r| < \delta\}$ for sufficiently small value of $\delta > 0$ and is a periodic function of θ of period 2π. The Hopf point at the origin for equation (2.5) corresponds to $R(0, \theta, \mu)$, so that $r = 0$ is a solution of equation (2.11). We can expand the function $R(r, \theta; \mu)$ in a power series in r,

$$\frac{dr}{d\theta} = R(r, \theta; \mu) = r^2 R_2(\theta; \mu) + r^3 R_3(\theta; \mu) + ... + O(r^n), \tag{2.12}$$

where $R_k(\theta; \mu)$ are $2\pi-$periodic functions of θ and satisfy $R_k(\theta + \pi; \mu) = (-1)^k R_k(\theta; \mu)$, $k = 2, 3, ...$ (see (Liu, 2001; Wang et al., 2010)). Here, the solution of system (2.12) with the initial condition $\theta = \theta_0$ and $r = r_0$ is denoted by $r = f(\theta, \theta_0, r_0; \mu)$ and also $f(\theta, \theta_0, 0; \mu) = 0$. Since the reduced system on the centre manifold at the origin has two complex eigenvalues with zero real part (the origin of system (2.5) is of centre-focus type), then in a sufficiently small neighbourhood of the origin every trajectory crosses each ray $\theta = c$, $0 \leq c < 2\pi$. This property implies that all trajectories of the system are passing through the segment $\Sigma = \{(x_1, x_2) : x_2 = 0,\ 0 \leq x_1 \leq \delta\}$ for δ sufficiently small, this set of points is equivalent to $\theta_0 = 0$, that is, all solutions $r = f(\theta, 0, r_0; \mu)$. We expand $f(\theta, 0, r_0; \mu)$ in a power series in r_0,

$$r = f(\theta, 0, r_0; \mu) = w_1(\theta; \mu)r_0 + w_2(\theta; \mu)r_0^2 + w_3(\theta; \mu)r_0^3 + ... + \ O(r_0^n), \quad (2.13)$$

which satisfies equation (2.12). Hence,

$$\dot{w}_1(\theta; \mu)r_0 + \dot{w}_2(\theta; \mu)r_0^2 + \dot{w}_3(\theta; \mu)r_0^3 + ... = R_2(\theta; \mu)(w_1(\theta; \mu)r_0 + w_2(\theta; \mu)r_0^2 +$$
$$w_3(\theta; \mu)r_0^3 + ...)^2 + R_3(\theta; \mu)(w_1(\theta; \mu)r_0 + w_2(\theta; \mu)r_0^2 + w_3(\theta; \mu)r_0^3 + ...)^3 + ... + \ O(r_0^n).$$

Equating the coefficients of r_0^i, $i = 1, 2, ...$, we obtain the following differential equations

$$\begin{aligned} \dot{w}_1(\theta, \mu) &= 0, \\ \dot{w}_2(\theta, \mu) &= R_2(\theta; \mu)w_1^2(\theta; \mu), \\ \dot{w}_3(\theta, \mu) &= 2R_2(\theta; \mu)w_1(\theta; \mu)w_2(\theta; \mu) + R_3(\theta; \mu)w_1^3(\theta; \mu), \\ &\vdots \end{aligned} \quad (2.14)$$

The initial condition $r = f(0, 0, r_0; \mu) = r_0$ leads to $w_1(0; \mu) = 1$, $w_i(0; \mu) = 0$ for all $i > 1$. Integrating the equations in (2.14) and using the above initial condition, the functions $w_i(\theta;\mu),\ i \geq 1$ will be obtained. In particular, we have $w_1(\theta;\mu) = 1$.

To obtain the next intersection point of the trajectory $r = f(\theta, 0, r_0; \mu)$ on Σ, we set $\theta = 2\pi$ in the solution function. Thus, $r = f(2\pi, 0, r_0; \mu)$ is the point on Σ where the trajectory of the system next intersects Σ. The map $R : \Sigma \subset \mathbb{R} \longrightarrow \mathbb{R}$ which is defined by

$$R(r_0;\mu) = f(2\pi, 0, r_0; \mu) = \tilde{\eta_1} r_0 + \eta_2 r_0^2 + \eta_3 r_0^3 + ... +\ O(r_0^n), \tag{2.15}$$

for $|r_0| < \delta$, where $\tilde{\eta_1} = w_1(2\pi;\mu) = 1$ and $\eta_i = w_i(2\pi;\mu)$ for $i > 1$ is called *Poincaré first return map* or just the *return map*. The difference between the first return map and its starting point, $d(r_0,\mu)$, is given by

$$\begin{aligned} d(r_0;\mu) &= R(r_0;\mu) - r_0 \\ &= \eta_1 r_0 + \eta_2 r_0^2 + \eta_3 r_0^3 + ... +\ O(r_0^n), \end{aligned} \tag{2.16}$$

and is called the *difference function.* In equation (2.16) the coefficient $\eta_i, i \in \mathbb{N}$ is called the *ith Liapunov number* at the origin on centre manifold of system (2.5) which are functions of μ. We note from the above two equations that, the first Liapunov number is zero and zeros of equation (2.16) correspond to cycles. Isolated zeros correspond to isolated closed orbits which are known as *limit cycles.* Liu (2001) presented an expression of the relation between the coefficients of $r_0^i,\ i = 1, 2, ...$ in equation (2.16). He proved that for every positive integer $m = 1, 2, ...,$ there exist an expression of the form

$$\eta_{2m} = \frac{1}{2} \sum_{k=1}^{m-1} \xi_m^{(k)} \eta_{2k+1}, \tag{2.17}$$

where $\xi_m^{(k)},\ k = 1, 2, ..., m-1$ are polynomials in $w_1(\pi),\ w_2(\pi), ...,\ w_{2m}(\pi)$ and

$\tilde{\eta_1},\ \eta_2, ...,\ \eta_{2m}$ with rational coefficients. We note in expression (2.17), if for each $1 \leq k \leq m-1,\ \eta_{2k+1} = 0$ then $\eta_2 = \eta_4 = ... = \eta_{2m} = 0$ and the first non-zero coefficient of r_0 in equation (2.16) is the coefficient of an odd power of r_0.

The origin of (2.5) is centre if for a fixed parameter $\mu^* \in \mathbf{K}$, $\tilde{\eta_1}(\mu^*) = 1$ ($\eta_1(\mu^*) = 0$) and $\eta_i(\mu^*) = 0,\ i \geq 2$. In this case the difference function $d(r_0; \mu^*)$ is zero. Otherwise, the difference function is non-zero and the origin is a focus. If for some $k \in \mathbb{N}$, $\eta_1 = \eta_2 = \eta_3 = ... = \eta_{2k} = 0$ and $\eta_{2k+1} \neq 0$, then the origin of (2.5) is called the *fine focus* or *weak focus* of order k. The coefficient η_{2i+1} in (2.16) is called the *ith Liapunov quantity* at the origin on centre manifold and denote it by $L(i)$. If the origin is a fine focus of order k at $\mu = \mu^*$, that is, $L(i) = 0$ for $i < k$ and $L(k) \neq 0$, then $d(r_0; \mu^*)$ has order $2k+1$. Thus, at most k limit cycles can be bifurcated from the point under perturbation. Moreover, the independence of the Liapunov quantities give us the exact number of limit cycles. That is, if we choose a parameter $\mu^* \in \mathbf{K}$ so that $L(i)$ for $1 \leq i \leq k-1$ are independent in a neighbourhood of the origin,(this will happen if the Jacobian matrix of the $L(i)$'s with respect to the parameters Λ at μ^* has rank $k-1$) then $k-1$ limit cycles can be produced by choosing one by one successively

$$|L(i-1)| \leq |L(i)|, \quad L(i-1)L(i) < 0,$$

working from $L(k-1)$ to $L(0)$.

The above method for finding Liapunov quantities from the return map $R(r_0; \mu)$ on the centre manifold is not the most efficient way to proceed. Instead, a method which is equivalence to it can be used. In this method, we only need to calculate the Liapunov quantities $L(k)$ modulo the previous $L(i)$ for $i < k$. The first Liapunov quantity is multiple of α_1, therefore the first Liapunov quantity of (2.8) is always zero. To find the Liapunov quantities of system (2.8), we seek a Lyapunov function of the form

$$F(x_1, x_2) = x_1^2 + x_2^2 + \sum_{k=3}^{\infty} F_k(x_1, x_2; \mu),$$

where F_k is a polynomial in x_1, x_2 of degree k and the coefficients of F satisfy

$$\mathcal{X}(F) = L_1 D + L_2 D^2 + L_3 D^3 + ..., \tag{2.18}$$

where $D = (x_1^2 + x_2^2)$ or x_1^2 or x_2^2 or $(x_1^2 + x_2^2)^2$ or other suitable forms (for more detail see Andronov et al. (1971); Lu and Luo (2002); Wang (1991)). Here, $L_i,\ i = 1, 2, 3, ...$ is a polynomial in the parameter μ of the system also called the *ith Liapunov quantity.* If the linear part of the system is not of the canonical form, we can transform the system or we can replace the term $x_1^2 + x_2^2$ in the Liapunov function F by an equivalent positive definite quadratic form which is annihilated by the linear part of the vector field $\mathcal{X}$.

Recently, an algorithm of computing the singular point quantities on centre manifold for the three dimensional system was introduced by Wang *et al.* in (Wang et al., 2010). This algorithm is more useful to investigate the multiple Hopf bifurcation at the origin of the three dimensional system (2.5). By the transformation

$$X = x_1 + ix_2,\ Y = x_1 - ix_2,\ Z = x_3,\ T = it,\ i = \sqrt{-1}\ ,$$

system (2.5) can be transformed into the following complex system

$$\begin{aligned}
\dot{X} &= X + G_1(X, Y, Z; \mu) = \tilde{G}_1(X, Y, Z; \mu), \\
\dot{Y} &= -Y + G_2(X, Y, Z; \mu) = \tilde{G}_2(X, Y, Z; \mu), \\
\dot{Z} &= -i\lambda Z + G_3(X, Y, Z; \mu) = \tilde{G}_3(X, Y, Z; \mu),
\end{aligned} \tag{2.19}$$

where $X,\ Y,\ Z$ and the coefficients of the $G_i,\ i = 1, 2, 3$ are complex and system (2.5) and (2.19) are called *concomitant*. In (Wang et al., 2010), a program of term by term calculations is presented for determining the formal power series below:

$$F(X, Y, Z) = XY + \sum_{\alpha+\beta+\gamma=3}^{\infty} C_{\alpha\beta\gamma} X^{\alpha} Y^{\beta} Z^{\gamma} \ , \tag{2.20}$$

such that

$$\begin{aligned} XF &= \frac{\partial F}{\partial X}\tilde{G}_1(X, Y, Z; \mu) + \frac{\partial F}{\partial Y}\tilde{G}_2(X, Y, Z; \mu) + \frac{\partial F}{\partial Z}\tilde{G}_3(X, Y, Z; \mu) \\ &= \sum_{m=1}^{\infty} \mu_m (XY)^{m+1} \ , \end{aligned} \tag{2.21}$$

where $C_{110} = 1, C_{101} = C_{011} = C_{200} = C_{020} = 0, C_{kk0} = 0, k = 2, 3, ...$ and the coefficient μ_m in equation (2.21) is called the *mth singular point quantity* at the origin on centre manifold of system (2.19) or (2.5). There exist a relationship between the *mth* singular point quantity μ_m and the *mth* focal value η_{2m+1} (*mth* Liapunov quantity) at the origin on centre manifold of system (2.5). This relation is proved in (Wang et al., 2010) and is given by

$$\eta_{2m+1} = i\pi\mu_m + i\pi \sum_{k=1}^{m-1} \xi_m^{(k)} \mu_m \ ,$$

where $\xi_m^{(k)},\ k = 1, 2, ..., m - 1$ are polynomial functions of coefficients of system (2.19). The above expression is usually called algebraic equivalence and written as $\eta_{2m+1} \sim i\pi\mu_m$. A good resource that provides a summery of the singular point quantities, focal values and their relationship for a critical point of three dimensional system is (Wang and Huang, 2012).

The existence of a power series F in (2.20) for system (2.19) is equivalent to the existence of a power series

$$F(x_1, x_2, x_3) = x_1^2 + x_2^2 + \sum_{k=3}^{\infty} F_k(x_1, x_2, x_3; \mu) \ , \tag{2.22}$$

where

$$F_k = \sum_{i=0}^{k} \sum_{j=0}^{i} C_{k-i,i-j,j} \ x_1^{k-i} x_2^{i-j} x_3^{j} \ ,$$

and the coefficients of F satisfy equation (2.18). In this method it does not necessary to find a centre manifold and the reduced system on it. We shall use this method in our calculations in chapter four.

2.4 The Darboux Theory of Integrability in 3DS

The studying of integrability of systems of differential equations is an enduring area of research in the theory of ordinary differential equations. Integrable systems are important in studying various mathematical models, especially when we perturb them, we obtain a rich picture of bifurcations. The structure of integrals helps us to understand such bifurcations. The problem of integrability for three dimensional systems has received much attention (see Aziz and Christopher (2012); Berrone and Giacomini (2003); Cairó and Llibre (2000); Christodoulides and Damianou (2009); Gao and Liu (1998); Hu et al. (2013); Llibre et al. (2012)).

The existence of a first integral is the key feature of integrability and leads to a reduction in order of the differential system by one. A non-constant analytic function $\phi : U \longrightarrow \mathbb{R}$ of system (2.5) where U is an open subset of $\mathbb{R}^3$ is called *first integral* if it is constant on every solution curve $(x_1(t), x_2(t), x_3(t))$ of (2.5) on U. That is, $\phi(x_1(t),\ x_2(t),\ x_3(t)) = c$ with $c \in \mathbb{R}$ for every time t for which the solution $(x_1(t),\ x_2(t),\ x_3(t))$ is defined on U. This means that ϕ satisfies the partial differential equation

$$\mathcal{X}(\phi) = (-x_2 + F_1)\frac{\partial \phi}{\partial x_1} + (x_1 + F_2)\frac{\partial \phi}{\partial x_2} + (\lambda x_3 + F_3)\frac{\partial \phi}{\partial x_3} = 0.$$

It is well known that the phase portrait of a two dimensional system is determined completely by the existence of a single first integral. With three dimensional systems, when there is one first integral then the system is partially integrable but when there are two independent first integrals the system is completely integrable and its trajectories are determined by intersection of the level curves of that two first integrals (Cairó and Llibre, 2000). In general, the $n-$dimensional system will be completely integrable if it has $(n-1)$ independent first integrals (Zhang, 2008). Many different methods have been used for studying the existence of first integrals. The algebraic theory of integrability is a classical one, which provides a link between the existence of first integrals of differential systems and the number of their invariant algebraic surfaces. This type of integrability is usually called *Darboux integrability* and it was found by Darboux in 1878 for curves in two dimensional systems (Darboux, 1878). He proved that if a planar polynomial differential system of degree n has at least $\frac{n(n+1)}{2}$ invariant algebraic curves, then it has a first integral which is an explicit function of the invariant algebraic curves. This method of integrability was extended by many authors such as Jouanolou (1979), Christopher (1994), Christopher and Llibre (1999) and Llibre and Zhang (2009).

The starting point in the Darboux theory of integrability in three dimensional systems is the concept of the invariant algebraic surface. The existence of invariant algebraic surfaces play an important role in the studying of integrability for polynomial differential systems. Given a polynomial $V \in \mathbb{C}[x_1, x_2, x_3]$, a surface $V = 0$ is called an *invariant algebraic surface* of system (2.5), if the polynomial

V satisfies the equation

$$\mathcal{X}(V) = (-x_2 + F_1)\frac{\partial V}{\partial x_1} + (x_1 + F_2)\frac{\partial V}{\partial x_2} + (\lambda x_3 + F_3)\frac{\partial V}{\partial x_3} = KV, \tag{2.23}$$

for some polynomial $K \in \mathbb{C}[x_1, x_2, x_3]$. The polynomial K is called the *cofactor* of the invariant algebraic surface $V = 0$. From equation (2.23), it is easy to see that the degree of the cofactor K is less than the degree of the invariant algebraic surface $V = 0$ by at least one. If system (2.5) admits several invariant algebraic surfaces, let us say $f_1,\ f_2,\ ...,\ f_n$, then the function

$$V = \Pi_{i=1}^{n} f_i^{\lambda_i}\ , \tag{2.24}$$

where the cofactors $k_i,\ i = 1, 2, ..., n$ satisfy $\sum_{i=1}^{n} \lambda_i k_i = 0$ and $\lambda_i \in \mathbb{R}$ not all zero, is called a *Darboux first integral* (Hu et al., 2013). For a nice summary of this subject see (Pan and Zhang, 2013). A function V which is defined in (2.24) is called *inverse Jacobi multiplier of Darboux type* for system (2.5) if satisfies

$$\sum_{i=1}^{n} \lambda_i k_i - div(\mathcal{X}) = 0,$$

where the f_i are invariant algebraic surfaces for the system, k_i are the corresponding cofactors and $\lambda_i \in \mathbb{R}$ not all zero.

Chapter 3

The Existence of Centre in 3DLVS Via the Darboux Method Using Inverse Jacobi Multipliers

In this chapter, sufficient conditions for the existence of a centre on a local centre manifold for the three dimensional Lotka-Volterra system were obtained by using the inverse Jacobi multiplier functions which are defined in a small neighbourhood of the Hopf point. The system always has three invariant algebraic surfaces given by the axis planes. However, for particular parameter values an additional fourth invariant algebraic surface which passes through the interior critical point can be found and this can be used to construct an inverse Jacobi multiplier for the system. This can be used to show the existence of a centre via Theorem 1.

3.1 The Inverse Jacobi Multiplier Function of Darboux Type

Here, we recall a function $V = \Pi_{i=1}^{n} f_i^{\lambda_i}$ is an *inverse Jacobi multiplier of Darboux type* for system (1.2) if satisfies

$$div(\mathcal{X}) = \sum_{i=1}^{n} \lambda_i k_i,$$

where the f_i are invariant algebraic surfaces for the system, k_i are the corresponding cofactors and $\lambda_i \in \mathbb{R}$ not all zero. This function can be used to study the Hopf point of the three dimensional Lotka-Volterra system (1.2). Invariant algebraic surfaces play an important role in constructing this type of map, therefore we now state and prove two main properties of invariant algebraic surfaces.

Proposition 1. Let $f_1, f_2 \in C[x_1, x_2, x_3]$. We assume that f_1 and f_2 are relatively prime in the ring $C[x_1, x_2, x_3]$. Then for the three dimensional system (1.2), $f_1 f_2 = 0$ is an invariant algebraic surface with cofactor K if and only if $f_1 = 0$ and $f_2 = 0$ are invariant algebraic surfaces with cofactors k_1 and k_2 respectively. Moreover, $K = \sum_{i=1}^{2} k_i$.

Proof. Suppose $f_1 = 0$ and $f_2 = 0$ are invariant algebraic surfaces of (1.2) with cofactors k_1 and k_2 respectively, then $\mathcal{X}(f_1) = k_1 f_1$, and $\mathcal{X}(f_2) = k_2 f_2$ and

$$\begin{aligned}
\mathcal{X}(f_1 f_2) &= (\mathcal{X} f_1) f_2 + f_1 (\mathcal{X} f_2) \\
&= (k_1 f_1) f_2 + f_1 (k_2 f_2) \\
&= (k_1 + k_2) f_1 f_2 \\
&= K f_1 f_2.
\end{aligned}$$

Thus, $f_1 f_2 = 0$ is an invariant algebraic surface of (1.2) with cofactor K.

Conversely, suppose $f_1 f_2 = 0$ is an invariant algebraic surface of (1.2) with cofactor K, then

$$(\mathcal{X} f_1) f_2 + f_1 (\mathcal{X} f_2) = \mathcal{X}(f_1 f_2) = K f_1 f_2. \tag{3.1}$$

Since f_1 and f_2 are relative prime polynomials, then there is no a polynomial of positive degree in $C[x_1, x_2, x_3]$ that divides both f_1 and f_2. From equation (3.1), we obtain that f_1 divides $\mathcal{X}(f_1)$ and f_2 divides $\mathcal{X}(f_2)$. That is, there exist two polynomials k_1 and k_2 with $\mathcal{X}(f_1) = k_1 f_1$ and $\mathcal{X}(f_1) = k_1 f_1$. Then, $f_1 = 0$ and $f_2 = 0$ are invariant algebraic surfaces of (1.2) with cofactors k_1 and k_2 respectively. □

Proposition 2. We suppose $V \in C[x_1, x_2, x_3]$ and let $V = f_1^{\lambda_1} f_2^{\lambda_2} \ ... \ f_n^{\lambda_n}$, where $f_i^{\lambda_i}$ are irreducible factor over $C[x_1, x_2, x_3]$. Then for system (1.2), $V = 0$ is an invariant algebraic surface with cofactor K_V if and only if $f_i = 0$ is an invariant algebraic surface with cofactor k_i for each $i = 1, 2, ..., n$. Moreover, $K_V = \sum_{i=1}^{n} \lambda_i k_i$.

Proof. We assume that $f_i = 0$ is invariant algebraic surface of (1.2) with cofactor $k_i, \ i = 1, 2, ..., n$, then

$$\begin{aligned}
\mathcal{X}(V) &= \mathcal{X}(f_1^{\lambda_1} f_2^{\lambda_2} f_3^{\lambda_3} ... f_n^{\lambda_n}) \\
&= (f_2^{\lambda_2} f_3^{\lambda_3} ... f_n^{\lambda_n}) \mathcal{X}(f_1^{\lambda_1}) + (f_1^{\lambda_1} f_3^{\lambda_3} ... f_n^{\lambda_n}) \mathcal{X}(f_2^{\lambda_2}) + ... + (f_1^{\lambda_1} f_2^{\lambda_2} ... f_{n-1}^{\lambda_{n-1}}) \mathcal{X}(f_n^{\lambda_n}) \\
&= (f_2^{\lambda_2} f_3^{\lambda_3} ... f_n^{\lambda_n})(\lambda_1 f_1^{\lambda_1 - 1} \mathcal{X}(f_1)) + (f_1^{\lambda_1} f_3^{\lambda_3} ... f_n^{\lambda_n})(\lambda_2 f_1^{\lambda_2 - 1} \mathcal{X}(f_2)) + ... \\
&+ (f_1^{\lambda_1} f_2^{\lambda_2} ... f_{n-1}^{\lambda_{n-1}})(\lambda_n f_n^{\lambda_n - 1} \mathcal{X}(f_n)) \\
&= (f_2^{\lambda_2} f_3^{\lambda_3} ... f_n^{\lambda_n})(\lambda_1 k_1 f_1^{\lambda_1}) + (f_1^{\lambda_1} f_3^{\lambda_3} ... f_n^{\lambda_n})(\lambda_2 k_2 f_2^{\lambda_2}) + ... + (f_1^{\lambda_1} f_2^{\lambda_2} ... f_{n-1}^{\lambda_{n-1}})(\lambda_n k_n f_n^{\lambda_n}) \\
&= V(\lambda_1 k_1 + \lambda_2 k_2 + ... + \lambda_n k_n) \\
&= K_V V.
\end{aligned}$$

Therefore, $V = 0$ is an invariant algebraic surface of (1.2) with cofactor K_V.

Now, we shall prove the converse statement. Suppose $V = 0$ is an invariant algebraic surface of (1.2) with cofactor K_V. From Proposition 1, we note that $V = 0$ is an invariant algebraic surface with cofactor K_V if and only if $f_i^{\lambda_i} = 0$ is an invariant algebraic surface for each $i = 1, 2, ..., n$ with cofactor k_{λ_i}. Furthermore, $K_V = \sum_{i=1}^{n} k_{\lambda_i}$. Thus, $f_i^{\lambda i} = 0$, is an invariant algebraic surface of (1.2) with cofactor $k_{\lambda_i},\ i = 1, 2, ..., n$. Then,

$$k_{\lambda_i} f_i^{\lambda_i} = \mathcal{X}(f_i^{\lambda_i}) = \lambda_i f_i^{\lambda_i - 1} \mathcal{X}(f_i).$$

The above equation is equivalent to

$$\mathcal{X}(f_i) = \frac{k_{\lambda_i}}{\lambda_i} f_i\ . \tag{3.2}$$

We denote $\dfrac{k_{\lambda_i}}{\lambda_i} = k_i$, therefore $\mathcal{X}(f_i) = k_i f_i\ i = 1, 2, ..., n$. That is, $f_i = 0$ is an invariant algebraic surface with cofactor k_i such that $k_{\lambda_i} = \lambda_i k_i,\ i = 1, 2, ..., n$. □

Remark 2. According to the definition of inverse Jacobi multiplier, from Proposition 2 if the cofactor $K_V = div(\mathcal{X})$, then $V = 0$ is an inverse Jacobi multiplier of (1.2).

3.2 Centre Conditions of 3DLVS

The aim of this section is to find sufficient conditions for the critical point at the origin to be a centre for the three dimensional Lotka-Volterra system (1.2) by using an inverse Jacobi multiplier. The explicit inverse Jacobi multiplier formula for system (1.2) is given by the following theorem.

Theorem 2. For system (1.2), if there exists an invariant algebraic surface L which is passing through the origin with cofactor given by $\lambda + \sum_{i=1}^{3} \beta_i x_i,\ \beta_i \in \mathbb{R}$,

$i = 1, 2, 3$, and $\lambda = \sum_{i=1}^{3} a_{i,i}$, then there exists $\alpha_i \in \mathbb{R},\ i = 1, 2, 3$ such that the function

$$V(x_1, x_2, x_3) = (x_1 + 1)^{\alpha_1}(x_2 + 1)^{\alpha_2}(x_3 + 1)^{\alpha_3} L, \tag{3.3}$$

is an inverse Jacobi multiplier of the Lotka-Volterra system (1.2). In addition, if the critical point at the origin is a Hopf point and $\nabla L(0) \neq 0$, then the critical point at the origin is a centre of (1.2) .

Proof. Since $(x_1+1)^{\alpha_1}$, $(x_2+1)^{\alpha_2}$ and $(x_3+1)^{\alpha_3}$ are always invariant algebraic surface of system (1.2) with cofactors, $K_i = \alpha_i(\sum_{j=1}^{3} a_{i,j}x_j),\ i = 1, 2, 3$ respectively, we can apply (2.10) to system (1.2) to obtain:

$$\begin{aligned}
\sum_{i=1}^{3} a_{i,1}\alpha_i &= \sum_{i=1}^{3} a_{i,1} + a_{1,1} - \beta_1, \\
\sum_{i=1}^{3} a_{i,2}\alpha_i &= \sum_{i=1}^{3} a_{i,2} + a_{2,2} - \beta_2, \\
\sum_{i=1}^{3} a_{i,3}\alpha_i &= \sum_{i=1}^{3} a_{i,3} + a_{3,3} - \beta_3.
\end{aligned} \tag{3.4}$$

From equation (2.3), it is clear that the determinant of the matrix of coefficients of system (3.4) is non-zero, then system (3.4) has a unique solution. As a result, the function V which is defined in equation (3.3) is an inverse Jacobi multiplier of the Lotka-Volterra system (1.2). Since

$$\begin{aligned}
\nabla V(0) &= (\frac{\partial}{x_1} L + \alpha_1 L,\ \frac{\partial}{x_2} L + \alpha_2 L,\ \frac{\partial}{x_3} L + \alpha_3 L)|_{(x_1,x_2,x_3)=(0,0,0)} \\
&= \nabla L(0) \neq 0,
\end{aligned}$$

then Theorem 1 guarantees that the critical point at the origin is a centre. □

We give two examples of three dimensional Lotka-Volterra systems (1.2) where we can apply the theorem above.

Proposition 3. The system (1.2) has an invariant algebraic surface of conic type if the following conditions are satisfied,

$$a_{1,1} + a_{2,3} = 0,\ a_{1,2} = a_{3,3} = 0,\ a_{1,3} + a_{2,3} = 0,\ a_{2,1} - 2a_{2,3} = 0,\ a_{2,2} + a_{2,3} = 0,$$
$$a_{3,1} - a_{2,3} = 0,\ a_{3,2} - a_{2,3} = 0,\ \text{and } a_{2,3} \neq 0. \tag{3.5}$$

Under these conditions the critical point at the origin is a centre on the centre manifold.

Proof. Suppose that the Lotka-Volterra system (1.2) satisfies the above conditions. Using equation (3.3) where $\alpha_i = 0, i = 1, 2, 3$ and $L = x_1x_2 + a_1x_1 + a_2x_2 + a_3x_3;\ a_i \in \mathbb{R},\ i = 1, 2, 3$ and not all zero. It is easy to show that, under the conditions (3.5), $L = 0$ is an invariant algebraic surface and the system has the inverse Jacobi multiplier

$$V(x_1, x_2, x_3) = x_1x_2 + x_1 - x_2 + x_3,$$

with its cofactor $K = a_{2,3}(-2 + x_1 - x_2)$. It is not difficult to check that under conditions (3.5) the critical point at the origin is a Hopf point and $\nabla V(0) \neq 0$, and hence the origin is a centre (see Figure 3.1). □

Proposition 4. The system (1.2) has an invariant plane that is passing through the origin if the following conditions hold,

$$a_{1,1} + a_{3,3} = 0,\ a_{1,3} + \frac{a_{3,3}((2-k)a_{3,3} + a_{3,1})}{a_{3,1}(1-k)} = 0,\ a_{2,1} = a_{2,3} = a_{3,2} = 0,$$

provided that $a_{2,2} \neq 0,\ k \in \mathbb{R}\backslash\{1\}$ and $\frac{a_{3,3}(a_{3,1}+a_{3,3})}{k-1} < 0$. Under these conditions the critical point at the origin is a centre on the centre manifold of (1.2).

Proof. Assume the above conditions hold. From equation (3.3) where $L = a_1x_1 + a_2x_2 + a_3x_3;\ a_i \in \mathbb{R},\ i = 1, 2, 3$ and not all zero, the following invariant algebraic surface can be found

$$V(x_1, x_2, x_3) = a_2x_2(x_1 + 1)^k(x_2 + 1)^{\frac{(1-k)a_{1,2}+a_{2,2}}{a_{2,2}}}(x_3 + 1)^{\frac{(k-2)a_{3,3}+a_{3,1}}{a_{3,1}}},$$

with its cofactor

$$K = a_{2,2} + (a_{3,1} - 2a_{3,3})x_1 + (a_{1,2} + 2a_{2,2})x_2 + (2a_{3,3} + \frac{a_{3,3}((2-k)a_{3,3} + a_{3,1})}{a_{3,1}(k-1)})x_3.$$

Since $K = div(\mathcal{X})$, then the invariant algebraic surface V is an inverse Jacobi multiplier for system (1.2). Moreover, $\nabla V(0) \neq 0$, then Theorem 1 allows us to decide the Lotka-Volterra system (1.2) admits a centre at the origin on a local centre manifold (see Figure 3.2). □

Remark 3. From equation (3.3), we can obtain more than the above two necessary conditions for the origin to be a centre for system (1.2). However, only two are presented here as an example, the others give the same number of limit cycles. The number of bifurcating limit cycles are illustrated in the next chapter.

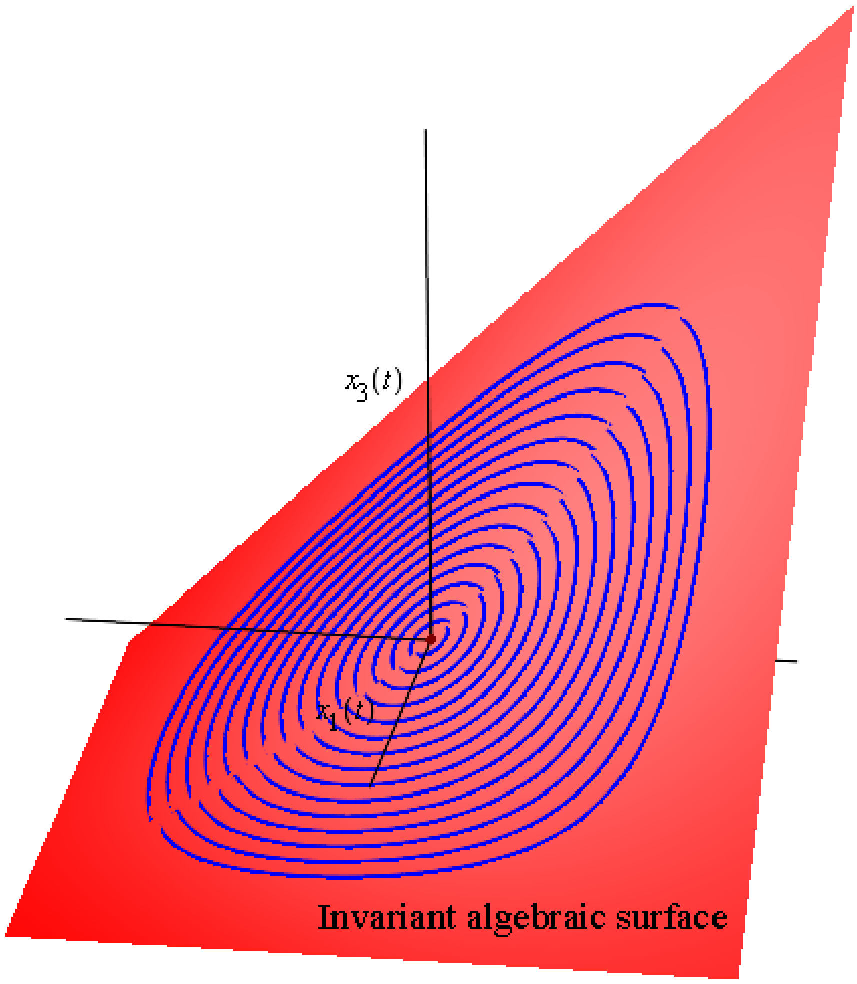

Figure 3.1: The zero set of the inverse Jacobi multiplier (3.3) where L is an invariant algebraic surface of conic type. The parameters satisfy the conditions of Proposition 3 and $a_{2,3} = 1$.

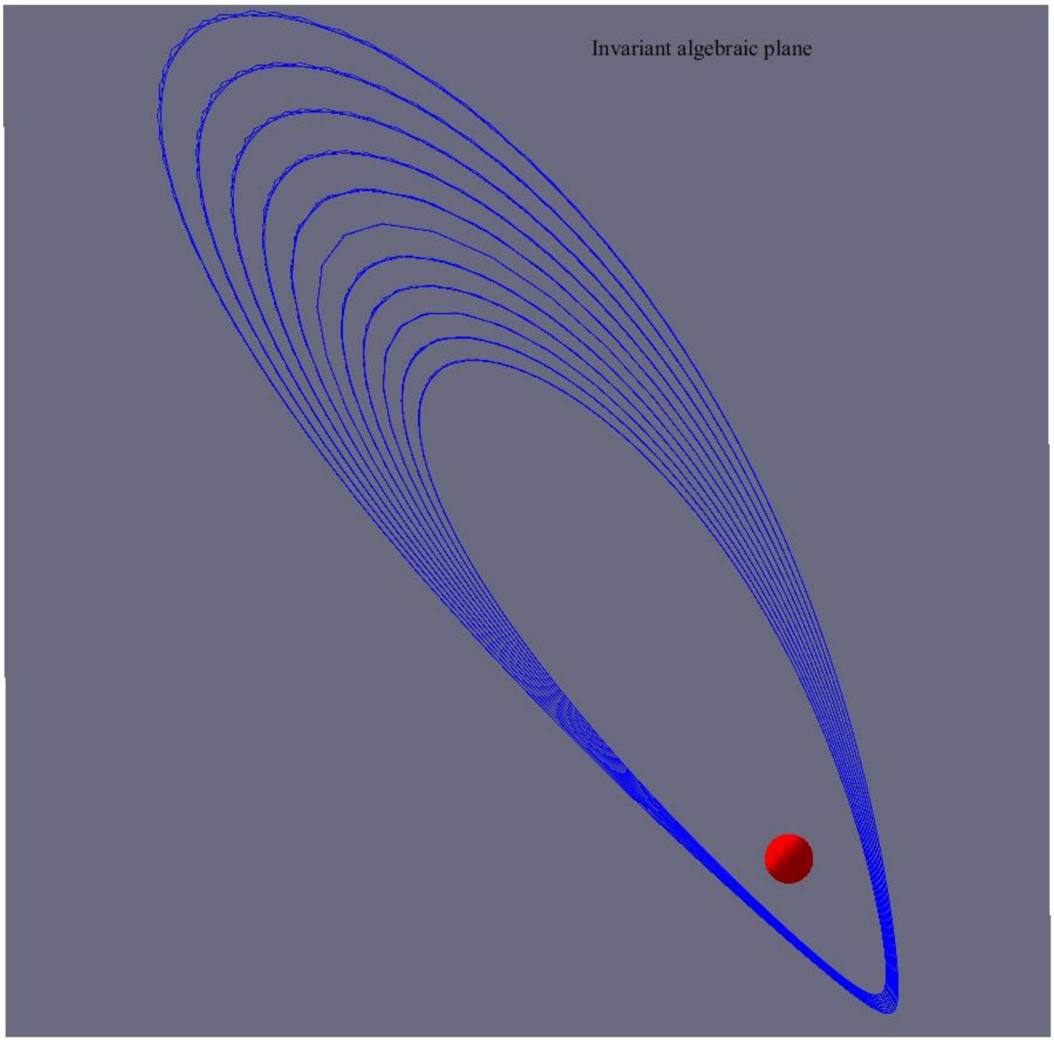

Figure 3.2: The zero set of the inverse Jacobi multiplier (3.3) where L is of type plane, the parameters satisfy the conditions of Proposition 4 with $a_{1,2} = 1,\ a_{2,2} = 1,\ a_{3,1} = -\dfrac{2}{\sqrt{3}},\ a_{3,3} = \sqrt{3},\ a_2 = 1$ and $k = 0$.

Chapter 4

Centre Bifurcations

This chapter investigates the cyclicity of the centres of the three dimensional Lotka-Volterra system by using centre bifurcations. We prove that two and four limit cycles can be bifurcated from the centre on a planar and a conic invariant surface respectively. Our technique is to use the linear and quadratic terms of the Liapunov quantities. Moreover, we apply the same technique to a quadratic 3DS having a plane of singularities and show that eight limit cycles can bifurcate from the centre.

4.1 The Basic Technique for Estimating Cyclicity from Centre

Bifurcation of limit cycles from critical points is the current research area in the bifurcation theory. A limit cycle is obtained by perturbing a focus or centre. One common approach is the centre bifurcation which is used to estimate the cyclicity and also to study the bifurcation of limit cycles from the centre (see (Bautin, 1952; Yu and Han, 2004)).

Christopher (2005) investigated a technique to examine the cyclicity bifurcating from centre in two dimensional systems by linearizing the Liapunov quantities. We generalized the technique to three dimensional systems to estimate the cyclicity of the centre. The idea of the technique used here to estimate the cyclicity in three dimensional differential system can be illustrated by the following steps. Firstly, a point on a centre variety will be chosen, after that, the Liapunov quantities about this point will be linearized. If the codimension of the point that was chosen on a centre variety is r provided that the first r linear terms of Liapunov quantities are linearly independent, then $r-1$ is the cyclicity. That is, we can bifurcate $r-1$ limit cycles by a small perturbation.

We recall the construction of the Liapunov quantities. We seek a function of the form

$$F(x_1, x_2, x_3) = x_1^2 + x_2^2 + \sum_{k=3}^{\infty} F_k(x_1, x_2, x_3),$$

where $F_k = \sum_{i=0}^{k} \sum_{j=0}^{i} C_{k-i,i-j,j} x_1^{k-i} x_2^{i-j} x_3^{j}$ for system (2.4) and the coefficients of F_k satisfy

$$\mathcal{X}(F) = L_1(x_1^2 + x_2^2) + L_2(x_1^2 + x_2^2)^2 + L_3(x_1^2 + x_2^2)^3 + ..., \tag{4.1}$$

where $L_i,\ i = 1, 2, ...$ are polynomials in the parameters of the system and the L_i is called the i^{th} Liapunov constant (focal value).

Explaining the technique in more detail, it is assumed that the centre critical point of (2.4) corresponds to $0 \in \mathbf{K}$, by using a perturbation technique in parameters.

This can be written:

$$\begin{aligned}
\mathcal{X} &= \mathcal{X}_o + \mathcal{X}_1 + ..., \\
F &= F_o + F_1 + ..., \qquad\qquad\qquad\qquad (4.2) \\
L_i &= L_{i0} + L_{i1} + ..., \qquad i = 1, 2, ...,
\end{aligned}$$

where $\mathcal{X}_o,\ F_o$ and L_{0i} are calculated at the unperturbed parameters and $\mathcal{X}_1,\ F_1$ and L_{1i} are obtained at a perturbed parameters of first order (they contain the terms of degree one in Λ), and so forth. The Liapunov function F_i and the Liapunov quantity L_i have degree i in parameters. Putting equation (4.2) into equation (4.1) and we obtain:

$$\mathcal{X}_o F_o = 0, \quad \mathcal{X}_0 F_1 + \mathcal{X}_1 F_o = L_{11}(x_1^2 + x_2^2) + L_{21}(x_1^2 + x_2^2)^2 + ... \ , \qquad (4.3)$$

and more general,

$$\mathcal{X}_o F_i + ... + \mathcal{X}_i F_o = L_{1i}(x_1^2 + x_2^2) + L_{2i}(x_1^2 + x_2^2)^2 + ... \qquad (4.4)$$

The linear terms of the Liapunov quantities L_k (modulo the $L_i,\ i < k$) would be obtained by solving the pair of equations (4.3) simultaneously by linear algebra. Equation (4.4) is used to generate the higher order terms of the Liapunov quantities.

4.2 Centre Bifurcation for the 3DLVS

Here, the technique which was shown in the previous section is applied to the 3DLVS. The system which satisfies the conditions of Proposition 3 and 4 are given individuality. As a result, we obtain the following theorems.

Theorem 3. If the parameters in the three-dimensional Lotka-Volterra system (1.2) satisfies the conditions that are mentioned in Proposition 3, then four limit cycles can bifurcate from the origin critical point.

Proof. Assume that the parameters in the three dimensional Lotka-Volterra system (1.2) satisfies the conditions of Proposition 3, then at the origin critical point, we obtain:

$$\begin{aligned} D &= -2a_{2,3}^3, \\ T &= -2a_{2,3}, \\ K &= -a_{2,3}^2. \end{aligned}$$

For $a_{2,3} \neq 0$, system (1.2) satisfies the Hopf bifurcation conditions which are mentioned in equation (2.3). More precisely, the linear part of system (1.2) at the origin has one non-zero real eigenvalue -2ω and a pair of pure imaginary eigenvalues $\pm i\omega$, where $\omega = a_{2,3}$. Using the linear transformation

$$X = PY, \ P = \begin{bmatrix} 1 & 1 & 1 \\ -1 & 1 & -3 \\ -2 & 0 & 1 \end{bmatrix}, \tag{4.5}$$

where $X = (x_1, x_2, x_3)$, $Y = (y_1, y_2, y_3)$, the linear part of system (1.2) at the origin, $A = \begin{bmatrix} -\omega & 0 & -\omega \\ 2\omega & -\omega & \omega \\ \omega & \omega & 0 \end{bmatrix}$, can be written in the real canonical form as

$$\begin{bmatrix} 0 & -\omega & 0 \\ \omega & 0 & 0 \\ 0 & 0 & -2\omega \end{bmatrix},$$

and the new system is given by

$$\dot{Y} = (P^{-1}AP)Y + P^{-1}\ diag(PY)APY, \tag{4.6}$$

where

$$P^{-1}AP = \begin{bmatrix} 0 & -\omega & 0 \\ \omega & 0 & 0 \\ 0 & 0 & -2\omega \end{bmatrix}$$

and $diag(PY)$ is the diagonal matrix of PY. It is easy to construct the Liapunov function F_o of equation (4.6) which satisfies $\mathcal{X}F_o = 0$. The same transformation in equation (4.5) is used for perturbed vector field part of system (1.2) which is obtained by putting $a_{i,j} = \overline{a}_{i,j} + b_{i,j},\ i,j = 1,2,3$, where $\overline{a}_{i,j}$ and $b_{i,j}$ are parameters before and after perturbation in the system, respectively. Using computer algebra package MAPLE, equation (4.3) give us the following linear independent terms of Liapunov quantities:

1. $L_1 = \frac{1}{5}(b_{2,1} - b_{3,1} + 2b_{2,2} + 3b_{3,2} + 3b_{1,2} + 4b_{1,1} - b_{1,3} + 4b_{3,3} + b_{2,3})$.
2. $L_2 = \frac{1}{50}(-28b_{1,1} + 4b_{1,2} + 7b_{1,3} - 12b_{2,1} - 4b_{2,2} + 3b_{2,3} + 12b_{3,1} - 16b_{3,2} - 23b_{3,3})$.
3. $L_3 = \frac{-1}{552500}(95712b_{3,3} + 90909b_{3,2} + 12197b_{3,1} + 51553b_{2,3} + 56356b_{2,2} - 12197b_{2,1} - 4803b_{1,3} + 129159b_{1,2} + 78712b_{1,1})$.
4. $L_4 = \frac{1}{26203196500000}(1553756234648b_{3,3} + 1322203912761b_{3,2} - 1530482987287b_{3,1} - 1046458652663b_{2,3} - 814906330776b_{2,2} + 1530482987287b_{2,1} - 231552321887b_{1,3} - 2115656380089b_{1,2} + 2852686900048b_{1,1})$.
5. $L_5 = \frac{0.00001}{675112268015688425}(9437762895902019945664b_{3,3} + 7976044124727350992153b_{3,2} + 11610358312567878l609b_{3,1} +$

$36654402974042322355501b_{2,3}+51271590685789011189012b_{2,2}-11610358312567878 1609b_{2,1}-$

$14617187711746689535111b_{1,3}+99229403357615879718 83b_{1,2}+78599405416016722105 44b_{1,1})$.

The origin of system (1.2) is a weak focus of order 4 if and only if

1. $b_{3,1} = b_{2,1} + 4b_{1,1} + 2b_{2,2} + 3b_{3,2} + 3b_{1,2} - b_{1,3} + 4b_{3,3} + b_{2,3}$.

2. $b_{1,1} = -\frac{3}{4}b_{2,3} - 2b_{1,2} + \frac{1}{4}b_{1,3} - b_{2,2} - b_{3,2} - \frac{5}{4}b_{3,3}$.

3. $b_{1,3} = \frac{15}{7}b_{2,3} + 6b_{1,2} + \frac{22}{7}b_{2,2} + b_{3,3}$.

4. $b_{2,2} = -b_{2,3} - 3b_{1,2}$.

Since

$$J = \begin{vmatrix} \frac{\partial L_1}{\partial b_{3,1}} & \frac{\partial L_1}{\partial b_{1,1}} & \frac{\partial L_1}{\partial b_{1,3}} & \frac{\partial L_1}{\partial b_{2,2}} \\ \frac{\partial L_2}{\partial b_{3,1}} & \frac{\partial L_2}{\partial b_{1,1}} & \frac{\partial L_2}{\partial b_{1,3}} & \frac{\partial L_2}{\partial b_{2,2}} \\ \frac{\partial L_3}{\partial b_{3,1}} & \frac{\partial L_3}{\partial b_{1,1}} & \frac{\partial L_3}{\partial b_{1,3}} & \frac{\partial L_3}{\partial b_{2,2}} \\ \frac{\partial L_4}{\partial b_{3,1}} & \frac{\partial L_4}{\partial b_{1,1}} & \frac{\partial L_4}{\partial b_{1,3}} & \frac{\partial L_4}{\partial b_{2,2}} \end{vmatrix} = \frac{63}{845000} \neq 0,$$

then by suitable perturbation of the coefficients of Liapunov quantities, four limit cycles can be bifurcated from the origin of system (1.2) in the neighbourhood of the origin. $\square$

Theorem 4. Two limit cycles can be bifurcated from the origin, when the three dimensional Lotka-Volterra system (1.2) satisfies the conditions in Proposition 4 with the additional conditions $a_{1,2} \neq 0, a_{2,2} - \frac{\omega^2}{a_{3,3}} \neq 0$ and $a_{3,3} - \frac{(\omega^2 \pm \sqrt{\omega^4 - a_{2,2}^4})\omega^2}{a_{2,2}^3} \neq 0$, where $k = 0$.

Proof. When the system (1.2) satisfies the conditions in Proposition 4, its characteristic polynomial is given by

$$\lambda^3 - a_{2,2}\lambda^2 - \frac{a_{3,3}(a_{3,1} + a_{3,3})}{k-1}\lambda + \frac{a_{2,2}a_{3,3}(a_{3,1} + a_{3,3})}{k-1} = 0,$$

its coefficients satisfy equation (2.3) and the eigenvalues are $\pm i\omega$ and $a_{2,2}$, where $a_{3,1} = -\frac{a_{3,3}^2+\omega^2(k-1)}{a_{3,3}}$. The linear transformation (4.5) bring system (1.2) to system (4.6) where

$$P=\begin{bmatrix} \frac{a_{3,3}}{\omega} & 1 & \frac{a_{1,2}(a_{2,2}-a_{3,3})}{\omega^2+a_{2,2}^2} \\ 0 & 0 & 1 \\ \frac{a_{3,3}^2+\omega^2(k-1)}{\omega a_{3,3}} & 0 & \frac{-a_{1,2}(a_{3,3}^2+\omega^2(k-1))}{a_{3,3}(\omega^2+a_{2,2}^2)} \end{bmatrix},\ A=\begin{bmatrix} -a_{3,3} & a_{1,2} & \frac{a_{3,3}(a_{3,3}^2+\omega^2)}{a_{3,3}^2+\omega^2(k-1)} \\ 0 & a_{2,2} & 0 \\ \frac{-(a_{3,3}^2+\omega^2(k-1))}{a_{3,3}} & 0 & a_{3,3} \end{bmatrix}$$

$$\text{and } P^{-1}AP = \begin{bmatrix} 0 & -\omega & 0 \\ \omega & 0 & 0 \\ 0 & 0 & a_{2,2} \end{bmatrix}.$$

The same transformation is also used for perturbed vector field. As we referred in the previous theorem and after applying (4.3) the following linear independent terms of Liapunov quantities are obtained, where $k = 0$:

1. $L_1 = \frac{1}{a_{3,3}(a_{2,2}^2+\omega^2)}(a_{1,2}b_{2,3}a_{3,3}^2 + a_{1,2}b_{2,1}a_{3,3}^2 + a_{3,3}b_{3,3}\omega^2 + a_{3,3}a_{2,2}^2b_{1,1} + a_{2,2}^2a_{3,3}b_{3,3} + \omega^2a_{3,3}b_{1,1} - a_{3,3}a_{2,2}a_{1,2}b_{2,1} - \omega^2a_{1,2}b_{2,3})$.

2. $L_2 = \frac{-1}{4\omega^2a_{3,3}^3(a_{2,2}^6+6\omega^2a_{2,2}^4+9\omega^4a_{2,2}^2+4\omega^6)}(b_{3,3}a_{3,3}^5a_{2,2}^6 + b_{1,1}a_{3,3}^5a_{2,2}^6 + 4\omega^8b_{3,3}a_{3,3}^3 + 4\omega^6b_{3,3}a_{3,3}^5 + 4\omega^6b_{1,1}a_{3,3}^5 + 4\omega^8b_{1,1}a_{3,3}^3 + 2a_{3,3}^4a_{1,2}a_{2,2}^4b_{2,3}\omega^2 + 5a_{3,3}^6a_{1,2}a_{2,2}^2b_{2,3}\omega^2 - 3\omega^6a_{1,2}a_{2,2}^2b_{2,3}a_{3,3}^2 - 2\omega^4a_{1,2}a_{2,2}^4b_{2,3}a_{3,3}^2 - 4\omega^2a_{3,3}^5a_{1,2}a_{2,2}^3b_{2,1} - \omega^6a_{1,2}b_{2,1}a_{3,3}^3a_{2,2} - \omega^6a_{1,2}a_{2,2}^2b_{2,1}a_{3,3}^2 + \omega^8a_{1,2}b_{2,1}a_{3,3}a_{2,2} - 4\omega^4a_{1,2}a_{2,2}^3b_{2,1}a_{3,3}^3 - \omega^2b_{2,1}a_{3,3}^3a_{2,2}^5a_{1,2} - 2\omega^4a_{3,3}^5a_{1,2}b_{2,1}a_{2,2} + 4\omega^2b_{2,3}a_{3,3}^5a_{2,2}^3a_{1,2} + 4\omega^4b_{2,3}a_{3,3}^5a_{2,2}a_{1,2} - \omega^4a_{3,3}^4a_{1,2}a_{2,2}^2b_{2,3} + 4\omega^4a_{3,3}^4a_{1,2}a_{2,2}^2b_{2,1} - 6\omega^4a_{3,3}^3a_{1,2}a_{2,2}^3b_{2,3} + 2\omega^6a_{1,2}a_{2,2}^3b_{2,3}a_{3,3} - 6\omega^6a_{3,3}^3a_{1,2}b_{2,3}a_{2,2} + 2\omega^8a_{1,2}b_{2,3}a_{3,3}a_{2,2} + 5a_{3,3}^6a_{1,2}a_{2,2}^2b_{2,1}\omega^2 + 2\omega^6b_{2,1}a_{3,3}^4a_{1,2} - \omega^8a_{1,2}a_{2,2}^2b_{2,3} - 2\omega^8a_{1,2}b_{2,1}a_{3,3}^2 + 9\omega^4b_{3,3}a_{3,3}^5a_{2,2}^2 + 6\omega^4b_{3,3}a_{3,3}^3a_{2,2}^4 + 9\omega^4b_{1,1}a_{3,3}^5a_{2,2}^2 + 6\omega^4b_{1,1}a_{3,3}^3a_{2,2}^4 + 9\omega^6a_{3,3}^3a_{2,2}^2b_{1,1} + 9\omega^6a_{3,3}^3a_{2,2}^2b_{3,3} + 6\omega^2b_{3,3}a_{3,3}^5a_{2,2}^4 + \omega^2b_{3,3}a_{3,3}^3a_{2,2}^6 + 6\omega^2b_{1,1}a_{3,3}^5a_{2,2}^4 + \omega^2b_{1,1}a_{3,3}^3a_{2,2}^6 + 4\omega^4a_{3,3}^6a_{1,2}b_{2,1} - b_{2,1}a_{3,3}^5a_{2,2}^5a_{1,2} - 4\omega^6a_{1,2}b_{2,3}a_{3,3}^4 + 4a_{3,3}^6a_{1,2}b_{2,3}\omega^4)$.

3. $$L_3 = \frac{-1}{288\omega^4 a_{3,3}^5 (9\omega^2 + a_{2,2}^2)(4\omega^2 + a_{2,2}^2)^2(\omega^2 + a_{2,2}^2)^3}(252\omega^{18}a_{1,2}a_{2,2}^2b_{2,3} - 252\omega^{18}a_{1,2}a_{2,2}a_{3,3}b_{2,1} -$$
$$504\omega^{18}a_{1,2}a_{2,2}a_{3,3}b_{2,3} + 504\omega^{18}a_{1,2}a_{3,3}^2b_{2,1} - 288\omega^{18}a_{1,2}a_{3,3}^2b_{2,3} - 1008\omega^{18}a_{3,3}^3b_{1,1} -$$
$$1008\omega^{18}a_{3,3}^3b_{3,3} + 573\omega^{16}a_{1,2}a_{2,2}^4b_{2,3} - 573\omega^{16}a_{1,2}a_{2,2}^3a_{3,3}b_{2,1} - 1650\omega^{16}a_{1,2}a_{2,2}^3a_{3,3}b_{2,3} +$$
$$1398\omega^{16}a_{1,2}a_{2,2}^2a_{3,3}^2b_{2,1} - 2612\omega^{16}a_{1,2}a_{2,2}^2a_{3,3}^2b_{2,3} + 2340\omega^{16}a_{1,2}a_{2,2}a_{3,3}^3b_{2,1} +$$
$$7032\omega^{16}a_{1,2}a_{2,2}a_{3,3}^3b_{2,3} - 4680\omega^{16}a_{1,2}a_{3,3}^4b_{2,1} + 2736\omega^{16}a_{1,2}a_{3,3}^4b_{2,3} - 3640\omega^{16}a_{2,2}^2a_{3,3}^3b_{1,1} -$$
$$3640\omega^{16}a_{2,2}^2a_{3,3}^3b_{3,3} + 7056\omega^{16}a_{3,3}^5b_{1,1} + 7056\omega^{16}a_{3,3}^5b_{3,3} + 186\omega^{14}a_{1,2}a_{2,2}^6b_{2,3} -$$
$$186\omega^{14}a_{1,2}a_{2,2}^5a_{3,3}b_{2,1} - 1518\omega^{14}a_{1,2}a_{2,2}^5a_{3,3}b_{2,3} + 945\omega^{14}a_{1,2}a_{2,2}^4a_{3,3}^2b_{2,1} -$$
$$1445\omega^{14}a_{1,2}a_{2,2}^4a_{3,3}^2b_{2,3} + 3043\omega^{14}a_{1,2}a_{2,2}^3a_{3,3}^3b_{2,1} + 16530\omega^{14}a_{1,2}a_{2,2}^3a_{3,3}^3b_{2,3} -$$
$$8086\omega^{14}a_{1,2}a_{2,2}^2a_{3,3}^4b_{2,1} + 316\omega^{14}a_{1,2}a_{2,2}^2a_{3,3}^4b_{2,3} - 4620\omega^{14}a_{1,2}a_{2,2}a_{3,3}^5b_{2,1} -$$
$$26136\omega^{14}a_{1,2}a_{2,2}a_{3,3}^5b_{2,3} + 10872\omega^{14}a_{1,2}a_{3,3}^6b_{2,1} - 12240\omega^{14}a_{1,2}a_{3,3}^6b_{2,3} - 4991\omega^{14}a_{2,2}^4a_{3,3}^3b_{1,1} -$$
$$4991\omega^{14}a_{2,2}^4a_{3,3}^3b_{3,3} + 25480\omega^{14}a_{2,2}^2a_{3,3}^5b_{1,1} + 25480\omega^{14}a_{2,2}^2a_{3,3}^5b_{3,3} - 7056\omega^{14}a_{3,3}^7b_{1,1} -$$
$$7056\omega^{14}a_{3,3}^7b_{3,3} + 9\omega^{12}a_{1,2}a_{2,2}^8b_{2,3} - 9\omega^{12}a_{1,2}a_{2,2}^7a_{3,3}b_{2,1} - 390\omega^{12}a_{1,2}a_{2,2}^7a_{3,3}b_{2,3} +$$
$$204\omega^{12}a_{1,2}a_{2,2}^6a_{3,3}^2b_{2,1} + 750\omega^{12}a_{1,2}a_{2,2}^6a_{3,3}^2b_{2,3} + 1864\omega^{12}a_{1,2}a_{2,2}^5a_{3,3}^3b_{2,1} +$$
$$11742\omega^{12}a_{1,2}a_{2,2}^5a_{3,3}^3b_{2,3} - 4816\omega^{12}a_{1,2}a_{2,2}^4a_{3,3}^4b_{2,1} - 9794\omega^{12}a_{1,2}a_{2,2}^4a_{3,3}^4b_{2,3} -$$
$$14713\omega^{12}a_{1,2}a_{2,2}^3a_{3,3}^5b_{2,1} - 58410\omega^{12}a_{1,2}a_{2,2}^3a_{3,3}^5b_{2,3} + 25786\omega^{12}a_{1,2}a_{2,2}^2a_{3,3}^6b_{2,1} -$$
$$5428\omega^{12}a_{1,2}a_{2,2}^2a_{3,3}^6b_{2,3} - 372\omega^{12}a_{1,2}a_{2,2}a_{3,3}^7b_{2,1} + 36744\omega^{12}a_{1,2}a_{2,2}a_{3,3}^7b_{2,3} +$$
$$936\omega^1 2a_{1,2}a_{3,3}^8b_{2,1} + 24912\omega^{12}a_{1,2}a_{3,3}^8b_{2,3} - 3220\omega^{12}a_{2,2}^6a_{3,3}^3b_{1,1} - 3220\omega^{12}a_{2,2}^6a_{3,3}^3b_{3,3} +$$
$$34937\omega^{12}a_{2,2}^4a_{3,3}^5b_{1,1} + 34937\omega^{12}a_{2,2}^4a_{3,3}^5b_{3,3} - 25480\omega^{12}a_{2,2}^2a_{3,3}^7b_{1,1} - 25480\omega^{12}a_{2,2}^2a_{3,3}^7b_{3,3} -$$
$$15120\omega^{12}a_{3,3}^9b_{1,1} - 15120\omega^{12}a_{3,3}^9b_{3,3} - 18\omega^{10}a_{1,2}a_{2,2}^9a_{3,3}b_{2,3} + 9\omega^{10}a_{1,2}a_{2,2}^8a_{3,3}^2b_{2,1} +$$
$$319\omega^{10}a_{1,2}a_{2,2}^8a_{3,3}^2b_{2,3} + 702\omega^{10}a_{1,2}a_{2,2}^7a_{3,3}^3b_{2,1} + 2310\omega^{10}a_{1,2}a_{2,2}^7a_{3,3}^3b_{2,3} -$$
$$828\omega^{10}a_{1,2}a_{2,2}^6a_{3,3}^4b_{2,1} - 9816\omega^{10}a_{1,2}a_{2,2}^6a_{3,3}^4b_{2,3} - 13858\omega^{10}a_{1,2}a_{2,2}^5a_{3,3}^5b_{2,1} -$$
$$39510\omega^{10}a_{1,2}a_{2,2}^5a_{3,3}^5b_{2,3} + 17680\omega^{10}a_{1,2}a_{2,2}^4a_{3,3}^6b_{2,1} + 25466\omega^{10}a_{1,2}a_{2,2}^4a_{3,3}^6b_{2,3} +$$
$$5521\omega^{10}a_{1,2}a_{2,2}^3a_{3,3}^7b_{2,1} + 84270\omega^{10}a_{1,2}a_{2,2}^3a_{3,3}^7b_{2,3} - 3922\omega^{10}a_{1,2}a_{2,2}^2a_{3,3}^8b_{2,1} +$$
$$46664\omega^{10}a_{1,2}a_{2,2}^2a_{3,3}^8b_{2,3} + 6840\omega^{10}a_{1,2}a_{2,2}a_{3,3}^9b_{2,1} - 17136\omega^{10}a_{1,2}a_{2,2}a_{3,3}^9b_{2,3} -$$
$$15120\omega^{10}a_{1,2}a_{3,3}^1 0b_{2,1} - 15120\omega^{10}a_{1,2}a_{3,3}^{10}b_{2,3} - 994\omega^{10}a_{2,2}^8a_{3,3}^3b_{1,1} - 994\omega^{10}a_{2,2}^8a_{3,3}^3b_{3,3} +$$
$$22540\omega^{10}a_{2,2}^6a_{3,3}^5b_{1,1} + 22540\omega^{10}a_{2,2}^6a_{3,3}^5b_{3,3} - 34937\omega^{10}a_{2,2}^4a_{3,3}^7b_{1,1} - 34937\omega^{10}a_{2,2}^4a_{3,3}^7b_{3,3} -$$

$54600\omega^{10}a_{2,2}^{2}a_{3,3}^{9}b_{1,1}-54600\omega^{10}a_{2,2}^{2}a_{3,3}^{9}b_{3,3}+16\omega^{8}a_{1,2}a_{2,2}^{10}a_{3,3}^{2}b_{2,3}+124\omega^{8}a_{1,2}a_{2,2}^{9}a_{3,3}^{3}b_{2,1}+$
$66\omega^{8}a_{1,2}a_{2,2}^{9}a_{3,3}^{3}b_{2,3}+8\omega^{8}a_{1,2}a_{2,2}^{8}a_{3,3}^{4}b_{2,1}-2258\omega^{8}a_{1,2}a_{2,2}^{8}a_{3,3}^{4}b_{2,3}-5490\omega^{8}a_{1,2}a_{2,2}^{7}a_{3,3}^{5}b_{2,1}-$
$7470\omega^{8}a_{1,2}a_{2,2}^{7}a_{3,3}^{5}b_{2,3}+4038\omega^{8}a_{1,2}a_{2,2}^{6}a_{3,3}^{6}b_{2,1}+24120\omega^{8}a_{1,2}a_{2,2}^{6}a_{3,3}^{6}b_{2,3}+$
$10756\omega^{8}a_{1,2}a_{2,2}^{5}a_{3,3}^{7}b_{2,1}+59106\omega^{8}a_{1,2}a_{2,2}^{5}a_{3,3}^{7}b_{2,3}-7204\omega^{8}a_{1,2}a_{2,2}^{4}a_{3,3}^{8}b_{2,1}+$
$15845\omega^{8}a_{1,2}a_{2,2}^{4}a_{3,3}^{8}b_{2,3}+23850\omega^{8}a_{1,2}a_{2,2}^{3}a_{3,3}^{9}b_{2,1}-40740\omega^{8}a_{1,2}a_{2,2}^{3}a_{3,3}^{9}b_{2,3}-$
$39192\omega^{8}a_{1,2}a_{2,2}^{2}a_{3,3}^{10}b_{2,1}-39192\omega^{8}a_{1,2}a_{2,2}^{2}a_{3,3}^{10}b_{2,3}-140\omega^{8}a_{2,2}^{10}a_{3,3}^{3}b_{1,1}-140\omega^{8}a_{2,2}^{10}a_{3,3}^{3}b_{3,3}+$
$6958\omega^{8}a_{2,2}^{8}a_{3,3}^{5}b_{1,1}+6958\omega^{8}a_{2,2}^{8}a_{3,3}^{5}b_{3,3}-22540\omega^{8}a_{2,2}^{6}a_{3,3}^{7}b_{1,1}-22540\omega^{8}a_{2,2}^{6}a_{3,3}^{7}b_{3,3}-$
$74865\omega^{8}a_{2,2}^{4}a_{3,3}^{9}b_{1,1}-74865\omega^{8}a_{2,2}^{4}a_{3,3}^{9}b_{3,3}+7\omega^{6}a_{1,2}a_{2,2}^{11}a_{3,3}^{3}b_{2,1}+2\omega^{6}a_{2,1}a_{2,2}^{10}a_{3,3}^{4}b_{2,1}-$
$104\omega^{6}a_{1,2}a_{2,2}^{10}a_{3,3}^{4}b_{2,3}-910\omega^{6}a_{1,2}a_{2,2}^{9}a_{3,3}^{5}b_{2,1}-234\omega^{6}a_{1,2}a_{2,2}^{9}a_{3,3}^{5}b_{2,3}+436\omega^{6}a_{1,2}a_{2,2}^{8}a_{3,3}^{6}b_{2,1}+$
$5450\omega^{6}a_{1,2}a_{2,2}^{8}a_{3,3}^{6}b_{2,3}+5142\omega^{6}a_{1,2}a_{2,2}^{7}a_{3,3}^{7}b_{2,1}+12090\omega^{6}a_{1,2}a_{2,2}^{7}a_{3,3}^{7}b_{2,3}-$
$1656\omega^{6}a_{1,2}a_{2,2}^{6}a_{3,3}^{8}b_{2,1}-8514\omega^{6}a_{1,2}a_{2,2}^{6}a_{3,3}^{8}b_{2,3}+26664\omega^{6}a_{1,2}a_{2,2}^{5}a_{3,3}^{9}b_{2,1}-$
$29820\omega^{6}a_{1,2}a_{2,2}^{5}a_{3,3}^{9}b_{2,3}-30645\omega^{6}a_{1,2}a_{2,2}^{4}a_{3,3}^{10}b_{2,1}-30645\omega^{6}a_{1,2}a_{2,2}^{4}a_{3,3}^{10}b_{2,3}-7\omega^{6}a_{2,2}^{12}a_{3,3}^{3}b_{1,1}-$
$7\omega^{6}a_{2,2}^{12}a_{3,3}^{3}b_{3,3}+980\omega^{6}a_{2,2}^{10}a_{3,3}^{5}b_{1,1}+980\omega^{6}a_{2,2}^{10}a_{3,3}^{5}b_{3,3}-6958\omega^{6}a_{2,2}^{8}a_{3,3}^{7}b_{1,1}-$
$6958\omega^{6}a_{2,2}^{8}a_{3,3}^{7}b_{3,3}-48300\omega^{6}a_{2,2}^{6}a_{3,3}^{9}b_{1,1}-48300\omega^{6}a_{2,2}^{6}a_{3,3}^{9}b_{3,3}-49\omega^{4}a_{1,2}a_{2,2}^{11}a_{3,3}^{5}b_{2,1}+$
$28\omega^{4}a_{1,2}a_{2,2}^{10}a_{3,3}^{6}b_{2,1}+272\omega^{4}a_{1,2}a_{2,2}^{10}a_{3,3}^{6}b_{2,3}+904\omega^{4}a_{1,2}a_{2,2}^{9}a_{3,3}^{7}b_{2,1}+510\omega^{4}a_{1,2}a_{2,2}^{9}a_{3,3}^{7}b_{2,3}+$
$140\omega^{4}a_{1,2}a_{2,2}^{8}a_{3,3}^{8}b_{2,1}-3223\omega^{4}a_{1,2}a_{2,2}^{8}a_{3,3}^{8}b_{2,3}+11343\omega^{4}a_{1,2}a_{2,2}^{7}a_{3,3}^{9}b_{2,1}-$
$6540\omega^{4}a_{1,2}a_{2,2}^{7}a_{3,3}^{9}b_{2,3}-6726\omega^{4}a_{1,2}a_{2,2}^{6}a_{3,3}^{10}b_{2,1}-6726\omega^{4}a_{1,2}a_{2,2}^{6}a_{3,3}^{10}b_{2,3}+49\omega^{4}a_{2,2}^{12}a_{3,3}^{5}b_{1,1}+$
$49\omega^{4}a_{2,2}^{12}a_{3,3}^{5}b_{3,3}-980\omega^{4}a_{2,2}^{10}a_{3,3}^{7}b_{1,1}-980\omega^{4}a_{2,2}^{10}a_{3,3}^{7}b_{3,3}-14910\omega^{4}a_{2,2}^{8}a_{3,3}^{9}b_{1,1}-$
$14910\omega^{4}a_{2,2}^{8}a_{3,3}^{9}b_{3,3}+49\omega^{2}a_{1,2}a_{2,2}^{11}a_{3,3}^{7}b_{2,1}+26\omega^{2}a_{1,2}a_{2,2}^{10}a_{3,3}^{8}b_{2,1}-184\omega^{2}a_{1,2}a_{2,2}^{10}a_{3,3}^{8}b_{2,3}+$
$1938\omega^{2}a_{1,2}a_{2,2}^{9}a_{3,3}^{9}b_{2,1}-324\omega^{2}a_{1,2}a_{2,2}^{9}a_{3,3}^{9}b_{2,3}-297\omega^{2}a_{1,2}a_{2,2}^{8}a_{3,3}^{10}b_{2,1}-297\omega^{2}a_{1,2}a_{2,2}^{8}a_{3,3}^{10}b_{2,3}-$
$49\omega^{2}a_{2,2}^{12}a_{3,3}^{7}b_{1,1}-49\omega^{2}a_{2,2}^{12}a_{3,3}^{7}b_{3,3}-2100\omega^{2}a_{2,2}^{10}a_{3,3}^{9}b_{1,1}-2100\omega^{2}a_{2,2}^{10}a_{3,3}^{9}b_{3,3}+$
$105a_{1,2}a_{2,2}^{11}a_{3,3}^{9}b_{2,1}-105a_{2,2}^{12}a_{3,3}^{9}b_{1,1}-105a_{2,2}^{12}a_{3,3}^{9}b_{3,3})$.

The origin is a weak focus of order two for system (1.2) if and only if the following conditions are held

1. $b_{1,1}=\dfrac{-\omega^2b_{3,3}a_{3,3}-a_{2,2}^2b_{3,3}a_{3,3}+\omega^2a_{1,2}b_{2,3}-b_{2,3}a_{3,3}^2a_{1,2}-b_{2,1}a_{3,3}^2a_{1,2}+a_{1,2}b_{2,1}a_{3,3}a_{2,2}}{\left(\omega^2+a_{2,2}^2\right)a_{3,3}}$.

2. $b_{2,1} = \dfrac{b_{2,3}(\omega^2 - a_{3,3}^2)(\omega^4 a_{2,2}^2 - 2\omega^4 a_{2,2}a_{3,3} - 4\omega^4 a_{3,3}^2 - \omega^2 a_{2,2}^3 a_{3,3} - 3\omega^2 a_{2,2}^2 a_{3,3}^2 + a_{2,2}^3 a_{3,3}^3)}{a_{3,3}(\omega^2 + a_{3,3}^2)(\omega^4 a_{2,2} - 2\omega^4 a_{3,3} + a_{2,2}^3 a_{3,3}^2)}.$

Since the Jacobian determinant of the functions (L_1, L_2) with respect to $(b_{1,1}, b_{2,1})$ is given by

$$J = \begin{vmatrix} \frac{\partial L_1}{\partial b_{1,1}} & \frac{\partial L_1}{\partial b_{2,1}} \\ \frac{\partial L_2}{\partial b_{1,1}} & \frac{\partial L_2}{\partial b_{2,1}} \end{vmatrix} = \frac{-\left(\omega^2 + a_{3,3}^2\right)\left(-a_{2,2}a_{3,3} + \omega^2\right)\left(a_{2,2}^3 a_{3,3}^2 - 2\omega^4 a_{3,3} + \omega^4 a_{2,2}\right) a_{1,2}}{4a_{3,3}^2\left(4\omega^2 + a_{2,2}^2\right)\left(\omega^2 + a_{2,2}^2\right)^2 \omega^2} \neq 0,$$

then two limit cycles can be bifurcated from the origin of the three dimensional Lotka-Volterra system (1.2) in the neighbourhood of the origin. □

Remark 4. In addition to the first order terms in the expansion of the Liapunov quantities $L(i)$, the second order terms can also be calculated. However, in the two cases above, the new results were the same as obtained by first order perturbation.

4.3 Perturbing the 3DS Having a Plane of Singularities

In this section, we consider the three dimensional system

$$\begin{aligned} \dot{x_1} &= -x_2(1 - x_1 - x_2 - x_3), \\ \dot{x_2} &= x_1(1 - x_1 - x_2 - x_3), \\ \dot{x_3} &= x_3(1 - x_1 - x_2 - x_3). \end{aligned} \tag{4.7}$$

This system has the plane $x_1 + x_2 + x_3 = 1$ of critical points, in addition to the origin, which is a centre. We perturbed system (4.7) inside the family of polynomial differential systems of degree two in $\mathbb{R}^3$ starting with terms of degree two.

Here, we apply the technique that is presented in the previous section to study the limit cycles bifurcating from the periodic orbits at the invariant plane $x_3 = 0$. The following theorem is the main result in this section.

Theorem 5. We consider the family of systems

$$\begin{aligned}
\dot{x_1} &= -x_2(1 - x_1 - x_2 - x_3) + F_1(x_1, x_2, x_3), \\
\dot{x_2} &= x_1(1 - x_1 - x_2 - x_3) + F_2(x_1, x_2, x_3), \\
\dot{x_3} &= x_3(1 - x_1 - x_2 - x_3) + F_3(x_1, x_2, x_3),
\end{aligned} \tag{4.8}$$

where $F_i,\ i = 1, 2, 3$ are polynomials of degree two starting with terms of degree two. Then, up to second order, eight limit cycles can be bifurcated from the centre at the origin respectively.

Proof. Let

$$\begin{aligned}
F_1 &= \sum_{i=0}^{2}\sum_{j=0}^{i} a_{2-i,i-j,j}x_1^{2-i}x_2^{i-j}x_3^{j}, \\
F_2 &= \sum_{i=0}^{2}\sum_{j=0}^{i} b_{2-i,i-j,j}x_1^{2-i}x_2^{i-j}x_3^{j}, \\
F_3 &= \sum_{i=0}^{2}\sum_{j=0}^{i} c_{2-i,i-j,j}x_1^{2-i}x_2^{i-j}x_3^{j}.
\end{aligned}$$

where $a_{2-i,i-j,j}, b_{2-i,i-j,j}$ and $c_{2-i,i-j,j},\ i, j = 0, 1, 2$ are real parameters. Using the same method as the previous section, we calculate the following expressions for the linear and quadratic terms of the Liapunov quantities in the parameters.

1. $L_1 = 0.$

2. $L_2 = \frac{1}{4}(3a_{200} + a_{110} + b_{200} + 3b_{020} + a_{020} + b_{110}) + \frac{1}{20}(-2a_{011}c_{020} - a_{011}c_{110} + 2a_{011}c_{200} + 5a_{020}a_{110} + 10a_{020}b_{020} - 9a_{101}c_{020} - 2a_{101}c_{110} - 11a_{101}c_{200} + 5a_{110}a_{200} -$

$10a_{200}b_{200} - 11b_{011}c_{020} + 2b_{011}c_{110} - 9b_{011}c_{200} - 5b_{020}b_{110} - 2b_{101}c_{020} - b_{101}c_{110} + 2b_{101}c_{200} - 5b_{110}b_{200})$.

3. $L_3 = \frac{1}{4}(a_{200} + a_{110} + b_{200} + b_{020} + a_{020} + b_{110}) + \frac{1}{480}(-300a_{011}c_{020} - 60a_{011}c_{110} - 108a_{011}c_{200} + 65a_{020}^2 - 470a_{020}a_{200} + 60a_{020}b_{020} - 110a_{020}b_{110} - 120a_{020}b_{200} - 180a_{020}c_{020} - 48a_{020}c_{110} - 60a_{020}c_{200} - 516a_{101}c_{020} - 300a_{101}c_{110} - 420a_{101}c_{200} + 55a_{110}^2 - 180a_{110}a_{200} - 10a_{110}b_{020} - 120a_{110}b_{110} - 130a_{110}b_{200} - 144a_{110}c_{020} - 36a_{110}c_{110} + 24a_{110}c_{200} - 555a_{200}^2 - 360a_{200}b_{020} - 470a_{200}b_{110} - 540a_{200}b_{200} - 348a_{200}c_{020} - 216a_{200}c_{110} - 372a_{200}c_{200} - 420b_{011}c_{020} - 108b_{011}c_{110} - 84b_{011}c_{200} + 195b_{020}^2 - 300b_{020}b_{110} - 10b_{020}b_{200} - 360b_{020}c_{020} + 84b_{020}c_{110} - 300b_{101}c_{020} - 60b_{101}c_{110} - 108b_{101}c_{200} - 175b_{110}^2 - 240b_{110}b_{200} - 180b_{110}c_{020} - 48b_{110}c_{110} - 60b_{110}c_{200} - 185b_{200}2 - 144b_{200}c_{200} - 36b_{200}c_{110} + 24b_{200}c_{200})$.

4. $L_4 = \dfrac{1}{16}(5a_{020} + 5a_{110} + 3a_{200} + 3b_{020} + 5b_{110} + 5b_{200}) + \dfrac{1}{32640}(-42096a_{011}c_{020} - 14400a_{011}c_{110} - 18288a_{011}c_{200} + 9605a_{020}^2 - 4080a_{020}a_{110} - 65450a_{020}a_{200} + 15300a_{020}b_{020} - 13430a_{020}b_{110} - 22440a_{020}b_{200} - 45684a_{020}c_{020} - 10452a_{020}c_{110} - 9804a_{020}c_{200} - 65568a_{101}c_{020} - 42096a_{101}c_{110} - 47040a_{101}c_{200} + 595a_{110}^2 - 54060a_{110}a_{200} - 3910a_{110}b_{020} - 22440a_{110}b_{110} - 31450a_{110}b_{200} - 42180a_{110}c_{020} - 15084a_{110}c_{110} - 11676a_{110}c_{200} - 95115a_{200}^2 - 38760a_{200}b_{020} - 65450a_{200}b_{110} - 84660a_{200}b_{200} - 62028a_{200}c_{020} - 48300a_{200}c_{110} - 65268a_{200}c_{200} - 47040b_{011}c_{020} - 18288b_{011}c_{110} - 10080b_{011}c_{200} + 56355b_{020}^2 - 15300b_{020}b_{110} - 3910b_{020}b_{200} - 47580b_{020}c_{020} + 10188b_{020}c_{110} + 10044b_{020}c_{200} - 42096b_{101}c_{020} - 14400b_{101}c_{110} - 18288b_{101}c_{200} - 23035b_{110}^2 - 40800b_{110}b_{200} - 45684b_{110}c_{020} - 10452b_{110}c_{110} - 9804b_{110}c_{200} - 32045b_{200}^2 - 42180b_{200}c_{020} - 15084b_{200}c_{110} - 11676b_{200}c_{200})$.

5. $L_5 = \dfrac{1}{16}(7a_{020} + 7a_{110} + 3a_{200} + 3b_{020} + 7b_{110} + 7b_{200}) + \dfrac{1}{424320}(-1058436a_{011}c_{020} - 457356a_{011}c_{110} - 498756a_{011}c_{200} + 273819a_{020}^2 - 132600a_{020}a_{110} - 1631422a_{020}a_{200} + 711620a_{020}b_{020} - 247962a_{020}b_{110} - 636480a_{020}b_{200} - 1569972a_{020}c_{020} - 407688a_{020}c_{110} - 324804a_{020}c_{200} - 1570644a_{101}c_{020} - 1058436a_{101}c_{110} - 1067316a_{101}c_{200} - 114699a_{110}^2 -$

$1816620a_{110}a_{200}-30498a_{110}b_{020}-636480a_{110}b_{110}-1024998a_{110}b_{200}-1572888a_{110}c_{020}-663612a_{110}c_{110}-606744a_{110}c_{200}-2664597a_{200}^2-742560a_{200}b_{020}-1631422a_{200}b_{110}-2373540a_{200}b_{200}-1816788a_{200}c_{020}-1543560a_{200}c_{110}-1889460a_{200}c_{200}-1067316b_{011}c_{020}-498756b_{011}c_{110}-283332b_{011}c_{200}+1922037b_{020}^2+154700b_{020}b_{110}-30498b_{020}b_{200}-1057272b_{020}c_{020}+284532b_{020}c_{110}+436392b_{020}c_{200}-1058436b_{101}c_{020}-457356b_{101}c_{110}-498756b_{101}c_{200}-521781b_{110}^2-1140360b_{110}b_{200}-1569972b_{110}c_{020}-407688b_{110}c_{110}-324804b_{110}c_{200}-910299b_{200}^2-1572888b_{200}c_{020}-663612b_{200}c_{110}-606744b_{200}c_{200})$.

6. $L_6=\frac{1}{32}(21a_{020}+21a_{110}+7a_{200}+7b_{020}+21b_{110}+21b_{200})+\frac{1}{62799360}(-299383152a_{011}c_{020}-147872304a_{011}c_{110}-148882800a_{011}c_{200}+90184133a_{020}^2-39249600a_{020}a_{110}-460463224a_{020}a_{200}+295271470a_{020}b_{020}-39429494a_{020}b_{110}-190360560a_{020}b_{200}-548103888a_{020}c_{020}-161777040a_{020}c_{110}-119895888a_{020}c_{200}-430244112a_{101}c_{020}-299383152a_{101}c_{110}-285245904a_{101}c_{200}-60746933a_{110}^2-609922430a_{110}a_{200}+22176024a_{110}b_{020}-190360560a_{110}b_{110}-341291626a_{110}b_{200}-578642688a_{110}c_{020}-269637744a_{110}c_{110}-250443840a_{110}c_{200}-809498469a_{200}^2-161577520a_{200}b_{020}-460463224a_{200}b_{110}-733558670a_{200}b_{200}-576082800a_{200}c_{020}-511909488a_{200}c_{110}-594183984a_{200}c_{200}-285245904b_{011}c_{020}-148882800b_{011}c_{110}-89756496b_{011}c_{200}+647920949b_{020}^2+171635230b_{020}b_{110}+22176024b_{020}b_{200}-256244256b_{020}c_{020}+97525584b_{020}c_{110}+166151328b_{020}c_{200}-299383152b_{101}c_{020}-147872304b_{101}c_{110}-148882800b_{101}c_{200}-129613627b_{110}^2-341471520b_{110}b_{200}-548103888b_{110}c_{020}-161777040b_{110}c_{110}-119895888b_{110}c_{200}-280544693b_{200}^2-578642688b_{200}c_{020}-269637744b_{200}c_{110}-250443840b_{200}c_{200})$.

7. $L_7=\frac{1}{32}(33a_{020}+33a_{110}+9a_{200}+9b_{020}+33b_{110}+33b_{200})+\frac{1}{549494400}(-5000767422a_{011}c_{020}-2697387546a_{011}c_{110}-2591142078a_{011}c_{200}+1746198350a_{020}^2-635352900a_{020}a_{110}-7726161105a_{020}a_{200}+6386727620a_{020}b_{020}-113660300a_{020}b_{110}-3262623000a_{020}b_{200}-10722852210a_{020}c_{020}-3511522140a_{020}c_{110}-2520916230a_{020}c_{200}-7016498454a_{101}c_{020}-5000767422a_{101}c_{110}-4603446246a_{101}c_{200}-1402764350a_{110}^2-11491301640a_{110}a_{200}+$

$921588785a_{110}b_{020}-3262623000a_{110}b_{110}-6411585700a_{110}b_{200}-11740337280a_{110}c_{020}-5857027050a_{110}c_{110}-5401512060a_{110}c_{200}-14265757740a_{200}^2-2108684760a_{200}b_{020}-7726161105a_{200}b_{110}-13191299940a_{200}b_{200}-10547693310a_{200}c_{020}-9627938880a_{200}c_{110}-10814191290a_{200}c_{200}-4603446246b_{011}c_{020}-2591142078b_{011}c_{110}-1643879454b_{011}c_{200}+12157072980b_{020}^2+4686729320b_{020}b_{110}+921588785b_{020}b_{200}-3566332140b_{020}c_{020}+1988265930b_{020}c_{110}+3402899640b_{020}c_{200}-5000767422b_{101}c_{020}-2697387546b_{101}c_{110}-2591142078b_{101}c_{200}-1859858650b_{110}^2-5889893100b_{110}b_{200}-10722852210b_{110}c_{020}-3511522140b_{110}c_{110}-2520916230b_{110}c_{200}-5008821350b_{200}^2-11740337280b_{200}c_{020}-5857027050b_{200}c_{110}-5401512060b_{200}c_{200})$.

8. $L_8=\frac{1}{256}(429a_{020}+429a_{110}+99a_{200}+99b_{020}+429b_{110}+429b_{200})+\frac{1}{17583820800}(-306026164416a_{011}c_{020}-175825776672a_{011}c_{110}-163947688128a_{011}c_{200}+122013309925a_{020}^2-36404004000a_{020}a_{110}-477767473170a_{020}a_{200}+471501683380a_{020}b_{020}+26426837450a_{020}b_{110}-201870505200a_{020}b_{200}-744465814344a_{020}c_{020}-264901558152a_{020}c_{110}-187611303096a_{020}c_{200}-421273784736a_{101}c_{020}-306026164416a_{101}c_{110}-275559010272a_{101}c_{200}-106284032725a_{110}^2-771878218020a_{110}a_{200}+88991026930a_{110}b_{020}-201870505200a_{110}b_{110}-430167847850a_{110}b_{200}-837273825864a_{110}c_{020}-439412974392a_{110}c_{110}-400975375416a_{110}c_{200}-912323221875a_{200}^2-102741715440a_{200}b_{020}-477767473170a_{200}b_{110}-860278129620a_{200}b_{200}-697063072440a_{200}c_{020}-647624052600a_{200}c_{110}-711505214280a_{200}c_{200}-275559010272b_{011}c_{020}-163947688128b_{011}c_{110}-108321820320b_{011}c_{200}+8095815506435b_{020}^2+383101771780b_{020}b_{110}+88991026930b_{020}b_{200}-175723324728b_{020}c_{020}+146011411896b_{020}c_{110}+243342558648b_{020}c_{200}-306026164416b_{101}c_{020}-175825776672b_{101}c_{110}-163947688128b_{101}c_{200}-95586472475b_{110}^2-367337006400b_{110}b_{200}-744465814344b_{110}c_{020}-264901558152b_{110}c_{110}-187611303096b_{110}c_{200}-323883815125b_{200}^2-837273825864b_{200}c_{020}-439412974392b_{200}c_{110}-400975375416b_{200}c_{200})$.

9. $L_9 = \frac{1}{256}(715a_{020} + 715a_{110} + 143a_{200} + 143b_{020} + 715b_{110} + 715b_{200}) + \frac{1}{2162809958400}(-72168505453800a_{011}c_{020} - 43497962460792a_{011}c_{110} - 39764608597224a_{011}c_{200} + 32315363560025a_{020}^2 - 7916222386800a_{020}a_{110} - 114401258119070a_{020}a_{200} + 128416519433280a_{020}b_{020} + 13889177861650a_{020}b_{110} - 47784582518400a_{020}b_{200} - 194973558969672a_{020}c_{020} - 74207530798128a_{020}c_{110} - 52307242311240a_{020}c_{200} - 97793060806728a_{101}c_{020} - 72168505453800a_{101}c_{110} - 64036208589192a_{101}c_{200} - 29358396820025a_{110}^2 - 196515664609680a_{110}a_{200} + 28180131064670a_{110}b_{020} - 47784582518400a_{110}b_{110} - 109458342898450a_{110}b_{200} - 223843642260336a_{110}c_{020} - 122227923315960a_{110}c_{110} - 110438527315536a_{110}c_{200} - 223595631389715a_{200}^2 - 19686398322240a_{200}b_{020} - 114401258119070a_{200}b_{110} - 214637646487680a_{200}b_{200} - 175641472336680a_{200}c_{020} - 165220771821840a_{200}c_{110} - 178674322123080a_{200}c_{200} - 64036208589192b_{011}c_{020} - 39764608597224b_{011}c_{110} - 27136661228712b_{011}c_{200} + 2039092330674\,75b_{020}^2 + 110294537555280b_{020}b_{110} + 28180131064670b_{020}b_{200} - 31760983766736b_{020}c_{020} + 40457388568968b_{020}c_{110} + 65123767738512b_{020}c_{200} - 72168505453800b_{101}c_{020} - 43497962460792b_{101}c_{110} - 39764608597224b_{101}c_{200} - 18426185698375b_{110}^2 - 87652942650000b_{110}b_{200} - 194973558969672b_{110}c_{020} - 74207530798128b_{110}c_{110} - 52307242311240b_{110}c_{200} - 800999460784\,25b_{200}^2 - 223843642260336b_{200}c_{020} - 122227923315960b_{200}c_{110} - 110438527315536b_{200}c_{200})$.

We note that, only the first three of the Liapunov quantities L_1, L_2 and L_3 have independent linear parts. Therefore, by considering the first order of the liapunov quantities, two limit cycles can bifurcate from the centre. Now, we are interesting in second order perturbation. For that reason, we perform the following analytic change of coordinates in parameters

1. $a_{020} = -3a_{200} - a_{110} - b_{200} - 3b_{020} - b_{110} + \frac{1}{5}(2a_{011}c_{020} + a_{011}c_{110} - 2a_{011}c_{200} + 9a_{101}c_{020} + 2a_{101}c_{110} + 11a_{101}c_{200} + 5a_{110}^2 + 10a_{110}a_{200} + 25a_{110}b_{020} + 5a_{110}b_{110} +$

$5a_{110}b_{200}+30a_{200}b_{020}+10a_{200}b_{200}+11b_{011}c_{020}-2b_{011}c_{110}+9b_{011}c_{200}+30b_{020}^2+15b_{020}b_{110}+10b_{020}b_{200}+2b_{101}c_{020}+b_{101}c_{110}-2b_{101}c_{200}+5b_{110}b_{200}).$

2. $a_{200}=-b_{020}+\frac{1}{20}(-3a_{011}c_{110}-13a_{011}c_{200}-21a_{101}c_{110}-13a_{101}c_{200}+20a_{110}^2+20a_{110}b_{110}+20a_{110}b_{200}+a_{110}c_{110}+7a_{110}c_{200}-13b_{011}c_{110}+11b_{011}c_{200}+25b_{020}c_{110}+31b_{020}c_{200}-3b_{101}c_{110}-13b_{101}c_{200}+20b_{110}b_{200}+b_{200}c_{110}+7b_{200}c_{200}-21a_{011}-25a_{101}+3a_{110}-13b_{011}-b_{020}-21b_{101}+3b_{200}).$

Under these substitution, the linear parts of the rest of the Liapunove quantities will become zero. Now, we expand the Liapunov quantities L_4, L_5, L_6, L_7, L_8 and L_9 in terms of the rest of the parameters. The order of the first non-zero terms of each of these Liapunov quantities is two. In this case, the Liapunov quantities can be written of the form

$$L_i = h_i(a_{110}, a_{101}, a_{011}, a_{002}, b_{200}, b_{110}, b_{101}, b_{020}, b_{011}, b_{002}, c_{200}, c_{110}, c_{101}, c_{020}, c_{011}, c_{002}) + ...$$

where $h_i,\ i=4,5,...,9$ are homogeneous polynomials of degree two. The first five of these homogeneous polynomials h_i have a common zero at wich the sixth does not vanish if the following conditions hold:

1. $a_{101}=\frac{-1}{(692+362c_{200}+513c_{110})}(362a_{011}c_{110}+269a_{011}c_{200}+244a_{110}c_{110}+435a_{110}c_{200}+269b_{011}c_{110}+216b_{011}c_{200}-1162b_{020}c_{110}-1557b_{020}c_{200}+362b_{101}c_{110}+269b_{101}c_{200}+244b_{200}c_{110}+435b_{200}c_{200}+513a_{011}+7a_{110}+362b_{011}-653b_{020}+513b_{101}+7b_{200}).$

2. $a_{011}=(-1/(83656c_{110}^2+101362c_{110}c_{200}+27660c_{200}^2+200898c_{110}+118505c_{200}+124781))(535271a_{110}c_{110}^2+760032a_{110}c_{110}c_{200}+226924a_{110}c_{200}^2+101362b_{011}c_{110}^2+117219b_{011}c_{110}c_{200}+27974b_{011}c_{200}^2-1469039b_{020}c_{110}^2-2131163b_{020}c_{110}c_{200}-652170b_{020}c_{200}^2+83656b_{101}c_{110}^2+101362b_{101}c_{110}c_{200}+27660b_{101}c_{200}^2+535271b_{200}c_{110}^2+760032b_{200}c_{110}c_{200}+226924b_{200}c_{200}^2+1507394a_{110}c_{110}+1186363a_{110}c_{200}+$

$285817b_{011}c_{110}+173348b_{011}c_{200}-4066527b_{020}c_{110}-3276055b_{020}c_{200}+200898b_{101}c_{110}+118505b_{101}c_{200}+1507394b_{200}c_{110}+1186363b_{200}c_{200}+981027a_{110}+200898b_{011}-2589949b_{020}+124781b_{101}+981027b_{200})$.

3. $a_{110} = (-1/(7069574c_{110}^3+13180278c_{110}^2c_{200}+7430940c_{110}c_{200}^2+1302764c_{200}^3+24863682c_{110}^2+29894343c_{110}c_{200}+7343787c_{200}^2+30583155c_{110}+18749598c_{200}+12801983))[373444b_{011}c_{110}^3+681198b_{011}c_{110}^2c_{200}+425580b_{011}c_{110}c_{200}^2+100354b_{011}c_{200}^3-20088390b_{020}c_{110}^3-37497240b_{020}c_{110}^2c_{200}-21016080b_{020}c_{110}c_{200}^2-3607230b_{020}c_{200}^3+7069574b_{200}c_{110}^3+13180278b_{200}c_{110}^2c_{200}+7430940b_{200}c_{110}c_{200}^2+1302764b_{200}c_{200}^3+1026282b_{011}c_{110}^2+101992b_{011}c_{110}c_{200}+211182b_{011}c_{200}^2-71512200b_{020}c_{110}^2-86623245b_{020}c_{110}c_{200}-21397815b_{020}c_{200}^2+24863682b_{200}c_{110}^2+29894343b_{200}c_{110}c_{200}+7343787b_{200}c_{200}^2+1031460b_{011}c_{110}+408978b_{011}c_{200}-88655085b_{020}c_{110}-55021860b_{020}c_{200}+30583155b_{200}c_{110}+18749598b_{200}c_{200}+391558b_{011}-37231275b_{020}+12801983b_{200}]$.

4. $c_{020} = 1$ and $c_{110} = \alpha$ where α is a real root of the equation below (it has exactly two real roots as we see in Figure 4.1.a, it was proved using Sturm sequence routine in Maple)

$$h(x) = 1645079678071649x^6 + 14962324997859279x^5 + 58385391188383563x^4 + 124809867725124797x^3 + 153170409627863643x^2 + 101457081348131271x + 27728667159920858 = 0. \tag{4.9}$$

5. $c_{200} = \dfrac{1}{6176836600663893}(6580318712286596\alpha^5 + 49874416659530930\alpha^4 + 157938617665759247\alpha^3 + 262914062348203945\alpha^2 + 223502331891049690\alpha + 79253734075676899)$.

Thus, the origin of system (4.8) can be bifurcated to give a weak focus of order eight. To bifurcate eight limit cycles, therefore using Theorem 3.1 in (Christopher, 2005), it is only necessary to verify that the Liapunov quantities are independent at the bifurcate point. This is easily verified since the first three Liapunov quantities including L_0 are linear and the Jacobian determinant of the next five of h_i with respect to the parameters $a_{101}, a_{011}, a_{110}, c_{110}$ and c_{200} is also non-zero. To make this calculation easier, we fix the free parameters as follows:

$$b_{011} = 0,\ b_{020} = 1,\ a_{002} = 0,\ c_{101} = 0,\ c_{011} = 0,\ c_{002} = 0, b_{200} = 0,\ b_{110} = 0,$$
$$b_{101} = 0,\ \text{and}\ b_{002} = 0.$$

The Jacobian determinant of the quadratic parts of the functions $(h_4, h_5, h_6, h_7, h_8)$ with respect to the parameters $(a_{1,0,1}, a_{0,1,1}, a_{1,1,0}, c_{1,1,0}, c_{2,0,0})$ is defined by

$$\begin{aligned} J(\alpha) = {} & \frac{0.00001}{151621245911581470750678208758602427541581836917986001767359601170562 56} \\ & (-2977901160700833716351566066721791672304750585981063106427867754 1\alpha^5 \\ & - 2417728528612514452034564572510025814310628359214343691296065962 62\alpha^4 \\ & - 8230921830404556197273240467900900394214600129016673651214751764 63\alpha^3 \\ & - 1479017166073315675228451877186866716902202423724504102039004310 110\alpha^2 \\ & - 1410958339653967061999414560604220683192656866109491277670750848 395\alpha \\ & - 5831080169224193379043447941365508967945403778136106663454792389 28). \end{aligned} \tag{4.10}$$

It is easy to see that this Jacobian determinant is non-zero or we can note from Figure 4.1.b. Then in a neighbourhood of the origin, eight limit cycles can bifurcate from the origin of the system (4.7).

□

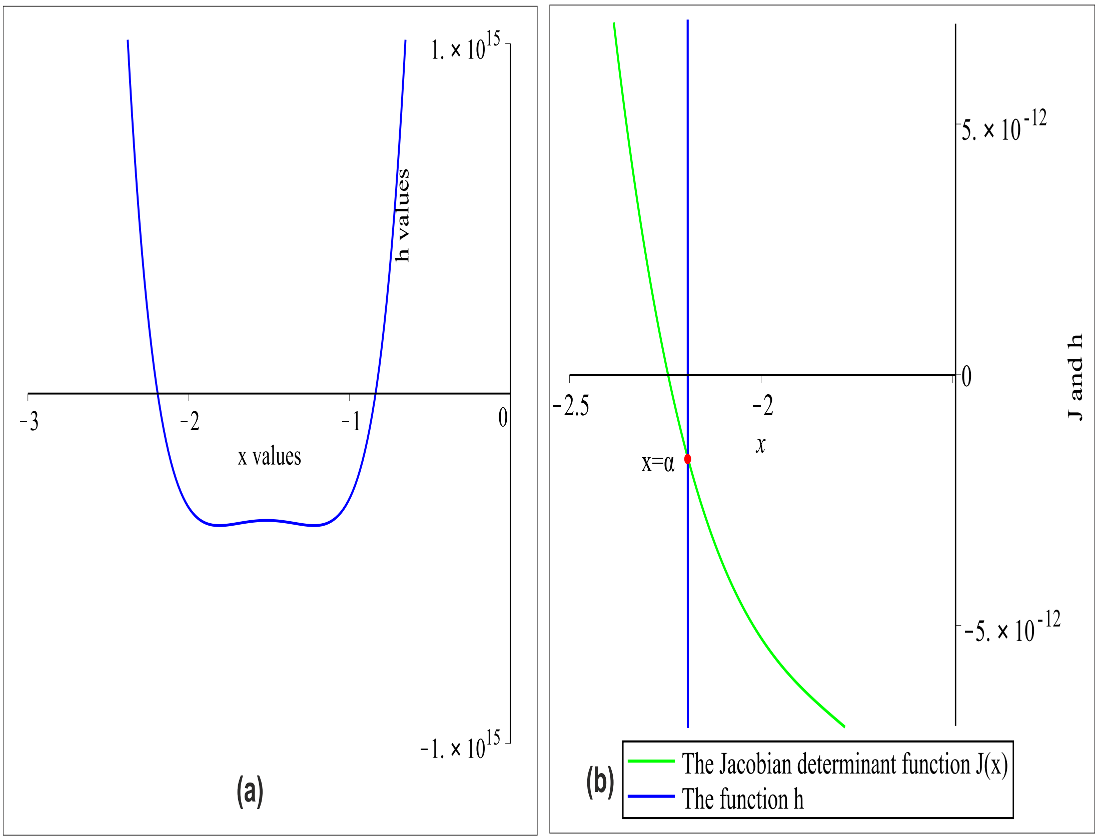

Figure 4.1: (a) The graph of function $h(x)$ in (4.9) has exactly two real roots. (b) The Jabian determinant function J(x) in (4.10) at these two real roots of function $h(x)$ is not equal zero.

Chapter 5

Some Chaotic Behaviour in Three Dimensional Systems

The aim of this chapter is to present some basic concepts relating to chaotic behaviour which will be useful in understanding the results which are shown in the next chapter. Until recently there has been no universally accepted mathematical definition of chaos. However, there are many possible definitions of chaos put forward, such the definition of Devaney, Wiggins and Lyapunov (Devaney, 2003; Wiggins, 1992; Robinson, 1995). The reader can consult these for more detailed information.

This chapter will not provide new results on chaotic behaviour, but will rather present some background on the horseshoe map including symbolic dynamics as well as the Shilnikov phenomena.

5.1 The Horseshoe Map

To define the horseshoe map, we consider a square region $S = [0, 1] \times [0, 1]$ in the plane. We define a map $\mathbf{F} : \mathbf{S} \to \mathbb{R}^2$ so that $\mathbf{F}(\mathbf{S}) \cap \mathbf{S}$ consists of two components which are mapped rectilinearly by $\mathbf{F}$. The horseshoe map $\mathbf{F}$ takes $\mathbf{S}$ inside itself by following steps. First, $\mathbf{F}$ linearly contracts $\mathbf{S}$ by factor $\lambda < \frac{1}{2}$ and expands $\mathbf{S}$ by factor $\mu > 2$ in the horizontal and vertical direction respectively, so that $\mathbf{S}$ is long and thin. Then $\mathbf{F}$ folds $\mathbf{S}$ and places it back over $\mathbf{S}$ as displayed in Figure 5.1. We note that the folding portion falls outside the square region $\mathbf{S}$, $\mathbf{F}$ maps the two horizontal boundaries AB, DC linearly onto the two horizontal intervals of length λ and $\mathbf{F}$ is one-to-one but is not onto, therefore the inverse of $\mathbf{F}$ is not globally defined (for more detail on this subject consult (Guckenheimer and Holmes, 2013; Hirsch et al., 2013)).

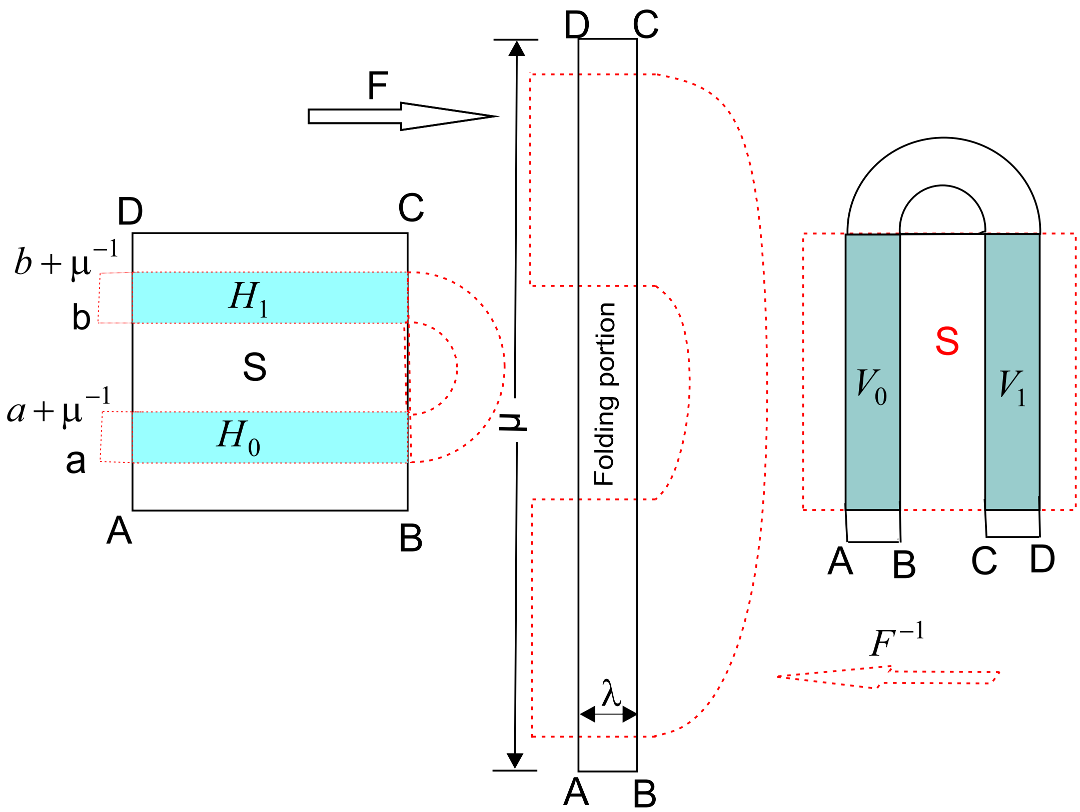

Figure 5.1: The geometrical Horseshoe map. The solid curves depict the Horseshoe map $\mathbf{F}$ and the dotted curves depict inverse of the Horseshoe map $\mathbf{F}^{-1}$.

Since $\mathbf{F}^{-1}(\mathbf{F}(\mathbf{S}) \cap \mathbf{S}) = \mathbf{S} \cap \mathbf{F}^{-1}(\mathbf{S})$, the preimage of $\mathbf{F}$ consists of two horizontal rectangles $H_0 = [0,1] \times [a, a+\mu^{-1}]$ and $H_1 = [0,1] \times [b, b+\mu^{-1}]$ which are obtained by reversing the compressing, stretching and folding where $a, b \in \mathbb{R}$. In addition, $\mathbf{F}$ has a constant Jacobian on each of them given by

$$\begin{bmatrix} \mp\lambda & 0 \\ 0 & \mp\mu \end{bmatrix}$$

with positive signs on H_0 and negative signs on H_1 (in addition to being compressing in the horizontal direction by factor λ and stretching in the vertical direction by factor μ, H_1 is also rotated 180^0, thus the matrix elements are negative). Therefore the two horizontal rectangles H_0 and H_1 are mapped linearly onto the two vertical rectangles V_0 and V_1 on $\mathbf{F}(\mathbf{S}) \cap \mathbf{S}$ and the width of these is λ, this means that:

$$\mathbf{F} : H_0 \to V_0 \quad \textit{and} \quad \mathbf{F} : H_1 \to V_1. \tag{5.1}$$

We note from equation (5.1) that the map $\mathbf{F}$ takes linearly the horizontal and vertical lines in H_i to horizontal and vertical lines in $V_i,\ i = 0, 1$. The relationship between the length of the horizontal line h with its image $\mathbf{F}(h)$ and the length of the vertical line v whose image lies in $\mathbf{S}$ and its image $\mathbf{F}(v)$ are illustrated below:

$$\text{length of } \mathbf{F}(h) = \lambda \times (\text{length of } h),$$
$$\text{length of } \mathbf{F}(v) = \mu \times (\text{length of } v).$$

We are interested in describing the set of all points whose orbits remain in $\mathbf{S}$ when the map $\mathbf{F}$ is iterated. We describe the forward and backward orbits for each point $x \in \mathbf{S}$. The forward orbit of $x \in \mathbf{S}$ is given by $\{\mathbf{F}^n(x) | \quad n \geq 0\}$. The set of all points that always remain in $\mathbf{S}$ under forward iterates of $\mathbf{F}$ is denoted by Λ_+ and defined by

$$\Lambda_+ = \{x \in \mathbf{S} \mid \mathbf{F}^n(x) \in \mathbf{S} \quad for \quad n = 0, 1, 2, ...\}.$$

If $x \in \Lambda_+$ then $\mathbf{F}(x) \in \mathbf{S}$, so we must have either $x \in H_0$ or $x \in H_1$. Since $\mathbf{F}^2(x) \in \mathbf{S}$ as well, we must also have $\mathbf{F}(x) \in H_0 \cup H_1$, so that $x \in \mathbf{F}^{-1}(H_0 \cup H_1)$. In general, since $\mathbf{F}^n(x) \in \mathbf{S}$, we have $x \in \mathbf{F}^{-n}(H_0 \cup H_1)$. Thus we may write the set Λ_+ as follows:

$$\Lambda_+ = \bigcap_{n=0}^{\infty} \mathbf{F}^{-n}(H_0 \cup H_1). \tag{5.2}$$

We denote one of the horizontal strips of height h that connects the right and left boundaries of $\mathbf{S}$ as H, then a pair of narrower horizontal strips of height $h\mu^{-1}$ one in each of H_0 and H_1 are obtained from $\mathbf{F}^{-1}(H)$ and their image under $\mathbf{F}$ are given by $H \cap V_0$ and $H \cap V_1$. Thus $\mathbf{F}^{-1}(H_i)$ consists of a pair of horizontal strips each of height μ^{-2} with one in H_0 and the other in H_1. Similarly, $\mathbf{F}^{-2}(H_i)$ gives us four narrower horizontal strips of height μ^{-3}. In general, $\mathbf{F}^{-n}(H_i)$ consist of 2^n narrower horizontal strips of height $\mu^{-(n+1)}$, therefore $\mathbf{F}^{-n}(H_0 \cup H_1)$ consists of 2^{n+1} narrower horizontal strips of height $\mu^{-(n+1)}$ (it can be symbolized by $H_{s_0 s_1 \ldots s_n}$, $s_i \in \{0, 1\}$, $i = 0, 1, ..., n$) and each strip can be labelled by a sequence of $0'$s and $1'$s of length n. When $n \longrightarrow \infty$, we obtain an infinite number of horizontal strips and the height of each of these strips is given by $lim_{n \longrightarrow \infty}(\frac{1}{\mu})^{n+1} = 0$, $\mu > 2$. Thus, Λ_+ consists of an infinite number of horizontal lines and each line can be labelled by a unique infinite sequence of $0'$s and $1'$s. The intersection of all these horizontal strips (n approaches ∞) which is denoted by Λ_+ forms a Cantor set of horizontal lines (see (Guckenheimer and Holmes, 2013)).

The backward orbit of a point $x \in \mathbf{S}$ is given by $\{x \in \mathbf{S} \mid \mathbf{F}^{-n}(x) \in \mathbf{S},\ n = 1, 2, 3, ...\}$, provided that $\mathbf{F}^{-n}(x)$ is defined and in $\mathbf{S}$. The set of all points whose backward orbit is defined and lies wholly in $\mathbf{S}$ is denoted by Λ_- and defined by

$$\Lambda_- = \left\{ x \in \mathbf{S} \mid \mathbf{F}^{-n}(x) \in \mathbf{S} \quad for \quad n = 1, 2, ... \right\}.$$

If we take $x \in \Lambda_-$, then we have $\mathbf{F}^{-n}(x) \in \mathbf{S}$, $\forall\ n \geq 1$, which implies that $x \in \mathbf{F}^n(\mathbf{S})$, $\forall\ n \geq 1$ and $x \in \mathbf{F}^n(H_0 \cup H_1)$, $\forall\ n \geq 1$. Thus we may write the set Λ_- as follows:

$$\Lambda_- = \bigcap_{n=1}^{\infty} \mathbf{F}^n(H_0 \cup H_1). \tag{5.3}$$

If $x \in \mathbf{S}$ and $\mathbf{F}^{-1}(x) \in \mathbf{S}$, then we must have $x \in \mathbf{F}(\mathbf{S}) \cap \mathbf{S}$ which consists of a pair of narrower vertical strips of width λ, one of them will be V_0 and the other is V_1. Similarly, if $\mathbf{F}^{-2}(x) \in \mathbf{S}$, we must have $x \in \mathbf{F}^2(\mathbf{S}) \cap \mathbf{S}$ which consists of four narrower vertical strips of width λ^2 (pictorially, this is described in Figure 5.2). In general, if $\mathbf{F}^{-n}(x) \in \mathbf{S}$, we must have $x \in \mathbf{F}^n(\mathbf{S}) \cap \mathbf{S}$, which consists of 2^n narrower vertical strips of width λ^n (it can be symbolized by $V_{s_{-1}s_{-2}...s_{-n}}$, $s_{-i} \in \{0, 1\}$, $i = 1,\ ...\ n$) and each strip can be labelled by a sequence of $0'$s and $1'$s of length n. When $n \longrightarrow \infty$, we obtain an infinite number of vertical strips of width zero, since $lim_{n\longrightarrow\infty}\lambda^n = 0$ for $0 < \lambda < \frac{1}{2}$. Thus, Λ_- consists of an infinite number of vertical lines and each line can be labelled by a unique infinite sequence of $0'$s and $1'$s. The intersection of all vertical strips (n approaches ∞) which is denoted by Λ_- forms a Cantor set of vertical lines (see (Guckenheimer and Holmes, 2013)). Let

$$\Lambda = \Lambda_+ \cap \Lambda_- = \bigcap_{n=-\infty}^{\infty} \mathbf{F}^n(H_0 \cup H_1) \tag{5.4}$$

be the intersection of these sets. The set Λ constructs an invariant set, therefore if a point $x \in \Lambda$, then both its forward and its backward orbits lie completely in $\mathbf{S}$. The map $\mathbf{F}$ restricted to its invariant set Λ, has a countable infinity of periodic orbits of all periods, an uncountable infinity of non-periodic orbits and a dense orbit (Wiggins, 2003) .

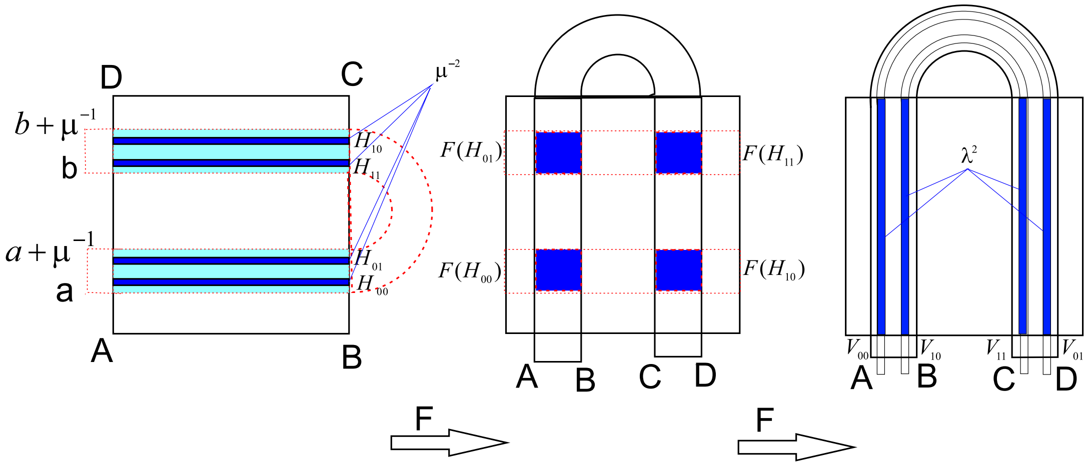

Figure 5.2: The second iteration of the Horseshoe map F: $V_{i,j} = F^2(H_{i,j}),\ i,j = 1,2$.

5.2 Symbolic Dynamics

Now, we represent the invariant set Λ_+ which is defined in (5.2) by using symbolic dynamics. When $n = 0$ in equation (5.2), by definition of the Horseshoe map $\mathbf{F}$, $H_0 \cup H_1 = \mathbf{S} \cap \mathbf{F}^{-1}(\mathbf{S})$ consists of two horizontal strips H_0 and H_1 of height μ^{-1} (see Figure 5.1). This set is denoted by $\Lambda+$ where,

$$\begin{aligned} \Lambda+ &= H_0 \cup H_1 \\ &= \mathbf{S} \cap \mathbf{F}^{-1}(\mathbf{S}) \\ &= \bigcup_{s_0 \in \{0,1\}} H_{s_0} \\ &= \{p \in \mathbf{S} : p \in H_{s_0},\ s_0 \in \{0,1\}\}. \end{aligned} \tag{5.5}$$

When $n = 1$, since H_0 and H_1 intersect both vertical boundaries of V_0 and V_1, the set $(H_0 \cup H_1) \cap \mathbf{F}^{-1}(H_0 \cup H_1) = \mathbf{S} \cap \mathbf{F}^{-1}(\mathbf{S}) \cap \mathbf{F}^{-2}(\mathbf{S})$ consists of four narrower horizontal strips, two each in H_0 and H_1, with each of height μ^{-2}. Using equation (5.5) we have

$$\begin{aligned}
\Lambda+ &= (H_0 \cup H_1) \cap \mathbf{F}^{-1}(H_0 \cup H_1) \\
&= \mathbf{S} \cap \mathbf{F}^{-1}(\mathbf{S}) \cap \mathbf{F}^{-1}(\mathbf{S} \cap \mathbf{F}^{-1}(\mathbf{S})) \\
&= \mathbf{S} \cap \mathbf{F}^{-1}(\mathbf{S}) \cap \mathbf{F}^{-2}(\mathbf{S}) \\
&= \mathbf{S} \cap \mathbf{F}^{-1}(\mathbf{S} \cap \mathbf{F}^{-1}(\mathbf{S})) \\
&= \mathbf{S} \cap \mathbf{F}^{-1}(\bigcup_{s_1 \in \{0,1\}} H_{s_1}). \qquad (5.6)
\end{aligned}$$

In the equation above, after substituting the value of $\mathbf{S} \cap \mathbf{F}^{-1}(\mathbf{S})$ we have changed the subscript s_0 on H_{s_0} to s_1, because s_i is merely a dummy variable and has no real effect. Since $\mathbf{F}^{-1}(H_{s_1})$ can not intersect all of $\mathbf{S}$ but only $H_0 \cup H_1$, so that equation (5.6) becomes

$$\begin{aligned}
\Lambda+ &= \bigcup_{\substack{s_i \in \{0,1\} \\ i=0,1}} (H_{s_0} \cap \mathbf{F}^{-1}(H_{s_1})) \\
&= \bigcup_{\substack{s_i \in \{0,1\} \\ i=0,1}} H_{s_0 s_1} \\
&= \{p \in \mathbf{S} : p \in H_{s_0},\ \mathbf{F}(p) \in H_{s_1},\ s_i \in \{0,1\},\ i = 0,1\}. \qquad (5.7)
\end{aligned}$$

This is represented pictorially in Figure 5.2.

For n=2, using the same reason as in the previous steps the set $(H_0 \cup H_1) \cap \mathbf{F}^{-1}(H_0 \cup H_1) \cap \mathbf{F}^{-2}(H_0 \cup H_1)$ consists of eight horizontal strips, four each in H_0 and H_1 and each having height μ^{-3}. This can be denoted as

$$\begin{aligned}
\Lambda+ &= (H_0 \cup H_1) \cap \mathbf{F}^{-1}(H_0 \cup H_1) \cap \mathbf{F}^{-2}(H_0 \cup H_1) \\
&= \mathbf{S} \cap \mathbf{F}^{-1}(\mathbf{S} \cap \mathbf{F}^{-1}(\mathbf{S}) \cap \mathbf{F}^{-2}(\mathbf{S}))
\end{aligned}$$

$$
\begin{aligned}
&= \mathbf{S} \cap \mathbf{F}^{-1}\big(\bigcup_{\substack{s_i \in \{0,1\} \\ i=1,2}} H_{s_1 s_2}\big) \\
&= \bigcup_{\substack{s_i \in \{0,1\} \\ i=0,1,2}} (H_{s_0} \cap \mathbf{F}^{-1}(H_{s_1 s_2})) \\
&= \bigcup_{\substack{s_i \in \{0,1\} \\ i=0,1,2}} H_{s_0 s_1 s_2} \qquad (5.8) \\
&= \{p \in \mathbf{S} : p \in H_{s_0},\ \mathbf{F}(p) \in H_{s_1},\ \mathbf{F}^2(p) \in H_{s_2},\ s_i \in \{0,1\},\ i = 0, 1,\ 2\}.
\end{aligned}
$$

If we continually repeat this procedure, it is not hard to see that at the k^{th} step $(n = k - 1)$ we obtain 2^k horizontal strips, 2^{k-1} each in H_0 and H_1 with each of height μ^{-k} and each strip can be labelled uniquely with sequence of $0's$ and $1's$ of length k. This is denoted by

$$
\begin{aligned}
\Lambda+ &= \bigcap_{n=0}^{k-1} \mathbf{F}^{-n}(H_0 \cup H_1) \\
&= (H_0 \cup H_1) \cap \mathbf{F}^{-1}(H_0 \cup H_1) \cap ... \cap \mathbf{F}^{-(k-1)}(H_0 \cup H_1) \\
&= \mathbf{S} \cap \mathbf{F}^{-1}(\mathbf{S}) \cap \mathbf{F}^{-2}(\mathbf{S}) \cap ... \cap \mathbf{F}^{-k}(\mathbf{S}) \\
&= \mathbf{S} \cap \mathbf{F}^{-1}(\mathbf{S} \cap \mathbf{F}^{-1}(\mathbf{S}) \cap ... \cap \mathbf{F}^{-(k-1)}(\mathbf{S})) \\
&= \mathbf{S} \cap \mathbf{F}^{-1}\big(\bigcup_{\substack{s_i \in \{0,1\} \\ i=1,2,\dots,k-1}} H_{s_1 s_2 \dots s_{k-1}}\big) \\
&= \bigcup_{\substack{s_i \in \{0,1\} \\ i=0,1,2,\dots,k-1}} (H_{s_0} \cap \mathbf{F}^{-1}(H_{s_1 s_2, \dots s_{k-1}})) \\
&= \bigcup_{\substack{s_i \in \{0,1\} \\ i=0,1,2,\dots,k-1}} H_{s_0 s_1 s_2, \dots s_{k-1}} \qquad (5.9) \\
&= \{p \in \mathbf{S} : \mathbf{F}^i(p) \in H_{s_i},\ s_i \in \{0,1\},\ i = 0, 1, 2, ..., k-1\}.
\end{aligned}
$$

Now, letting $n \longrightarrow \infty$, since a decreasing intersection of compact sets is non-empty, then we obtain an infinite number of horizontal strips of height zero which is obtained by $\lim_{n\to\infty}(\frac{1}{\mu})^{n+1} = 0,\ \mu > 0$. Each line can be labelled by a unique infinite sequence of $0'$s and $1'$s as follows

$$\begin{aligned}
\Lambda_+ &= \bigcap_{n=0}^{\infty} \mathbf{F}^{-n}(H_0 \cup H_1) \\
&= \bigcup_{\substack{s_i\in\{0,1\}\\ i=0,1,2,\dots}} (H_{s_0} \cap \mathbf{F}^{-1}(H_{s_1 s_2 \dots s_k \dots})) \\
&= \bigcup_{\substack{s_i\in\{0,1\}\\ i=0,1,2,\dots}} H_{s_0 s_1 s_2 \dots s_k \dots} \\
&= \{p \in \mathbf{S} :\ \mathbf{F}^i(p) \in H_{s_i},\ s_i \in \{0,1\},\ i = 0,1,2,\dots\}. \qquad (5.10)
\end{aligned}$$

Now, we describe the invariant set Λ_- by using symbolic dynamics. When $n = 1$ in equation (5.3), by definition of the Horseshoe map $\mathbf{F}$, $\mathbf{F}(H_0 \cup H_1) = \mathbf{S} \cap \mathbf{F}(\mathbf{S})$ and it consists of the two vertical strips V_0 and V_1 of width λ (see Figure 5.1). This set is denoted as follows

$$\begin{aligned}
\Lambda_- &= \mathbf{F}(H_0 \cup H_1) \\
&= \mathbf{S} \cap \mathbf{F}(\mathbf{S}) \\
&= V_0 \cup V_1,
\end{aligned}$$

we denote $V_0 \cup V_1 = \bigcup_{s_{-1}\in\{0,1\}} V_{s_{-1}}$, therefore

$$\begin{aligned}
\Lambda_- &= \bigcup_{s_{-1}\in\{0,1\}} V_{s_{-1}} \qquad (5.11) \\
&= \{p \in \mathbf{S} : p \in V_{s_{-1}},\ s_{-1} \in \{0,1\}\}.
\end{aligned}$$

When $n = 2$, since $\mathbf{F}(H_0 \cup H_1) = \mathbf{S} \cap \mathbf{F}(\mathbf{S})$ consists of two vertical strips V_0 and V_1 that intersecting the horizontal boundaries of H_0 and H_1, then $\mathbf{F}(H_0 \cup H_1) \cap \mathbf{F}^2(H_0 \cup H_1) = \mathbf{S} \cap \mathbf{F}(\mathbf{S}) \cap \mathbf{F}^2(\mathbf{S})$ corresponds to four vertical strips, two each in

V_0 and V_1, with each of width λ^2. Using equation (5.11), we have

$$\begin{aligned}\Lambda- &= \mathbf{F}(H_0 \cup H_1) \cap \mathbf{F}^2(H_0 \cup H_1)\\ &= \mathbf{S} \cap \mathbf{F}(\mathbf{S}) \cap \mathbf{F}(\mathbf{S} \cap \mathbf{F}(\mathbf{S}))\\ &= \mathbf{S} \cap \mathbf{F}(\mathbf{S} \cap \mathbf{F}(\mathbf{S}))\\ &= \mathbf{S} \cap \mathbf{F}(\bigcup_{s_{-2}\in\{0,1\}} V_{s_{-2}}). \qquad (5.12)\end{aligned}$$

In the above equation, after substituting the value of $\mathbf{S}\cap\mathbf{F}(\mathbf{S})$ we have changed the subscript s_{-1} on $V_{s_{-1}}$ to s_{-2}, because s_i is only a dummy variable. Since $\mathbf{F}(V_{s_{-2}})$ can not intersect all of $\mathbf{S}$ but only $V_0 \cup V_1$, so that equation (5.12) becomes

$$\begin{aligned}\Lambda- &= \bigcup_{\substack{s_{-i}\in\{0,1\}\\ i=1,2}} (V_{s_{-1}} \cap \mathbf{F}(V_{s_{-2}}))\\ &= \bigcup_{\substack{s_{-i}\in\{0,1\}\\ i=1,2}} V_{s_{-1}s_{-2}} \qquad (5.13)\\ &= \{p \in \mathbf{S} : p \in V_{s_{-1}},\ \mathbf{F}^{-1}(p) \in V_{s_{-2}},\ s_{-i} \in \{0,1\},\ i = 1,2\}.\end{aligned}$$

Pictorially, the second positive iterate for the Horseshoe map $\mathbf{F}$ is described in Figure 5.2.

For n=3, $\mathbf{F}(H_0 \cup H_1) \cap \mathbf{F}^2(H_0 \cup H_1) \cap \mathbf{F}^3(H_0 \cup H_1) = \mathbf{S} \cap \mathbf{F}(\mathbf{S}) \cap \mathbf{F}^2(\mathbf{S}) \cap \mathbf{F}^3(\mathbf{S})$, using the same reason as in the previous steps this set consists of eight vertical strips, four each in V_0 and V_1, with each of width λ^3. This can be represented as

$$\begin{aligned}\Lambda- &= \mathbf{F}(H_0 \cup H_1) \cap \mathbf{F}^2(H_0 \cup H_1) \cap \mathbf{F}^3(H_0 \cup H_1)\\ &= \mathbf{S} \cap \mathbf{F}(\mathbf{S} \cap \mathbf{F}(\mathbf{S}) \cap \mathbf{F}^2(\mathbf{S}))\\ &= \mathbf{S} \cap \mathbf{F}(\bigcup_{\substack{s_{-i}\in\{0,1\}\\ i=2,3}} V_{s_{-2}s_{-3}})\end{aligned}$$

$$= \bigcup_{\substack{s_{-i}\in\{0,1\}\\ i=1,2,3}} (V_{s_{-1}} \cap \mathbf{F}(V_{s_{-2}s_{-3}}))$$

$$= \bigcup_{\substack{s_{-i}\in\{0,1\}\\ i=1,2,3}} V_{s_{-1}s_{-2}s_{-3}} \tag{5.14}$$

$$= \{p \in \mathbf{S} : p \in V_{s_{-1}},\ \mathbf{F}^{-1}(p) \in V_{s_{-2}},\ \mathbf{F}^{-2}(p) \in V_{s_{-3}},\ s_{-i} \in \{0,1\},\ i = 1,2,3\}.$$

Continuing this procedure, at the k^{th} step we obtain 2^k vertical strips, 2^{k-1} each in V_0 and V_1 with each of width λ^k and each of the strips can be labelled uniquely with sequence of $0'$s and $1'$s of length k. That is

$$\begin{aligned}
\Lambda- &= \mathbf{F}(H_0 \cup H_1) \cap \mathbf{F}^2(H_0 \cup H_1) \cap ... \cap \mathbf{F}^k(H_0 \cup H_1) \\
&= \mathbf{S} \cap \mathbf{F}(\mathbf{S} \cap \mathbf{F}(\mathbf{S}) \cap ... \cap \mathbf{F}^k(\mathbf{S})) \\
&= \mathbf{S} \cap \mathbf{F}(\bigcup_{\substack{s_{-i}\in\{0,1\}\\ i=2,3,\ldots,k}} V_{s_{-2}s_{-3}\ldots s_{-k}}) \\
&= \bigcup_{\substack{s_{-i}\in\{0,1\}\\ i=1,2,3,\ldots,k}} (V_{s_{-1}} \cap \mathbf{F}(V_{s_{-2}s_{-3}\ldots s_{-k}})) \\
&= \bigcup_{\substack{s_{-i}\in\{0,1\}\\ i=1,2,3,\ldots,k}} V_{s_{-1}s_{-2}s_{-3},\ldots,s_k} \qquad (5.15) \\
&= \{p \in \mathbf{S} : \mathbf{F}^{-i+1}(p) \in V_{s_{-i}},\ s_{-i} \in \{0,1\},\ i = 1,2,3,\ldots\ k\}.
\end{aligned}$$

As in the case of the horizontal strip, we let $n \longrightarrow \infty$, since $\lim_{n\to\infty}(\lambda)^n = 0$, for $0 < \lambda < \dfrac{1}{2}$, it is clear that we obtain an infinite number of vertical strips of width zero. Thus, we have shown that

$$\begin{aligned}
\Lambda_- &= \bigcap_{n=1}^{\infty} \mathbf{F}^n(H_0 \cup H_1) \\
&= \bigcup_{\substack{s_{-i}\in\{0,1\}\\ i=1,2,\ldots}} (V_{s_{-1}} \cap \mathbf{F}(V_{s_{-2}s_{-3}\ldots s_{-k}\ldots}))
\end{aligned}$$

$$= \bigcup_{\substack{s_{-i}\in\{0,1\}\\ i=1,2,...}} V_{s_{-1}s_{-2}s_{-3}...s_{-k}...}$$

$$= \{p \in \mathbf{S} : \mathbf{F}^{-i+1}(p) \in V_{s_{-i}},\ s_{-i} \in \{0,1\},\ i = 1,2,3,...\}. \tag{5.16}$$

This set consists of an infinite number of vertical lines and each line can be labelled by a unique infinite sequence of $0'$s and $1'$s .

Since each horizontal line in Λ_+ and each vertical line in Λ_- are intersected in a unique point, then equation (5.4) indicates that the invariant set Λ consists of an infinite set of points and each point $x \in \Lambda$ can be labelled uniquely by a bi-infinite sequence of $0's$ and $1's$. From equation (5.10) and (5.16), we can describe the invariant set Λ as follows

$$\begin{aligned}
\Lambda =& \Lambda_+ \cap \Lambda_- \\
=& \bigcup_{\substack{s_{\mp i}\in\{0,1\}\\ i=0,1,2,...}} (H_{s_0s_1s_3....} \cap V_{s_{-1}s_{-2}s_{-3}....}) \\
=& \{p \in \mathbf{S} : \mathbf{F}^{i}(p) \in H_{s_i},\ i = 0, \pm1, \pm2,\ ...\} \qquad (5.17)\\
& \text{since} \quad \mathbf{F}(H_{s_i}) = V_{s_i}.
\end{aligned}$$

Now, we explain the direct relationship between any point $p \in \Lambda$ and the bi-infinite sequence of $0'$s and $1'$s. Let $s_{-1}s_{-2}...s_{-k}...$ be a particular infinite sequence of $0'$s and $1'$s, then $V_{s_{-1}s_{-2}...s_{-k}...}$ corresponds to a unique vertical line. We let $s_0s_1s_2...s_k...$ be another particular infinite sequence of $0'$s and $1'$s, then $H_{s_0s_1s_2...s_k...}$ be a unique horizontal line. Since each vertical line intersects each horizontal line in a unique point p, then there is a well-defined map from $p \in \Lambda$ to infinite sequence of $0'$s and $1'$s, which is called the *itinerary map I*.

To present symbolic dynamics into the horseshoe map $\mathbf{F}$, a doubly infinite sequence (bi-infinite sequences) of $0's$ and $1's$ corresponding to each point in Λ

will be chosen. For $x \in \Lambda$, the itinerary map I from Λ into sequence space Σ where

$$\Sigma = \{s = (...s_{-2}s_{-1}.s_0s_1s_2...), s_i = 0, \text{or } 1\}$$

is defined by

$$I(x) = (...s_{-2}s_{-1}.s_0s_1s_2...)$$

where $s_i = 0$ or 1, $s_i = k$ if and only if $\mathbf{F}^i(x) \in H_k$ and the decimal point refers to separate the forward and backward parts of the sequences. We define the shift map $\sigma : \Sigma \to \Sigma$ as follows

$$s = (...s_{-2}s_{-1}.s_0s_1s_2...) \in \Sigma$$
$$\sigma(s) = (...s_{-2}s_{-1}s_0.s_1s_2...)$$

or, more compactly,

$$(\sigma(s))_i = s_{i+1}$$

that is the map σ shifts each sequence in Σ one unit to the left. This map has inverse, shifting one unit to the right gives us its inverse and also the map is chaotic in Σ (see (Wiggins, 2003)). Suppose $x \in \Lambda$ and $I(x) = (...s_{-2}s_{-1}.s_0s_1s_2...)$, then we have $x \in H_{s_0}, \mathbf{F}(x) \in H_{s_1},\ \mathbf{F}^{-1}(x) \in H_{s_{-1}}$ and so forth. And also we have $\mathbf{F}(x) \in H_{s_1},\ \mathbf{F}(\mathbf{F}(x)) \in H_{s_2},\ x = \mathbf{F}^{-1}(\mathbf{F}(x)) \in H_{s_0}$ and so forth. Therefore,

$$I(\mathbf{F}(x)) = (...s_{-2}s_{-1}s_0.s_1s_2...) = \sigma(I(x))$$
$$I \circ \mathbf{F} = \sigma \circ I \quad \Rightarrow \quad \mathbf{F} = I^{-1} \circ \sigma \circ I.$$

This is a conjugacy equation, this means that the itinerary map I gives a topological conjugacy between the shifting map σ on Σ and the horseshoe map $\mathbf{F}$ on Λ. Since the itinerary map $I : \Lambda \to \Sigma$ is a homomorphism (for the proof see (Wiggins, 1992, 2003)), then the orbit of $x \in \Lambda$ under the horseshoe map $\mathbf{F}$ and the orbit $I(x)$ under the shift map σ in Σ are directly corresponding. This means that the whole orbit structure of σ on Σ and $\mathbf{F}$ on Λ are identical. Therefore, the horseshoe map $\mathbf{F}$ is chaotic in the invariant set Λ (Wiggins, 2003).

5.3 The Shilnikov Phenomena

In this section, we consider a three dimensional system in which there is a homoclinic loop to a saddle-focus critical point.

5.3.1 Saddle-Focus and Saddle Index

We consider a three dimensional system of the form

$$\begin{aligned} \dot{x} &= \mu x - \omega y + F_1(x, y, z), \\ \dot{y} &= \omega x + \mu y + F_2(x, y, z), \\ \dot{z} &= \lambda z + F_3(x, y, z), \end{aligned} \tag{5.18}$$

where $F_i,\ i = 1, 2, 3$ are real analytic functions in the neighbourhood of the origin in $\mathbb{R}^3$ and with their derivatives vanish at the origin. It is clear that the origin is a critical point of saddle type and the eigenvalues of (5.18) linearized about the origin are given by $\lambda_{1,2} = \mu \pm \omega i,\ \omega \neq 0$ and $\lambda_3 = \lambda$. We assume that

$$\lambda > -\mu > 0\ ,$$

by this algebraic assumption, the saddle-focus critical point at the origin possesses a two dimensional stable manifold, W^s, which is a surface that is tangent to the plane $z = 0$ and a one dimensional unstable manifold, W^u, which is a curve that is tangent to the $z-$axis at the origin. The unstable manifold consists of the origin and two separatrices that tend to the point as $t \longrightarrow -\infty$. If we restrict the system to the stable manifold only, the above assumption indicates that the critical point at the origin will be a stable focus, i.e. when $t \longrightarrow +\infty$ the orbits on the stable manifold, W^s, spiral onto the critical point. Therefore, in the full system, the critical point at the origin is called a *saddle-focus*. The second assumption, which is a geometric assumption, is that equation (5.18) possesses a homoclinic orbit Γ connecting the origin to itself which is a trajectory bi-asymptotic to the origin as $t \longrightarrow \pm\infty$ ($\Gamma \in W^s \cap W^u$). Now, we introduce the other ingredients of the Shilnikov phenomena which are saddle index $\upsilon = -\dfrac{\mu}{\lambda}$ and saddle value (saddle quality) $\sigma = \mu + \lambda$. Depending on the sign of the saddle value σ, or whether the saddle index υ is less or greater than 1, the dynamics of (5.18) near the homoclinic loop Γ is simple if the saddle index υ is greater than 1 (saddle value $\sigma < 0$) (Shilnikov, 1963), or complex if the saddle index υ is less than 1 (saddle value $\sigma > 0$). The condition $\upsilon < 1$ ($\sigma > 0$) is known as the Shilnikov condition.

5.3.2 Poincaré Map

In order to analyse the nature of the orbit structure near the homoclinic loop Γ, we construct a two dimensional Poincaré map $\mathbf{T}$ on a small cross-section Π_1 perpendicular to Γ at M^+. This map is obtained by dividing the trajectory close to the critical point at the origin and its unstable manifold. The first part is the local map $\mathbf{T}_1$ which is defined by trajectories near the origin which takes points from Π_1 to the second cross-section Π_2. This second cross-section Π_2 is transversal to unstable manifold, W^u, (parallel to the stable manifold W^s) which intersects

Γ at M^- . The second part, the global map $\mathbf{T}_2$, is defined by trajectories close to Γ and takes points on Π_2 and brings them back to Π_1. The composition of $\mathbf{T}_1$ and $\mathbf{T}_2$ constructs the Poincaré map $\mathbf{T}$, i.e. $\mathbf{T} = \mathbf{T}_2 \circ \mathbf{T}_1$.

We observe that the stable manifold, W^s, breaks the cross section Π_1 into the top Π_1^+ and bottom Π_1^- components. The orbits that start at the bottom part Π_1^- leave a small neighbourhood of the origin in the opposite direction of the loop Γ and therefore do not intersect Π_2. The orbits that start at the upper part Π_1^+, will intersect Π_2 and then follow the loop Γ until they return to Π_1. If the returning orbits intersect Π_1^-, then they leave the neighbourhood of Γ; otherwise they follow the loop Γ to construct another circuit and return to Π_1 and so forth. Hence, the map $\mathbf{T}_1$ is defined only on the top part Π_1^+ ($\mathbf{T}_1 : \Pi_1^+ \longrightarrow \Pi_2$). Let Π_1 and Π_2 be two rectangles are defined as follows

$$\Pi_1 = \{(x, y, z) \in \mathbb{R}^3 \mid x = 0,\ \epsilon e^{\frac{2\pi\mu}{\omega}} \leq y \leq \epsilon,\ 0 < z \leq \epsilon\}$$
$$\Pi_2 = \{(x, y, z) \in \mathbb{R}^3 \mid z = \epsilon\}.$$

The cross-section Π_1 is taken as a small rectangle on $yz-$plane, such that each trajectory only strikes Π_1 once when it spirals into the origin. The flow generated by (5.18) linearized about the origin which starts from $(0, y, z)$ at $t = 0$ and ends at $z = \epsilon$ at $t = \tau$ must satisfy the relation

$$\begin{pmatrix} x(\tau) \\ y(\tau) \end{pmatrix} = e^{\tau\begin{pmatrix} \mu & -\omega \\ \omega & \mu \end{pmatrix}} \begin{pmatrix} 0 \\ y \end{pmatrix} = e^{\mu\tau} \begin{pmatrix} \cos(\omega\tau) & -\sin(\omega\tau) \\ \sin(\omega\tau) & \cos(\omega\tau) \end{pmatrix} \begin{pmatrix} 0 \\ y \end{pmatrix} \tag{5.19}$$
$$z = \epsilon e^{-\lambda\tau}.$$

The time τ from $(0, y, z) \in \Pi_1$ to Π_2 which is called the flight time is given by

$\tau = \frac{-1}{\lambda}\ln(\frac{z}{\epsilon})$. Substituting this expression into equation (5.19), we obtain the formula for the local map $T_1 : \Pi_1 \longrightarrow \Pi_2$ which is given by

$$T_1 : \begin{pmatrix} y \\ z \end{pmatrix} \mapsto \begin{pmatrix} x_1 \\ y_1 \end{pmatrix} = y\left(\frac{z}{\epsilon}\right)^v \begin{pmatrix} \sin(\frac{\omega}{\lambda}\ln(\frac{z}{\epsilon})) \\ \cos(\frac{\omega}{\lambda}\ln(\frac{z}{\epsilon})) \end{pmatrix}, \tag{5.20}$$

where $z > 0$ and v be a saddle index. From the above equation, we can see that the image $T_1(\Pi_1^+)$ on the cross-section Π_2 spirals onto the point M^- as we see in Figure 5.3. The global map T_2 maps this spiral difformorphically into the cross-section Π_1 and takes the point M^- on Π_2 to the point M^+ on Π_1. This map also preserves the spiralling shape too. It intersects the stable manifold, W^s, infinitely many times close to M^+. Combing the local and global maps, the Poincaré return map $T = T_2 \circ T_1$ is obtained. We strip Π_1^+ down into a countable number of the segments Σ_k provided that the image of the segment Σ_k and the bounded region between the segment and its successive segment Σ_{k+1} spirals rotate to 2π in the x_1y_1-plane. The global map T_2 sends the image of $T_1(\Sigma_k)$ to the half-curl on Π_1^+ and it also brings the image of $T_1(\Sigma_{k^*})$ (where Σ_{k^*} is a bounded region of Σ_k *and* Σ_{k+1}) to the next half-curl on Π_1^- (see Figure 5.3). The relation between the position $z \sim z_k$ of Σ_k (distance of the top of Σ_k from the stable manifold W^s) and its image under the local map T_1 (distance of $T_1(z_k)$ of the half-curl $T_1(\Sigma_k)$ from the origin in Π_2) is follows

$$T_1(z_k) \sim z_k^v.$$

Since the global map T_2 preserves the distance i.e. the distance of the half-curl in Π_1^+ from M^+ is of the same order, then

$$T(z_k) \sim z_k^v.$$

Suppose $z_k = e^{\frac{-2\pi k}{\omega}}$, $k = 1, 2, 3, ...$, then $T(z_k) \sim e^{\frac{-2\pi k \upsilon}{\omega}}$. Thus, when $\upsilon > 1$, there is no intersection between the segment Σ_k and $T(\Sigma_k)$, in this case the image of Σ_k lies below its pre-image. On the contrary, when $\upsilon < 1$, for each k large enough the intersection of Σ_k with its image $T(\Sigma_k)$ is non-empty and consists of two connected components. This leads to a form Smale horseshoe, thus the chaos in the return map is defined near the homoclinic orbit. This is geometrically evidence for having fixed point on each components of the Poincaré return map, T. We recall that a fixed point of the Poincaré return map corresponds to a periodic orbit of the system. As a result, if the saddle index $\upsilon < 1$ (or saddle value $\sigma > 0$), then there exist infinitely many saddle periodic orbits in any neighbourhood of the homoclinic loop Γ. For more detailed justification on this subject the reader should consult references (Glendinning and Sparrow, 1984; Shilnikov et al., 2001).

In this thesis, we try to construct an example of a three dimensional Lotka-Volterra system to apply these ideas. Since the 3DLVS has always three invariant planes, therefore none of the planar critical points have a homoclinic loop. However, by using some specific parameters, we try to construct a loop connecting three critical points so that the product of their ratio of eigenvalues around the loop is less than 1. This condition plays the same role as the Shilinikov condition.

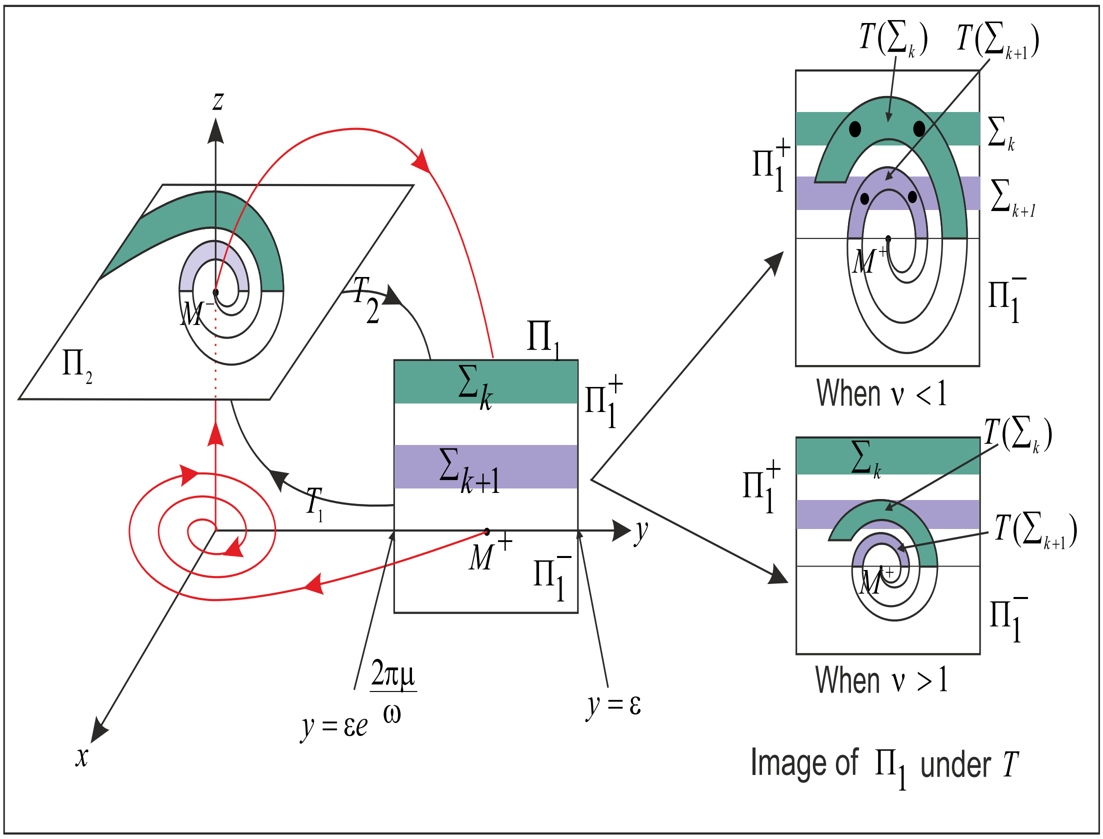

Figure 5.3: The Shilnikov phenomena.

Chapter 6

The Existence of Horseshoe Dynamics in 3DLVS

This chapter focuses on the chaotic behaviour of the three dimensional Lotka-Volterra system. The sufficient conditions on parameters for the existence of the horseshoe map for the three dimensional Lotka-Volterra system were obtained.

6.1 A Heteroclinic Cycle

In this chapter, we consider the three dimensional Lotka-Volterra system

$$\begin{aligned} \dot{x_1} &= x_1(r_1 - x_1 - x_2 - x_3), \\ \dot{x_2} &= x_2(r_2 - 2x_1 + \frac{5}{2}x_2 + a_{2,3}x_3), \\ \dot{x_3} &= x_3(r_3 + x_1 - 3x_2 - x_3). \end{aligned} \tag{6.1}$$

The main goal in this section is to investigate the heteroclinic cycle that connects the following three critical points:

$$A_1(\frac{r_1 - r_3}{2}, 0, \frac{r_1 + r_3}{2}), \quad A_2(\frac{5r_1 + 2r_2}{9}, \frac{4r_1 - 2r_2}{9}, 0) \quad \text{and} \quad A_3(r_1, 0, 0).$$

For the sake of simplicity, we can scale such that the first planar critical point is $A_1(1,0,1)$ in this case $r_1 = 2$ and $r_3 = 0$.

In the first subsection below, a line that connects A_1 to A_2 is found and it satisfies the conditions of invariant and non-singularity of the line. In the two subsequent subsections, isoclines are used to collect some information of the orbit directions. This information is useful to show that the three dimensional Lotka-Volterra system in this study has a heteroclinic orbit.

6.1.1 A Heteroclinic Orbit Between Two Different Planar Critical Points

In this subsection, some conditions on the parameters of the three dimensional Lotka-Volterra system have been found for a heteroclinic orbit that joins two planar critical points to exist. A line C is called an invariant of system (6.1) if any trajectory which starts in or enters C and remains in C. This is equivalent to the vector field (6.1) and the direction vector for the given line being parallel and have a zero cross product. Such a line is a heteroclinic orbit if it joins two critical points.

The line that joins the two above planar critical points A_1 and A_2 is defined by:

$$\begin{aligned}
x_1 &= 1 + \frac{1}{9}(2r_2 + 1)t, \\
x_2 &= \frac{2}{9}(4 - r_2)t, \\
x_3 &= 1 - t \ , \quad t \in [0, 1] \, .
\end{aligned}$$

The above line is invariant if the following conditions are held:

$$a_{2,3} = \frac{9}{2} \quad \text{and} \quad r_2 = -\frac{1}{2}.$$

After scaling the first planar critical point A_1 and applying the above invariant conditions, the three critical points and the invariant line will be:
$A_1(1,0,1),\ A_2(1,1,0),\ A_3(2,0,0)$ and

$$x_1 = 1,\ x_2 = t,\ x_3 = 1 - t,\ t \in [0,1]\,. \tag{6.2}$$

The above line is a heteroclinic orbit that joins the two planar critical points A_1 and A_2.

6.1.2 A Planar Heteroclinic Orbit on the x_1x_2-plane

To show that the three dimension Lotka-Volterra system (6.1) has a heteroclinic orbit on x_1x_2-plane that connecting the planar critical point A_2 and axial critical point A_3 we study the isoclines. That is, the lines with equal slope. These lines are used to help to draw the phase portrait. It is easy to know where the trajectories have vertical and horizontal tangent lines by finding the isoclines for $\dot{x}_1 = 0$ and $\dot{x}_2 = 0$. If $\dot{x}_1 = 0$ and $\dot{x}_2 = 0$, then there are no motion horizontally and vertically respectively. The vertical trajectories are given by $x_1 = 0$, and $x_1 + x_2 = 2$ which are obtained from $\dot{x}_1 = 0$ and the horizontal trajectories are given by $x_2 = 0$ and $4x_1 - 5x_2 = -1$ which are obtained from $\dot{x}_2 = 0$.

Since the planar critical point A_2 is in the first quadrant in x_1x_2-plane, we are interested in collecting the information in the first quadrant. We fix a value of x_1 and suppose x_2 is above the isocline $x_1 + x_2 = 2$, in this case we can write $x_2 = 2 - x_1 + \epsilon,\ \epsilon \in \mathbb{R}^+$ and we obtain $\dot{x}_1 = -\epsilon x_1 < 0$. The reverse holds if x_2 is below the line, in this case $\dot{x}_1 = \epsilon x_1 > 0$. Similarly, if x_2 is above the line $4x_1 - 5x_2 = -1$ which is obtained from $\dot{x}_2 = 0$, then $\dot{x}_2 = \frac{5}{2}\epsilon x_2 > 0$, with the opposite being true when x_2 is below i.e. $\dot{x}_2 = -\frac{5}{2}\epsilon x_2 < 0$.

When a trajectory of the system crosses an isocline, it is either horizontal or vertical because either $\dot{x}_1$ or $\dot{x}_2$ is zero there. Moreover, with $x_1 = 0$, one seems that $\dot{x}_2 < 0$ when $x_2 \in (0, \frac{1}{5})$ and $\dot{x}_2 > 0$ when $x_2 > \frac{1}{5}$ and $x_2 < 0$. A similar result holds when $x_2 = 0$ in this case $\dot{x}_1 > 0$ when $0 < x_1 < 2$, otherwise $\dot{x}_1 < 0$. Now we have sufficient information to sketch the orbit directions of the system. The vertical and horizontal information on the isoclines tell us how arrows must bend. As shown in Figure 6.1, any separatrix of A_2 passing through the region that is bounded by the four isoclines in x_1x_2-plane tends toward the critical point A_3. This separatrix is called heteroclinic orbit and its image is depicted by a dotted curve (see Figure 6.1).

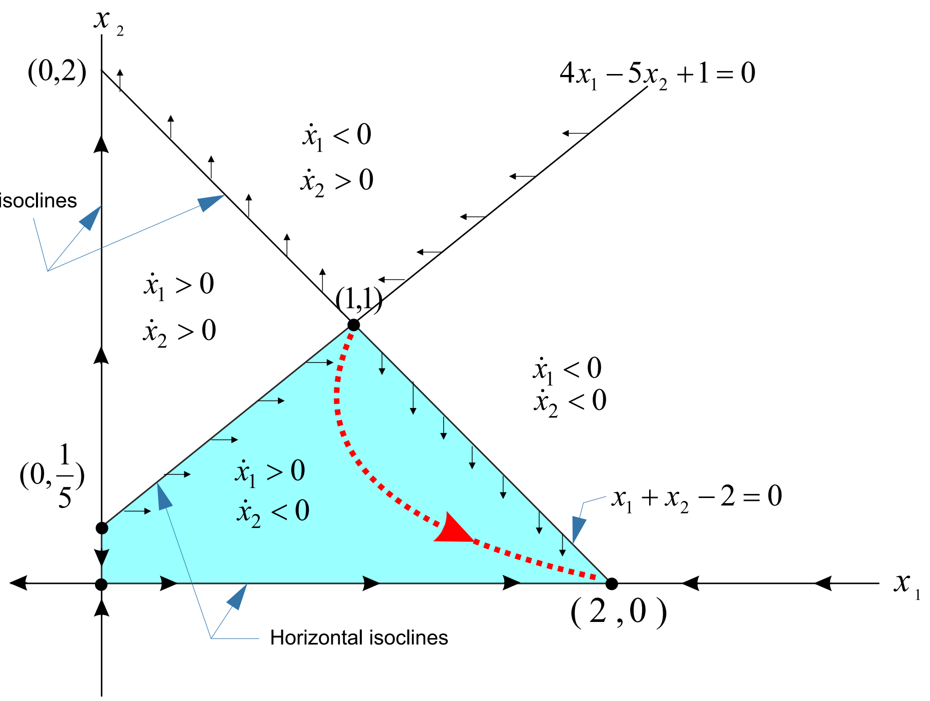

Figure 6.1: Isoclines and their analysis for system (6.1) on x_1x_2-plane with heteroclinic orbit that connects the two critical points A_2 and A_3 which is depicted by a dotted curve.

6.1.3 A Planar Heteroclinic Orbit on the x_1x_3-plane

To show that a heteroclinic orbit that connects the axial critical point A_3 with the planar critical point A_1 exist, we consider the isoclines again. The vertical trajectories are given by $x_1 = 0$, $x_1 + x_3 = 2$ and the horizontal trajectories are given by $x_3 = 0$, $x_1 - x_3 = 0$ which are obtained from $\dot{x}_1 = 0$ and $\dot{x}_3 = 0$ respectively.

Since the planar critical point A_1 is belong to the first quadrant of x_1x_3-plane, we are only interested in collecting the information in the first quadrant. We fix a value of x_1 and suppose x_3 is above the isocline $x_1 + x_3 = 2$, in this case we can write $x_3 = 2 - x_1 + \epsilon,\ \epsilon \in \mathbb{R}^+$ and we obtain $\dot{x}_1 = -\epsilon x_1 < 0$ but if x_3 is below the isocline, $\dot{x}_1 = \epsilon x_1 > 0$ is obtained. Similarly, if x_3 is above the isocline $x_1 - x_3 = 0$, then $\dot{x}_3 = -\epsilon x_3 < 0$ and if x_3 is below the isocline then $\dot{x}_3 = \epsilon x_3 > 0$ will be obtained. This means that the trajectory that starts in this region spiral toward A_1.

In addition to the above information, to sketch the phase portrait, the orbit directions information on the axial isoclines are needed. On the axial isoclines $x_1 = 0$ and $x_3 = 0$ the following information are obtained. On the line $x_1 = 0$ always $\dot{x}_3$ is negative and on the line $x_3 = 0,\ \dot{x}_1$ is positive where $0 < x_1 < 2$ otherwise it is negative. After combining these information, sufficient information for sketching the orbit directions are obtained which are shown in Figure 6.2. The spiral orbit that connects the axial critical point A_3 with planar critical point A_1 is the heteroclinic orbit.

Combining the three heteroclinic orbits which are obtained from the above subsections give us the heteroclinic cycle (see Figure 6.3).

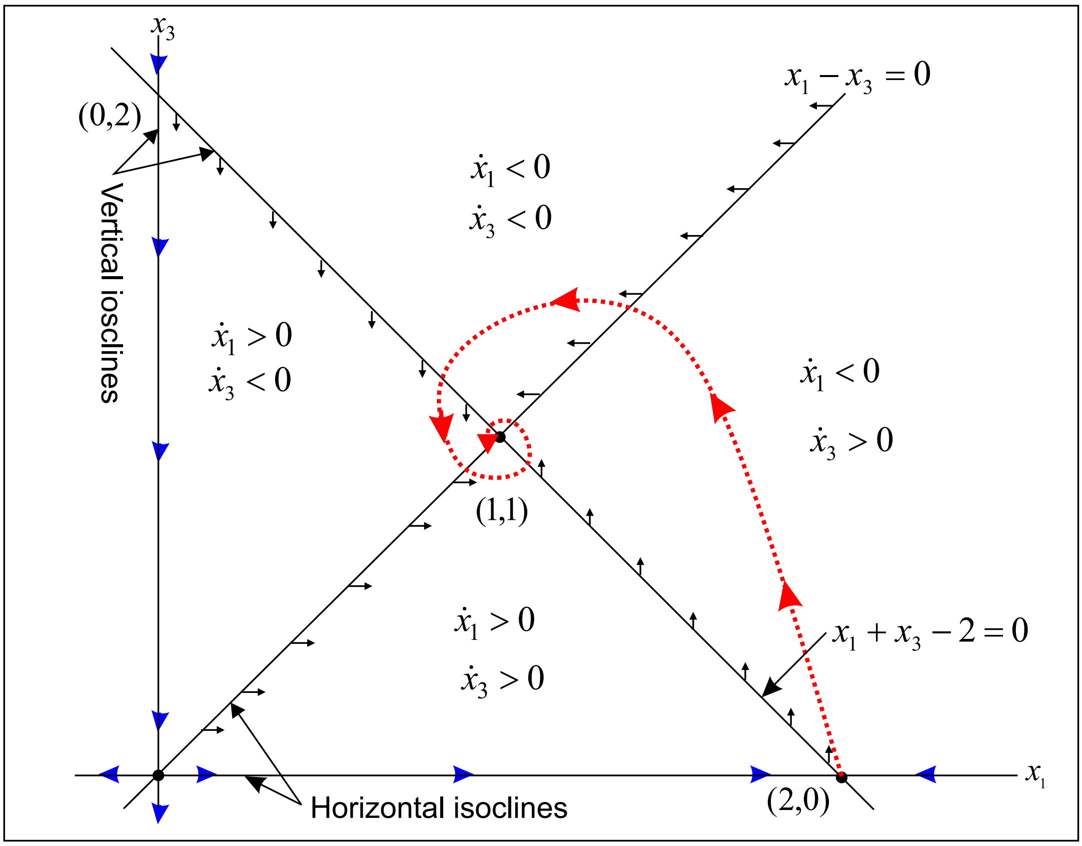

Figure 6.2: Isoclines and their analysis for system (6.1) on x_1x_3-plane with heteroclinic orbit that connects the two critical points A_3 and A_1 which is depicted by a dotted curve.

6.2 The Local Study of Trajectories

In this section, we investigate the local behaviour of the three dimensional Lotka-Volterra system that possesses a heteroclinic cycle joining the three critical points, they are of type planar saddle-focus, another planar saddle and the third of type axial saddle. Here, we do not examine the full system. Instead, a linear part of the three dimensional system in a neighbourhood of the critical points is studied. According to the Grobman-Hartman Theorem (Zhang, 2005) the nonlinear and its linear system are locally topologically equivalent near the hyperbolic critical points, for the sake of simplicity we assume that the three dimensional system (6.1)

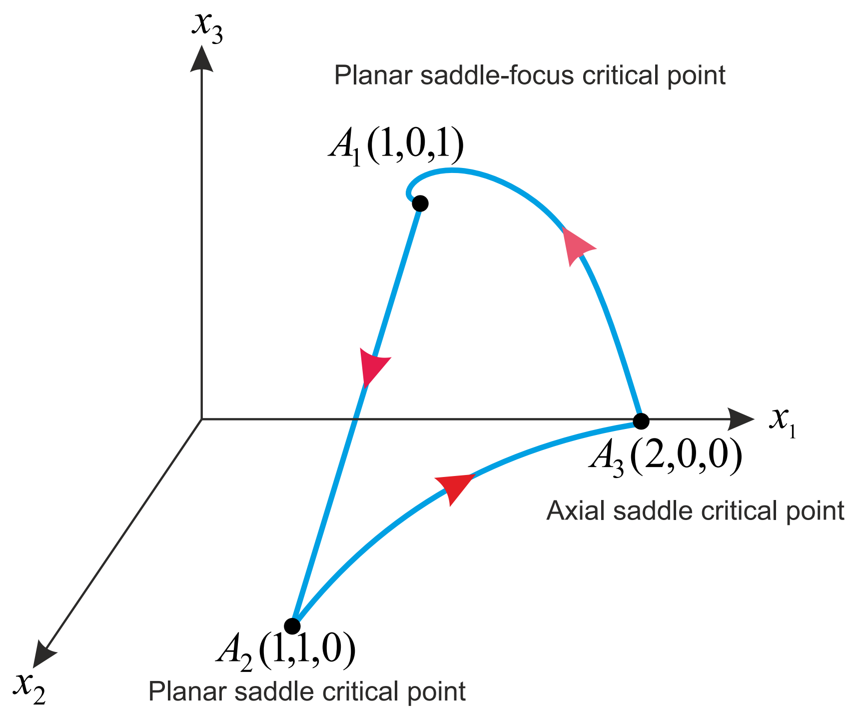

Figure 6.3: The Heteroclinic cycle connecting the three critical points.

is linear near the three chosen critical points. The study of the expected phenomena depends on the qualitative properties of the linear system and the heteroclinic assumption.

6.2.1 Planar Saddle-Focus Critical Point

In this subsection, the local behaviour of trajectories of the three dimensional Lotka-Volterra system in a small neighbourhood of the critical point A_1 is studied. A linear system of the three dimensional system in a certain cylindrical neighbourhood of the planar saddle-focus critical point A_1 is analyzed. In this case, the system has two complex eigenvalues $\mu \pm \omega i$ where $\mu < 0$, $\omega \neq 0$ and positive eigenvalue λ, provided that $\lambda > -\mu$ (Shilnikov condition). Then, the system has a two-dimensional stable surface which lies on x_1x_3-plane on which the trajectories spiral toward the critical point and a one-dimensional unstable curve which is a heteroclinic orbit that joins the two planar critical points.

The linearized system of the three dimensional Lotka-Volterra system (6.1) at $A_1(1,0,1)$ is given by

$$\begin{aligned} \dot{x}_1 &= -x_1 - x_2 - x_3, \\ \dot{x}_2 &= 2x_2, \\ \dot{x}_3 &= x_1 - 3x_2 - x_3. \end{aligned} \tag{6.3}$$

We use the transformation

$$X_{old} = PX_{new}, \ P = \begin{bmatrix} 1 & 0 & 1 \\ 0 & -1 & 0 \\ -1 & 1 & 1 \end{bmatrix},$$

where $X_{old} = (x_1, x_2, x_3)$ and $X_{new} = (y_1, y_2, y_3)$. Then, system (6.3) can be transformed to the normal form

$$\begin{aligned} \dot{y}_1 &= -y_1 - y_3, \\ \dot{y}_2 &= 2y_2, \\ \dot{y}_3 &= y_1 - y_3. \end{aligned} \tag{6.4}$$

The associated eigenvalues are $\mu \pm i\omega$ and λ where $\mu = -1,\ \omega = 1$ and $\lambda = 2$, hence the origin is a saddle-focus critical point. To analyse the flow near the critical point, we introduce the cylindrical region S_1 of $\mathbb{R}^3$ given by $y_1^2 + y_3^2 \leq r_o^2$ and $0 \leq y_2 \leq a$. The flow ϕ_t generated by system (6.4) is given by

$$\begin{aligned} y_1(t) &= e^{\mu t}(y_1^0 \cos(\omega t) - y_3^0 \sin(\omega t)), \\ y_2(t) &= y_2^0 e^{\lambda t}, \end{aligned} \tag{6.5}$$

$$y_3(t) \quad = \quad e^{\mu t}(y_1^0 \sin(\omega t) + y_3^0 \cos(\omega t)).$$

Using polar coordinates in the y_1y_3-plane where $y_1 = r\cos(\theta)$ and $y_3 = r\sin(\theta)$, solutions in S_1 are given by

$$\begin{aligned} r(t) &= r_0 e^{\mu t}, \\ y_2(t) &= y_2^0 e^{\lambda t}, \\ \theta(t) &= \theta_0 + \omega t. \end{aligned} \tag{6.6}$$

This system has a one dimensional unstable manifold lying on the y_2-axis and a two dimensional stable manifold lying on y_1y_3-plane. Note that the boundary of the cylindrical region S_1 consists of two pieces: the upper disk D_1 given by $y_2 = a,\ r \leq r_0$, where $a \in \mathbb{R}^+$, which can be parametrized by r and θ, and the cylindrical boundary C given by $r = r_0,\ 0 \leq y_2 < a$, which can be parametrized by θ and y_2.

Depending on the eigenvalues, any solution of this system originating in C must eventually leave S_1 through D_1 and it has the shape of a spiral. Hence, we can define a map $\Psi_1 : C \to D_1$ given by following solution curves starting in C until they first meet D_1. We denote the time taken for the solution curves to passes from a point (y_2^0, θ_0) in C to D_1 by $T = T(y_2^0,\ \theta_0)$. We compute directly from the second equation in (6.6) that $T = -\ln(\sqrt[\lambda]{y_2^0/a})$. Clearly, the time increases logarithmically when the initial point goes closer to the stable manifold. Thus, we obtain

$$\Psi_1 : \begin{pmatrix} r_0 \\ \theta_0 \\ y_2^0 \end{pmatrix} \mapsto \begin{pmatrix} r_1 \\ \theta_1 \\ a \end{pmatrix}, \tag{6.7}$$

where $r_1 = r_0(\sqrt[\lambda]{y_2^0/a})^{-\mu}$, $\theta_1 = \theta_0 - \omega \ \ln(\sqrt[\lambda]{y_2^0/a})$ and (r_1, θ_1) are polar the coordinates on D_1. We note that the map Ψ_1 brings the vertical line $\theta = \theta^*$ in C to the spiral in D_1:

$$y_2^0 \to (r_0(\sqrt[\lambda]{y_2^0/a})^{-\mu},\ \theta^* - \omega \ \ln(\sqrt[\lambda]{y_2^0/a})). \tag{6.8}$$

Since, as $y_2^0 \to 0$ in equation (6.8), $\ln(\sqrt[\lambda]{y_2^0/a}) \to -\infty$ and $\theta^* - \omega \ \ln(\sqrt[\lambda]{y_2^0/a}) \to \infty$, the image of the vertical line $\theta = \theta^*$ spirals down to the point $r_1 = 0$ in D_1. Geometrically, the circles $y_2 = \Gamma$ in C are mapped by Ψ_1 to circles $r_1 = r_0(\sqrt[\lambda]{\Gamma/a})^{-\mu}$ centred at $r_1 = 0$ in D_1.

In another way, in order to know what the image of any strips look like, we introduce two cross sections. The first one, Π_0, lies in the y_1y_2-plane and the second one, Π_1, is parallel to y_1y_3-plane (it coincides with D_1). The flow, ϕ_t, generated by system (6.4) is also given by (6.5) where (y_1^0, y_2^0, y_3^0) lies in Π_0 and the flight time of trajectories starting on Π_0 to reach Π_1 is also given by $T = \ln(\sqrt[\lambda]{\frac{a}{y_2^0}})$. Thus the map $\Psi_1^1 : \Pi_0 \to \Pi_1$ is given by

$$\Psi_1^1 : \begin{pmatrix} y_1 \\ y_2 \\ 0 \end{pmatrix} \mapsto \begin{pmatrix} y_1 \left(\frac{a}{y_2}\right)^{\frac{\mu}{\lambda}} \cos(\frac{\omega}{\lambda} \ln \frac{a}{y_2}) \\ a \\ y_1 \left(\frac{a}{y_2}\right)^{\frac{\mu}{\lambda}} \sin(\frac{\omega}{\lambda} \ln \frac{a}{y_2}) \end{pmatrix}. \tag{6.9}$$

This map is not a diffeomorphism, hence we restrict it to the cross section Π_0 as follows

$$\Pi_0 = \left\{(y_1, y_2, y_3) \in \mathbb{R}^3 |\ y_3 = 0,\ ae^{\frac{2\pi\mu}{\omega}} \le y_1 \le a,\ 0 \le y_2 \le a\right\}. \tag{6.10}$$

Thus, the map $\Psi_1^1 : \Pi_0 \longrightarrow \Pi_1$ is a diffeomorphism . Now, we want to describe the geometry of $\Psi_1^1(\Pi_0)$ on Π_1. In polar coordinates, $\Psi_1^1(\Pi_0)$ is defined as follows

$$\begin{pmatrix} r \\ \theta \end{pmatrix} = \begin{pmatrix} y_1 \left(\frac{a}{y_2}\right)^{\frac{\mu}{\lambda}} \\ \frac{\omega}{\lambda} \ln \frac{a}{y_2} \end{pmatrix}. \tag{6.11}$$

From the above equation, we note the following. Firstly, a vertical line $y_1 =$ *constant* in Π_0 is mapped to a logarithmic spiral. Secondly, a horizontal line $y_2 =$ *constant* in Π_0 is mapped to a radial line emanating from the point $(0, a, 0)$. To illustrate this, we consider a closed set

$$R_k = \{(y_1, y_2, y_3) \in \mathbb{R}^3 |\ y_3 = 0, ae^{\frac{2\pi\mu}{\omega}} \leq y_1 \leq a,\ ae^{\frac{-2\pi(k+1)\lambda}{\omega}} \leq y_2 \leq ae^{\frac{-2\pi k\lambda}{\omega}}\}.$$

Studying the behaviour of the image of the horizontal and vertical boundaries of the closed set R_k gives us a geometric picture of the image of R_k under Ψ_1^1. We denote these four boundaries of R_k as

$$H^u = \{(y_1, y_2, y_3) \in \mathbb{R}^3 |\ y_3 = 0,\ y_2 = ae^{\frac{-2\pi k\lambda}{\omega}},\ ae^{\frac{2\pi\mu}{\omega}} \leq y_1 \leq a\},$$
$$H^l = \{(y_1, y_2, y_3) \in \mathbb{R}^3 |\ y_3 = 0,\ y_2 = ae^{\frac{-2\pi(k+1)\lambda}{\omega}},\ ae^{\frac{2\pi\mu}{\omega}} \leq y_1 \leq a\},$$
$$V^r = \{(y_1, y_2, y_3) \in \mathbb{R}^3 |\ y_3 = 0,\ ae^{\frac{-2\pi(k+1)\lambda}{\omega}} \leq y_2 \leq ae^{\frac{-2\pi k\lambda}{\omega}},\ y_1 = a\},$$
$$V^l = \{(y_1, y_2, y_3) \in \mathbb{R}^3 |\ y_3 = 0,\ ae^{\frac{-2\pi(k+1)\lambda}{\omega}} \leq y_2 \leq ae^{\frac{-2\pi k\lambda}{\omega}},\ y_1 = ae^{\frac{2\pi\mu}{\omega}}\}.$$

The image of these boundaries under Ψ_1^1 are given by

$$\Psi_1^1(H^u) = \{(r,\ \theta,\ y_2) \in \mathbb{R}^3 |\ y_2 = a,\ \theta = 2k\pi,\ ae^{\frac{2(k+1)\pi\mu}{\lambda}} \leq r \leq ae^{\frac{2k\pi\mu}{\lambda}}\},$$
$$\Psi_1^1(H^l) = \{(r,\ \theta,\ y_2) \in \mathbb{R}^3 |\ y_2 = a,\ \theta = 2(k+1)\pi,\ ae^{\frac{2(k+2)\pi\mu}{\lambda}} \leq r \leq ae^{\frac{2(k+1)\pi\mu}{\lambda}}\},$$
$$\Psi_1^1(V^r) = \{(r,\ \theta,\ y_2) \in \mathbb{R}^3 |\ y_2 = a,\ 2k\pi \leq \theta \leq 2(k+1)\pi,\ r = ae^{\frac{\mu}{\omega}\theta}\},$$
$$\Psi_1^1(V^l) = \{(r,\ \theta,\ y_2) \in \mathbb{R}^3 |\ y_2 = a,\ 2k\pi \leq \theta \leq 2(k+1)\pi,\ r = ae^{(2\pi+\theta)\frac{\mu}{\omega}}\}.$$

The closed set R_k and its horizontal and vertical boundaries are displayed in Figure 6.5. The geometry of this figure is a fundamental part of showing that a horseshoe map may happen in the three dimensional system (6.1).

From equation (6.6), we note that the ratio of the eigenvalues between the stable and unstable manifold is $\frac{-\mu}{\lambda}$. We denote the distance of the upper bound of a strip on the cylindrical boundary C from the stable manifold by h_1 (it means $y_2 = h_1$) and the distance of its image under Ψ_1 on D_1 from the unstable manifold by h_2 (it means $r_1 = h_2$). Thus, equation (6.8) indicates that

$$h_2 = k_1 h_1^{\frac{-\mu}{\lambda}}, \tag{6.12}$$

where k_1 is a positive constant. This is shown in Figure 6.4.

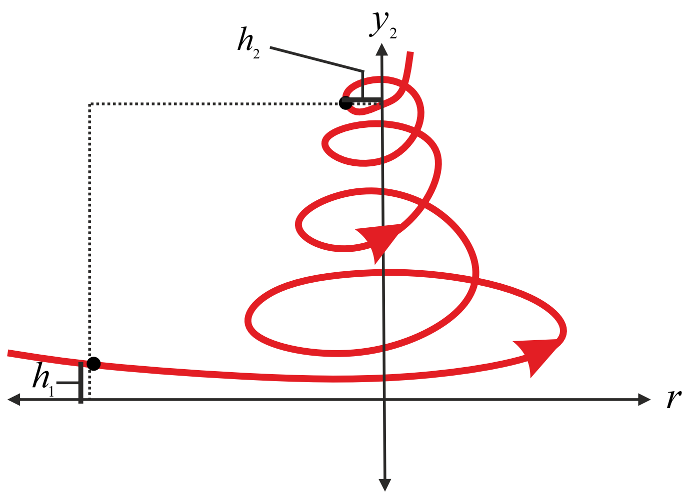

Figure 6.4: The behaviour of trajectories near the planar saddle-focus critical point where the ratio of the eigenvalues around the point is equal to $\frac{-\mu}{\lambda}$.

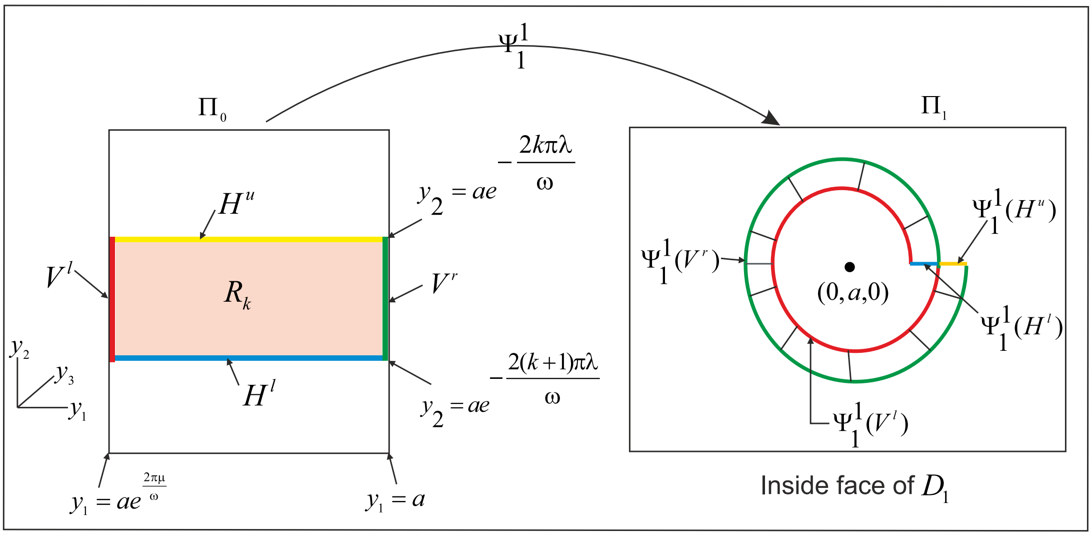

Figure 6.5: The boundaries of the closed region R_k with their images under Ψ_1^1.

6.2.2 Planar Saddle Critical Point

In order to study the local behaviour of trajectories of the three dimensional Lotka-Volterra system (6.1) in a small neighbourhood of the planar critical point A_2, we use a linear change of coordinates to transform the system to normal form. The linearized system at the critical point is given by

$$
\begin{aligned}
\dot{x}_1 &= -x_1 - x_2 - x_3, \\
\dot{x}_2 &= -2x_1 + \frac{5}{2}x_2 + \frac{9}{2}x_3, \\
\dot{x}_3 &= -2x_3.
\end{aligned}
\tag{6.13}
$$

We apply the linear change of coordinates

$$
X_{old} = PX_{new}, \;\; P = \begin{bmatrix} 2 & 1 & 0 \\ 1 & -4 & -1 \\ 0 & 0 & 1 \end{bmatrix}, \tag{6.14}
$$

where $X_{old} = (x_1, x_2, x_3)$ and $X_{new} = (y_1, y_2, y_3)$, to bring system (6.13) to the normal form:

$$\begin{aligned}
\dot{y}_1 &= \alpha_1 y_1, \\
\dot{y}_2 &= \alpha_2 y_2, \\
\dot{y}_3 &= -\lambda y_3,
\end{aligned} \tag{6.15}$$

the associated eigenvalues are α_1, α_2 and $-\lambda$ where $\alpha_1 = -\frac{3}{2}$, $\alpha_2 = 3$ and $\lambda = 2$, hence the origin is a saddle critical point. We note that system (6.15) has one positive and two negative eigenvalues, therefore it has a one-dimensional unstable manifold (the unstable subspace E^u coincides with the y_2-axis) and a two dimensional stable manifold (the stable subspace E^s is the y_1y_3-plane). We recall the extended stable invariant subspace E^{se} and the extended unstable invariant subspace E^{ue} as follows

$$E^{se} = E^s \oplus E^{uL},$$
$$E^{ue} = E^u \oplus E^{sL},$$

where $\oplus$ is a direct sum and E^{uL}, E^{sL} are unstable and stable leading respectively. Furthermore, the leading subspace, E^L, is defined by $E^L = E^{se} \cap E^{ue}$. Here, the y_1-axis is the stable leading subspace E^{sL} and y_3-axis is the stable non-leading subspace E^{ss}. The extended stable subspace E^{se} is the entire space $\mathbb{R}^3$ and y_1y_2-plane is the extended unstable invariant subspace, E^{ue}, and is also the leading subspace, E^L.

In a small neighbourhood of the origin we introduce two cross sections

$$S_2 = \left\{(y_1,\ y_2,\ y_3) \in \mathbb{R}^3 : |y_1| \leq \epsilon,\ |y_2| \leq \epsilon,\ y_3 = \epsilon\right\},$$
$$D_2 = \left\{(y_1,\ y_2,\ y_3) \in \mathbb{R}^3 : |y_1| \leq \delta,\ y_2 = \delta,\ 0 \leq y_3 \leq \delta\right\}, \quad \delta,\ \epsilon \in \mathbb{R}^+$$

as a transverse to the stable manifold and unstable manifold respectively. The stable manifold of A_2 divides the cross section S_2 into three parts which are denoted by S_2^0 S_2^+ and S_2^-. The first portion S_2^0 is the set of all points on S_2 belonging to the intersection of S_2 with the stable manifold and any trajectory starts or passing through it will approach the critical point A_2. The second portion S_2^+ is the set of all points on S_2 belonging to one side of the stable manifold, any trajectory that starts or passes through it leaves the small neighbourhood of the origin and moves directly towards the stable critical point at infinity which lies on the positive y_2-axis (opposite side of the cross section D_2, see the Figure 6.10). The third portion S_2^- is the set of all points on S_2 belonging to the other side of the stable manifold and any trajectory that starts or passes through it tends toward the cross section D_2. Thus, a local map $\Psi_2 : S_2^- \to D_2$ can be defined. The solution $(y_1(t), y_2(t), y_3(t))$ of equation (6.15) that starts from a point $(y_1^0, y_2^0, \epsilon) \in S_2^-$ at $t = 0$ and ends up the point $(y_1^1, \delta, y_3^1) \in D_2$ when $t = T$ is written as follows:

$$\begin{aligned} y_1(T) &= y_1^0 e^{\alpha_1 T}, \\ y_2(T) &= y_2^0 e^{\alpha_2 T}, \\ y_3(T) &= \epsilon\ e^{-\lambda T}. \end{aligned} \tag{6.16}$$

The flight time $T = \frac{-1}{\alpha_2} \ln(\frac{y_2^0}{\delta})$ of the trajectory connecting the cross sections can be evaluated from the second equation in (6.16). Clearly, the time increases logarithmically fast when the initial point goes closer to the stable manifold. Substituting the value of T into the first and third equation of (6.16) gives the map

$$\Psi_2 : \begin{pmatrix} y_1 \\ y_2 \\ \epsilon \end{pmatrix} \mapsto \begin{pmatrix} y_1^1 \\ \delta \\ y_3^1 \end{pmatrix} = \begin{pmatrix} y_1(\frac{y_2}{\delta})^{\alpha\upsilon} \\ \delta \\ \epsilon(\frac{y_2}{\delta})^{\upsilon} \end{pmatrix}, \tag{6.17}$$

where $\upsilon = \frac{\lambda}{\alpha_2} < 1$ and $\alpha = \frac{-\alpha_1}{\lambda} < 1$. Since $\upsilon < 1$ and $\alpha\upsilon < 1$, from the above equation we observe the following notes. Firstly, in a small neighbourhood of the critical point A_2, the $y_1$coordinate of the image gets becomes smaller when $y_1 > 0$ and it gets become bigger when $y_1 < 0$, this means there is a contraction in the $y_1$direction. Secondly, the y_3 coordinates in S_2^- are mapped to $\epsilon(\frac{y_2}{\delta})^{\upsilon}$ in D_2 and the value of $\epsilon(\frac{y_2}{\delta})^{\upsilon} > y_2$ in a small neighbourhood of the critical point. This indicate that the expansion will be happen in the vertical direction. As a result, the map Ψ_2 contracts the region S_2^- in the y_1-direction (horizontal) and expands the reign S_2^- in the y_3-direction (vertical), as shown in Figure 6.7. Moreover, if the starting points approach the stable manifold of A_2 on S_2 (i.e. $y_2 \longrightarrow 0$), then the contracting becomes infinitely strong. From the above map the bellow relation is obtained

$$y_1^1 = (\frac{y_1}{\epsilon^{\alpha}})(y_3^1)^{\alpha}.$$

If we take the maximum and minimum values of y_1 on S_2 i.e. $y_1 = \pm\epsilon$, then their images on D_2 are given by

$$y_1^1 = \pm(\epsilon)^{1-\alpha}(y_3^1)^{\alpha}$$

and the values of y_1^1 satisfies the following relation

$$C_2(y_3^1)^\alpha \leq y_1^1 \leq C_1(y_3^1)^\alpha, \text{ where } C_{1,2} = \pm(\epsilon)^{1-\alpha}.$$

Thus, the rectangle S_2^- mapped by Ψ_2 to a curvilinear wedge on D_2 and the wedge adjoins to the point $(0, \delta, 0)$ on D_2, as shown in Figure 6.7 .

To find a relation between the trajectories and the stable and unstable manifold of the planar saddle critical point, we let the distance between the starting point of a trajectory and the stable manifold on S_2 is h_2 (it means $y_2 = h_2$) and we denote the distance between the image of h_2 under Ψ_2 and the unstable manifold on D_2 by h_3 (it means $y_3 = h_3$), as we see in Figure 6.6. Thus, from equation (6.17), the following relation is obtained

$$h_3 = k_2 h_2^{\frac{-\lambda}{\alpha_2}}, \tag{6.18}$$

where k_2 is a positive constant.

Remark 5. Since the value of δ is positive, therefore equation (6.17) will indicate that the map is defined only for non-negative values of y_2.

6.2.3 Axial Saddle Critical Point

This subsection is devoted to studying the local behaviour of trajectories of the three dimensional Lotka-Volterra system (6.1) in a small neighbourhood of the axial critical point A_3. The linearized system at A_3 is given by

$$\begin{aligned} \dot{x}_1 &= -2x_1 - 2x_2 - 2x_3, \\ \dot{x}_2 &= -\frac{9}{2}x_2, \\ \dot{x}_3 &= 2x_3. \end{aligned} \tag{6.19}$$

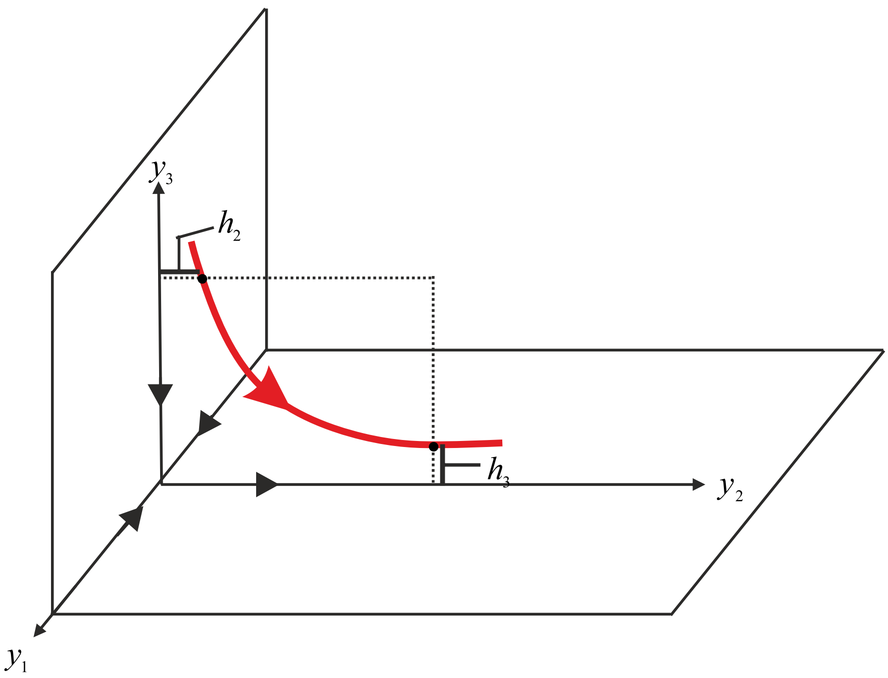

Figure 6.6: The behaviour of trajectories near the planar saddle critical point where the ratio of the eigenvalues around the point is equal to $\frac{\lambda}{\alpha_2}$.

The linear change of coordinates

$$X_{old} = PX_{new}, \;\; P = \begin{bmatrix} 1 & 1 & 0 \\ 0 & \frac{5}{4} & 0 \\ 0 & 0 & -2 \end{bmatrix}, \tag{6.20}$$

where $X_{old} = (x_1, x_2, x_3)$ and $X_{new} = (y_1,\; y_2,\; y_3)$, brings the system (6.19) to the normal form

$$\begin{aligned} \dot{y}_1 &= \beta_1 y_1, \\ \dot{y}_2 &= \beta_2 y_2, \\ \dot{y}_3 &= \beta_3 y_3, \end{aligned} \tag{6.21}$$

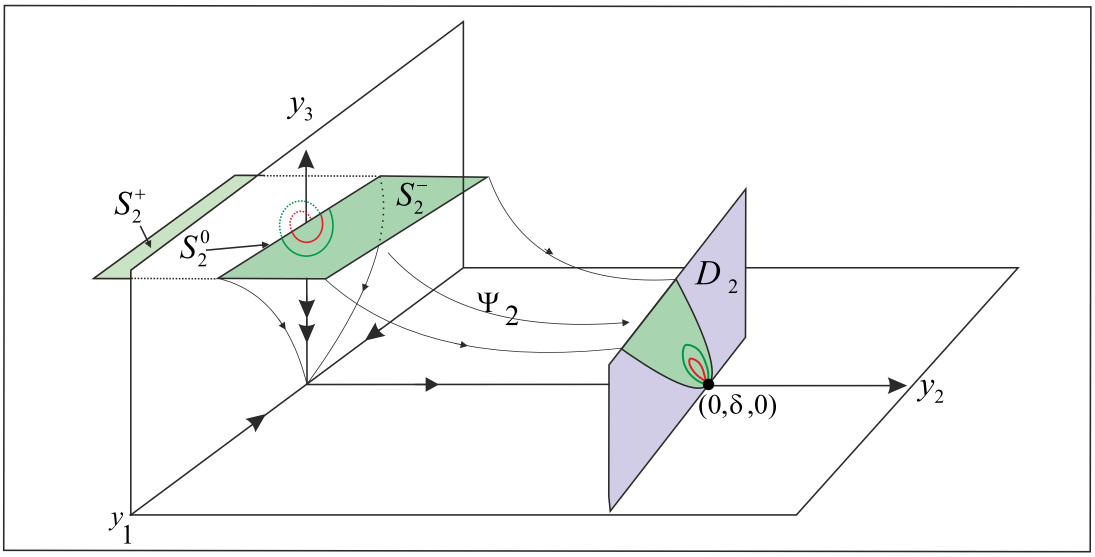

Figure 6.7: The image of S_2 under Ψ_2, which shows the local behaviour of trajectories near the critical point A_2. On S_2, the solid curves depict the points that tend toward the cross section D_2 and the doted curves depict the points that tend toward infinity. Double arrows label the stable non-leading (strong stable).

where $\beta_1 = -2,\ \beta_2 = -\frac{9}{2}$ and $\beta_3 = 2$. Since system (6.21) has one positive and two negative eigenvalues, thus it has a one dimensional unstable manifold (y_3-axis) and a two dimensional stable manifold (y_1y_2-plane). In a small neighbourhood of the origin we introduce the cross sections

$$S_3 = \left\{(y_1,\ y_2,\ y_3) \in \mathbb{R}^3 : |y_1| \leq \epsilon,\ y_2 = \epsilon,\ 0 \leq y_3 \leq \epsilon\right\},$$

$$D_3 = \left\{(y_1,\ y_2,\ y_3) \in \mathbb{R}^3 : |y_1| \leq \delta,\ 0 \leq y_2 \leq \delta,\ y_3 = \delta\right\}, \quad \delta,\ \epsilon \in \mathbb{R}^+$$

as a transverse to the stable and unstable manifold of the critical point A_3. If a trajectory that starts or passes through the intersection points of the cross section S_3 with the stable manifold, then the trajectory approach the point $(0, 0, \delta)$ on D_3. Any trajectory that starts or passes through any other points on S_3 goes toward the cross section D_3. Thus, a map $\Psi_3 : S_3 \to D_3$ can be defined. the solution $(y_1(t), y_2(t), y_3(t))$ of equation (6.21) that starts from a point $(y_1^0, \epsilon, y_3^0) \in S_3$ at

$t = 0$ and ends up the point $(y_1^1, y_2^1, \delta) \in D_3$ when $t = T$ is written as follows:

$$\begin{aligned} y_1(T) &= y_1^0 e^{\beta_1 T}, \\ y_2(T) &= \epsilon e^{\beta_2 T}, \\ y_3(T) &= y_3^0 e^{\beta_3 T}. \end{aligned} \tag{6.22}$$

The dwelling time $T = -\frac{1}{\beta_3}\ln(\frac{y_3^0}{\delta})$ of the trajectory connecting the cross sections can be evaluated from the third equation in (6.22). Clearly, the time increases logarithmically fast when the initial point will closer the stable manifold. Substituting the value of T into the first and second equation of (6.22) gives the map

$$\Psi_3 : \begin{pmatrix} y_1 \\ \epsilon \\ y_3 \end{pmatrix} \mapsto \begin{pmatrix} y_1^1 \\ y_2^1 \\ \delta \end{pmatrix} = \begin{pmatrix} y_1(\frac{y_3}{\delta})^{\alpha\upsilon} \\ \epsilon(\frac{y_3}{\delta})^{\upsilon} \\ \delta \end{pmatrix}, \tag{6.23}$$

where $\upsilon = -\frac{\beta_2}{\beta_3} > 1$ and $\alpha = \frac{\beta_1}{\beta_2} < 1$. From equation (6.23), we note the following. Firstly, in a small neighbourhood of the critical point A_3, the y_1-coordinate of the image gets become smaller and bigger when $y_1 > 0$ and $y_1 < 0$ respectively, this means there is a contraction in the y_1 direction. Secondly, since $\upsilon > 1$, in a small neighbourhood of the critical point, the map Ψ_3 is also contraction with respect to the non-leading coordinate y_2 as well. Finally, if the starting points come near the stable manifold of A_3 on S_3 (*i.e.* $y_3 \longrightarrow 0$), then the contracting becomes infinitely strong. As a result, the map Ψ_3 contracts the region S_3 in both the y_1-direction (horizontal) and the y_2-direction (vertical), as shown in Figure 6.8.

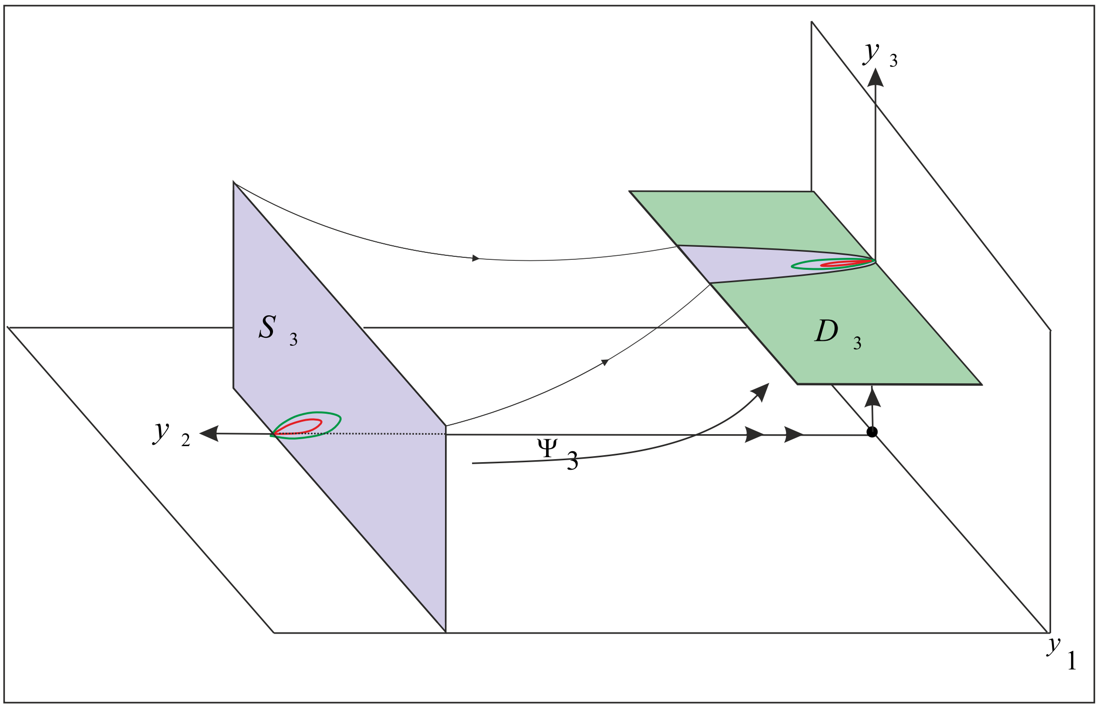

Figure 6.8: The image of S_3 under Ψ_3, which shows the local behaviour of trajectories near the critical point A_3. Double arrows label the stable non-leading (strong stable).

From equation (6.23), it is easy to obtain the relation below

$$y_1^1 = (\frac{y_1}{\epsilon^\alpha})(y_2^1)^\alpha.$$

The image of the maximum and minimum values of y_1 on D_3 ($y_1 = \pm\epsilon$, respectively) are given by

$$y_1^1 = \pm(\epsilon)^{1-\alpha}(y_2^1)^\alpha$$

and the values of y_1^1 satisfies the following relation

$$C_2(y_2^1)^\alpha \leq y_1^1 \leq C_1(y_2^1)^\alpha, \text{ where } C_{1,2} = \pm(\epsilon)^{1-\alpha}.$$

Thus, the map Ψ_3 takes the cross section S_3 onto a curvilinear wedge on D_3 and the wedge touches the extended unstable subspace E^{ue} ($y1y3-$plane) at the point $(0,0,\delta)$ on D_3, as shown in Figure 6.8.

To explain the relation between the trajectories and the stable and unstable manifolds of the axial saddle critical point, we denote the distance between a starting point of a trajectory and the stable manifold on S_3 by h_3 (it means $y_3 = h_3$) and distance between the image of h_3 under Ψ_3 and the unstable manifold on D_3 by $\tilde{h}$ (it means $y_2 = \tilde{h}$) as shown in Figure 6.9. From (6.23), the following relation is obtained

$$\tilde{h} = k_3 h_3^{\frac{-\beta_2}{\beta_3}}, \tag{6.24}$$

where k_3 is a positive constant.

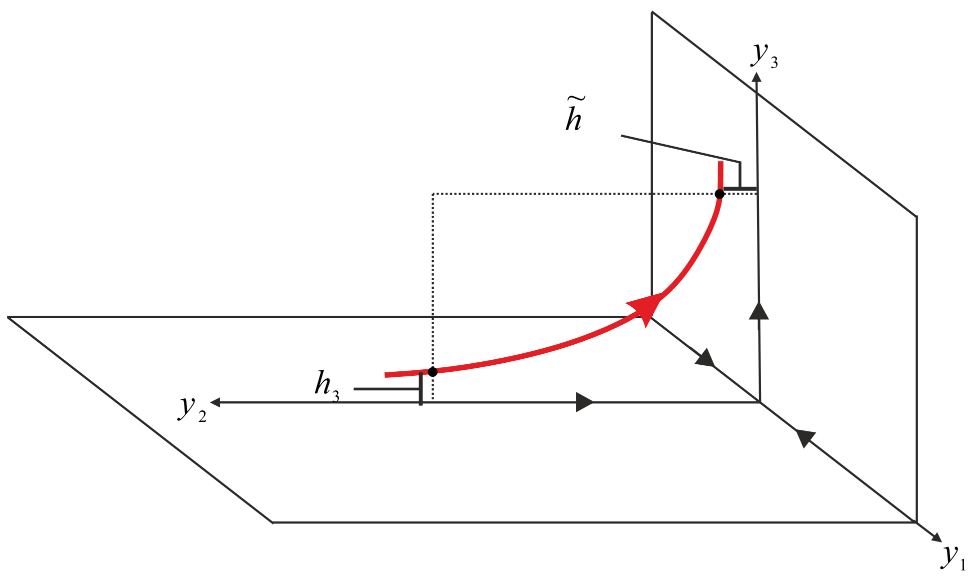

Figure 6.9: The behaviour of trajectories near the axial saddle critical point where the ratio of the eigenvalues around the point is equal to $\frac{-\beta_2}{\beta_3}$.

6.3 The Behaviour at Infinity

In this section, we shall examine the global phase portrait for the three dimensional Lotka-Volterra system (6.1) by studying the behaviour at infinity. The plane at infinity is a projective plane that is added to the affine 3-space. Finding them including critical points and studying the behaviour at infinity of system (6.1) is very important to an understanding its global dynamics. For this purpose, the three below nonlinear change of variables are used individually.

$$X = \frac{1}{x_1}, Y = \frac{x_2}{x_1} \text{ and } Z = \frac{x_3}{x_1} \ ; \ x_1 \neq 0. \tag{6.25}$$

$$X = \frac{x_1}{x_2}, Y = \frac{1}{x_2} \text{ and } Z = \frac{x_3}{x_2} \ ; \ x_2 \neq 0. \tag{6.26}$$

$$X = \frac{x_1}{x_3}, Y = \frac{x_2}{x_3} \text{ and } Z = \frac{1}{x_3} \ ; \ x_3 \neq 0. \tag{6.27}$$

The points $(0, Y_0, Z_0), (X_0, 0, Z_0)$ and $(X_0, Y_0, 0)$ where $\dot{X}, \dot{Y}$ and $\dot{Z}$ vanish are obtained from the nonlinear change of coordinates (6.25), (6.26) and (6.27) respectively. These are the critical points of the new system that is corresponding to the critical points at infinity for system (6.1).

Applying the nonlinear change of variables (6.25) on system (6.1) and after a rescaling of the variables the new system is obtained

$$\begin{aligned} \dot{X} &= X(1 - 2X + Y + Z), \\ \dot{Y} &= \frac{1}{2}Y(-2 - 5X + 7Y + 11Z), \\ \dot{Z} &= 2Z(1 - X - Y). \end{aligned} \tag{6.28}$$

The above system has two critical points $x_{1\infty}(0, 0, 0)$ and $L_{1\infty}(0, \frac{2}{7}, 0)$ where $x_i \geq 0,\ i = 1, 2, 3$. The first one is the intersection point of the line at infinity $L_\infty =$

$\{X = 0\}$ and x_1-axis, the system at that point has Jacobian matrix

$$J = \begin{bmatrix} 1 & 0 & 0 \\ 0 & -1 & 0 \\ 0 & 0 & 2 \end{bmatrix},$$

with one negative -1 and two positive eigenvalues $1, 2$, therefore the critical point is unstable. The Jacobian at the second critical point $L_{1\infty}(0, \frac{2}{7}, 0)$ is given by

$$J = \begin{bmatrix} \frac{9}{7} & 0 & 0 \\ -\frac{5}{7} & 1 & \frac{11}{7} \\ 0 & 0 & \frac{10}{7} \end{bmatrix},$$

with three positive eigenvalues $\frac{10}{7}, 1$ and $\frac{9}{7}$, the critical point is also unstable. The system below is obtained when we apply the nonlinear change of variables (6.26) on system (6.1) after a rescaling of variables

$$\begin{aligned} \dot{X} &= \frac{1}{2}X(-7 + 2X + 5Y - 11Z), \\ \dot{Y} &= \frac{1}{2}Y(-5 + 4X + Y - 9Z), \\ \dot{Z} &= \frac{1}{2}Z(-11 + 6X + Y - 11Z). \end{aligned} \tag{6.29}$$

Corresponding to the critical points at infinity of (6.1) where $x_i \geq 0,\ i = 1, 2, 3,$ system (6.29) has only two critical points $x_{2\infty}(0, 0, 0)$ and $L_{2\infty}(\frac{7}{2}, 0, 0)$. We note that the second one is coincidental with the critical point $L_{1\infty}(0, \frac{2}{7}, 0)$. At the first critical point $x_{2\infty}(0,0,0)$, system (6.1) has Jacobian matrix

$$J = \begin{bmatrix} -\frac{7}{2} & 0 & 0 \\ 0 & -\frac{5}{2} & 0 \\ 0 & 0 & -\frac{11}{2} \end{bmatrix},$$

which it has three negative eigenvalues $-\frac{7}{2}, -\frac{5}{2}$ and $-\frac{11}{2}$. Therefore such critical point is stable. If we apply the last change of variables (6.27) to the three dimensional Lotka-Volterra system (6.1) then this system would be obtained

$$\begin{aligned} \dot{X} &= 2X(-X+Y+Z), \\ \dot{Y} &= \frac{1}{2}Y(11-6X+11Y-Z), \\ \dot{Z} &= Z(1-X+3Y). \end{aligned} \tag{6.30}$$

The system (6.30) has only one critical point $x_{3\infty}(0,0,0)$ which corresponds to the critical point at infinity of (6.1) where $x_i \geq 0,\ i = 1,2,3$ and has a Jacobian matrix:

$$J = \begin{bmatrix} 0 & 0 & 0 \\ 0 & \frac{11}{2} & 0 \\ 0 & 0 & 1 \end{bmatrix}.$$

This matrix has three eigenvalues 0, $\frac{11}{2}$ and 1.

The diagram 6.10 below shows the dynamics behaviour at an affine plane and also at infinity, which exams a good understanding of the global behaviour of the three dimensional Lotka-Volterra system (6.1). Moreover, diagram 6.11 shows all eigenvector directions of the Jacobian matrices of the system at the critical points. The sum of the ratio of eigenvalues of either line is unity according to an index formula by Lins Neto (Lins Neto, 1988).

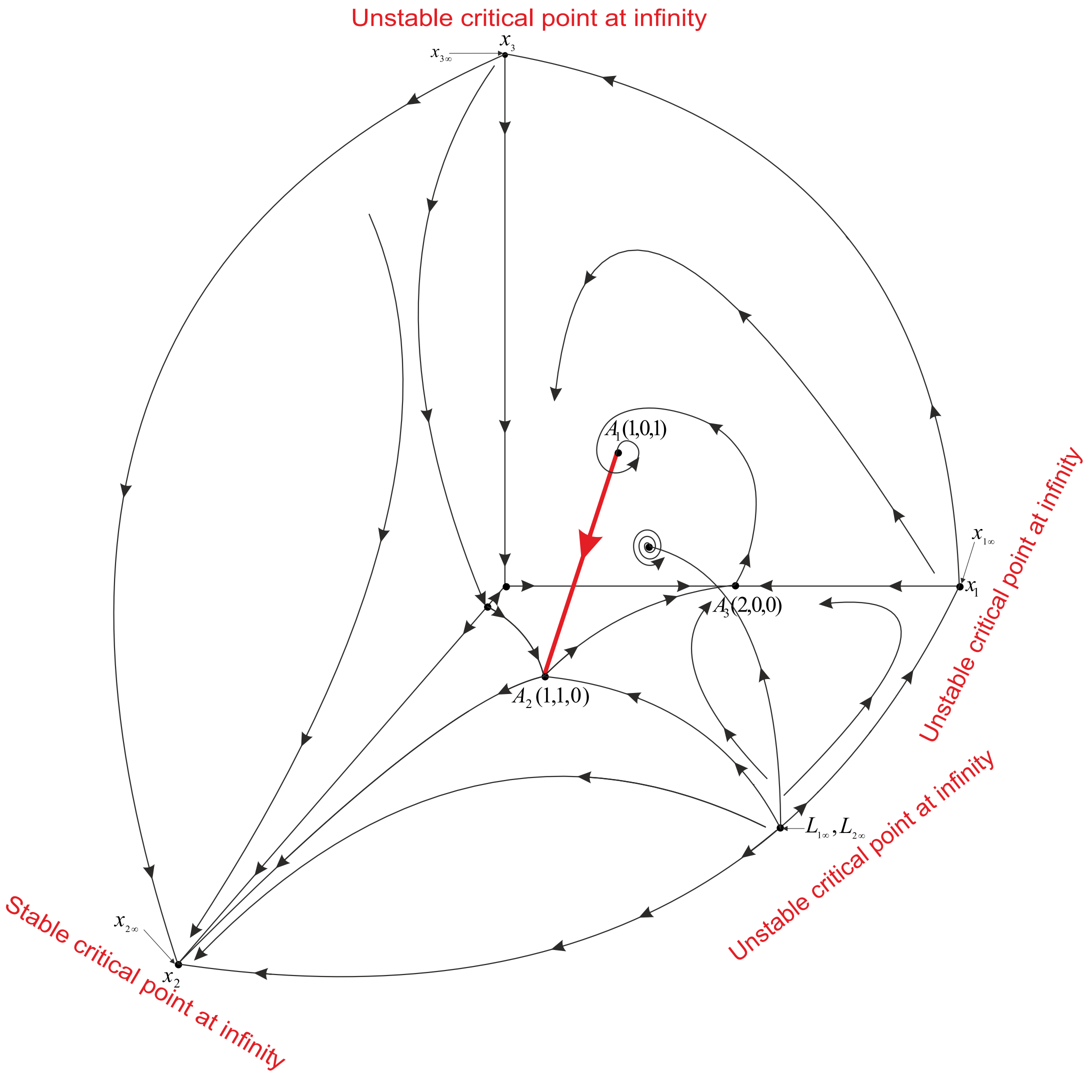

Figure 6.10: Global phase portraits of Lotka-Volterra system (6.1) for $x_i \geq 0,\ i = 1, 2, 3$.

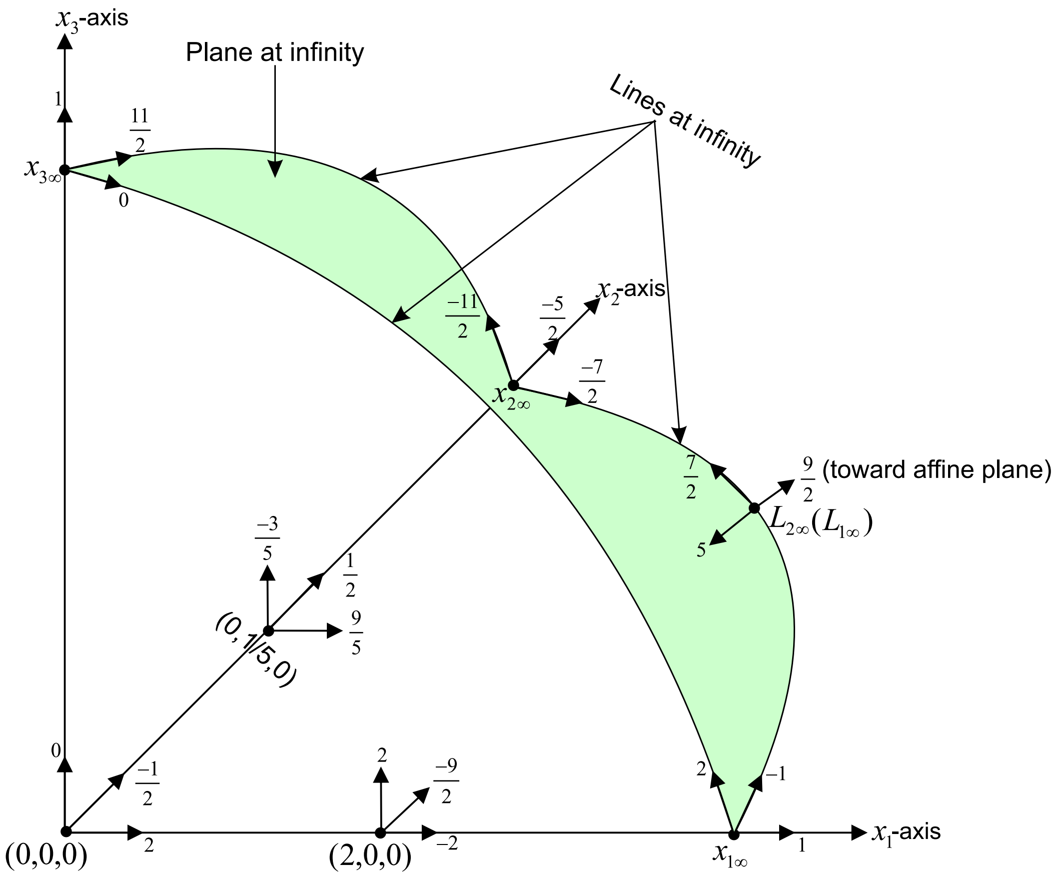

Figure 6.11: The eigenvalues at the origin, axial and infinity critical points for the three dimensional Lotka-Volterra system (6.1).

6.4 The Horseshoe Map of the 3D Lotka-Volterra System

In this section, we will show that the three dimensional Lotka-Volterra system (6.1) can exhibit a horseshoe map. Firstly we choose two cross sections $C_1 = \{(x_1,\ x_2,\ x_3) \in \mathbb{R}^3 : x_3 = 0.5\}$ and $C_2 = \{(x_1,\ x_2,\ x_3) \in \mathbb{R}^3 : x_2 - x_3 = 0\}$, the first one is transverse to the heteroclinic orbit connecting the two critical points A_3 and A_1, the second one is transverse to the invariant line introduced in equation (6.2). Then, we define a map $\mathbf{F}_t : C_1 \longrightarrow C_2$ by the trajectories close to the homoclinic cycle. Under the effect of the planar saddle-focus critical point A_1, the map $\mathbf{F_t}$ takes C_1 inside C_2 by some steps. Firstly, the map $\mathbf{F_t}$ contracts C_1 in the horizontal direction (x_1-axis direction) and expands C_1 in the vertical direction (x_2-axis direction). Then it folds the cross section C_1. The shape of the image $\mathbf{F_t}(C_1)$ on C_2 is a spiral around the invariant line that is introduced in equation (6.2) having the appearance of a snail shell shape. These behaviour of the critical points have been obtained under the assumption that the vector field was given by its linear parts. Since around the critical points the nonlinear system differs from the system given by its linear terms due to a C^1 transformation tangent to the identity, then the behaviour of trajectories for the linear and nonlinear systems will be C^1 equivalent.

The stable manifold of the critical point A_2 divides the image $\mathbf{F_t}(C_1)$ on C_2 into two parts: C_2^1 and C_2^2. The first one C_2^1 is the set of all points on $\mathbf{F_t}(C_1) \cap C_2$ belonging to one side of the stable manifold where $\mathbf{F_t}(C_1)$ tends toward a stable critical point at infinity on the positive x_2-axis as $t \longrightarrow \infty$. These leave the cross section C_2 and never return. The second one C_2^2 is the set of all points on $\mathbf{F_t}(C_1) \cap C_2$ belonging to the other side of the stable manifold where the trajectories turn towards the positive x_1x_3-plane to intersect C_1 and then follow the invariant line introduced in (6.2) until they intersect C_2. If the orbit passes through C_2^1, then it will leave the neighbourhood of the heteroclinic cycle towards the stable critical point at infinity and never return; otherwise it will make another round following the heteroclinic cycle and return to C_1 again and so forth. We denote $\mathbf{F_t}^{-1}(C_2^2)$ by H_k which are horizontal strips on C_1, then $\mathbf{F_t}(H_k)$ lie in C_2^2 and the flow continues to intersect C_1 and the image of $\mathbf{F_t}(H_k)$ is a horseshoe shaped region that crosses H_k twice as shown in Figure 6.15. It is geometrically evident that there is a fixed point of $\mathbf{F}_t$ within each of the components of H. These fixed points correspond to a periodic orbit of the system. Thus the Poincaré map with respect to C_1 contains a horseshoe. Such a map $\mathbf{F_t}$ is called a horseshoe map.

The sufficient condition for the intersection of H_k and $F_t(H_k)$ on C_1 is determined by the value of the ratio of eigenvalues. In addition to the maps $\Psi_i,\ i = 1, 2, 3$ which are introduced in (6.7), (6.17) and (6.23) there are three other diffeomorphism maps $\Phi_i,\ i = 1, 2, 3$. The first one $\Phi_1 : D_1 \to S_2$, maps the spirals on D_1 diffeomorphically into the cross section S_2 and takes the intersection point of the invariant line (6.2) with cross section D_1 to the intersection point of the given line with cross section S_2. The second one, $\Phi_2 : D_2 \to S_3$, maps the intersection point of the cross section D_2 with the heteroclinic orbit connecting A_2 and A_3 to the intersection point of cross section S_3 with the heteroclinic orbit. The last one, $\Phi_3 : D_3 \to C$, maps the intersection point of the cross section D_3 with the heteroclinic orbit connecting A_3 and A_1 to the intersection point of the cross section C with the heteroclinic orbit. These maps locally preserve the shapes of these structures. From equations (6.12), (6.18)and (6.24), for system (6.1), we obtain

$$h_2 \sim k_1 h_1^{\rho_1},\ h_3 \sim k_2 h_2^{\rho_2},\ \text{and}\ \tilde{h} \sim k_3 h_3^{\rho_3},$$

where $\rho_1 = \dfrac{-\mu}{\lambda}$, $\rho_2 = \dfrac{\lambda}{\alpha_2}$ and $\rho_3 = \dfrac{-\beta_2}{\beta_3}$. The composition of the maps Ψ_i and $\Phi_i,\ i = 1, 2, 3$ gives the following relation

$$\tilde{h} \sim c h_1^{\rho}, \tag{6.31}$$

where $\rho = \rho_1\rho_2\rho_3$ and c is a positive constant (see Figure 6.12). In our case, the ratio of eigenvalues $\rho = \dfrac{3}{4} < 1$. This property plays the same role as the saddle index in Shilnikov theory. Here, we explain how the intersection of the horizontal strip, H_k, and its image, $F_t(H_k)$, on the cross section C_1 is non-empty. We denote the distance of the upper and lower boundaries of the horizontal strip, H_k, from the stable manifold of the critical point A_1 by d_k and d_{k+1} respectively, where $d_{k+1} = a d_k,\ 0 < a < 1$.

Let

$$d_k = e^{-nk},\ n \in \mathbb{R}^+ \text{ and } k = 1, 2, ...$$

From (6.31), the following relation is obtained

$$\begin{aligned}\tilde{d}_k &\sim c(e^{-nk})^{\frac{3}{4}},\\ \tilde{d}_{k+1} &\sim c(ae^{-nk})^{\frac{3}{4}},\end{aligned}$$

where $\tilde{d}_k$ and $\tilde{d}_{k+1}$ are images of d_k and d_{k+1} on the cross section C_1 respectively. Since,

$$\begin{aligned}\frac{\tilde{d}_k}{d_k} &\sim ce^{\frac{1}{4}nk},\\ \frac{\tilde{d}_{k+1}}{d_{k+1}} &\sim c_1 e^{\frac{1}{4}nk},\ c_1 = ca^{\frac{-1}{4}}\end{aligned}$$

$$\frac{\tilde{d}_{k+1}}{d_k} \sim c_2 e^{\frac{1}{4}nk}, \ c_2 = ca^{\frac{3}{4}}$$

and $e^{\frac{1}{4}nk}$ approaches ∞ as k tends to ∞. Thus, the intersection of H_k and $F_t(H_k)$ is non-empty and consists of two connected components for k sufficiently large. We have performed a numerical simulation to obtain the horseshoe map visually (see Figure 6.15).

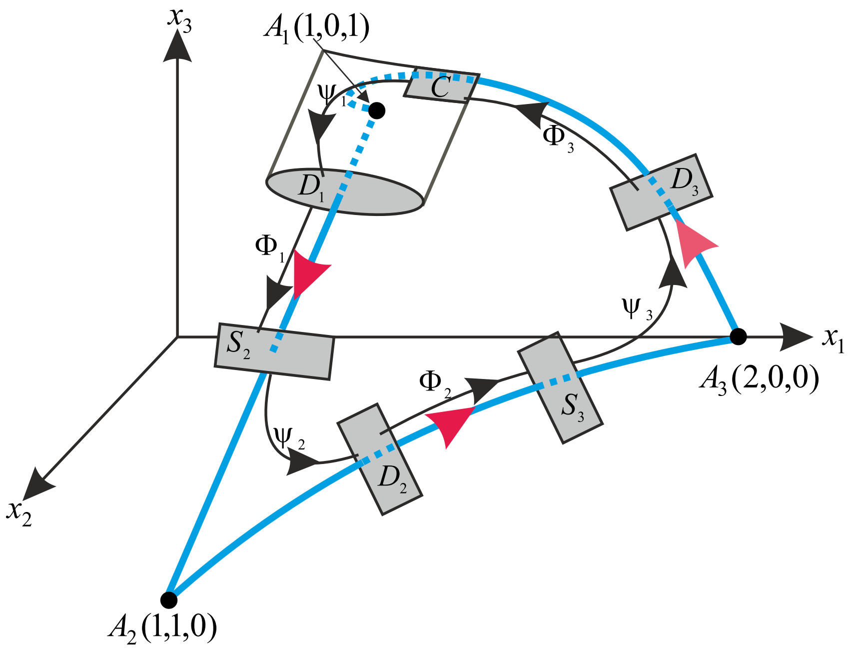

Figure 6.12: The Poincaré return map around the cycle.

The technique of choosing the horizontal strip H_k in this thesis is illustrated below. Its left and right sides are the backward orbits of the lines $\theta = \frac{39}{20}\pi$ and $\theta = \frac{1}{20}\pi$ of the cylinder parallel with the line that is introduced in (6.2) having centre A_1 and radius 0.3 respectively, provided that their images lie on that side of the stable manifold of the critical point A_2 where the trajectories goes toward the positive x_1x_3- plane. The upper and bottom of the strip are the backward orbits of the curve that connecting the end points of the images of the lines $\theta = \frac{39}{20}\pi$ and $\theta = \frac{1}{20}\pi$ on the stable manifold of the critical point A_2. The image of the horizontal strip H_k on C_1 and $\mathbf{F_t}(H_k)$ on C_2 are shown in Figure 6.13 and 6.14 respectively.

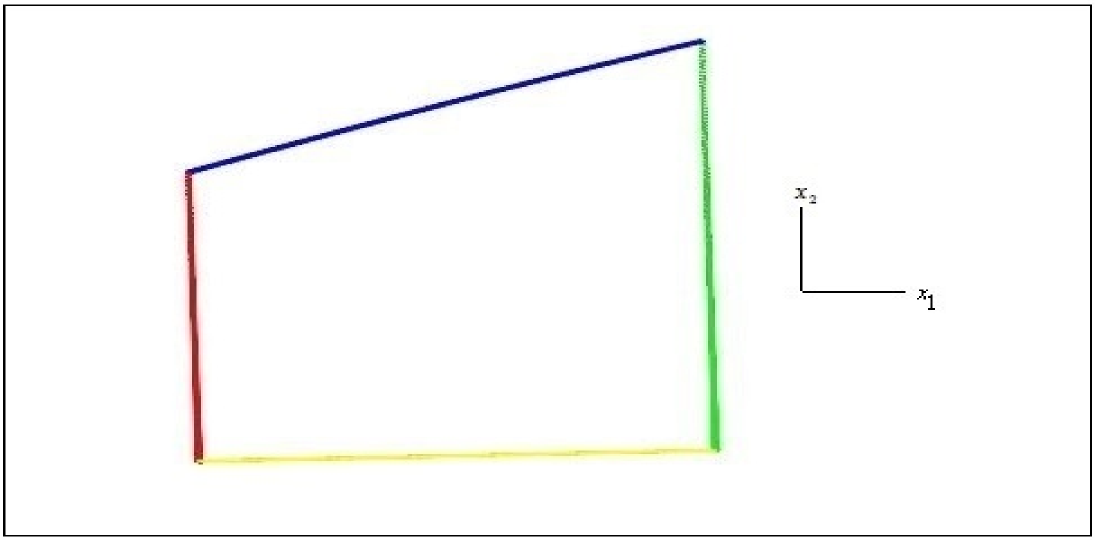

Figure 6.13: The horizontal strip H_k on C_1.

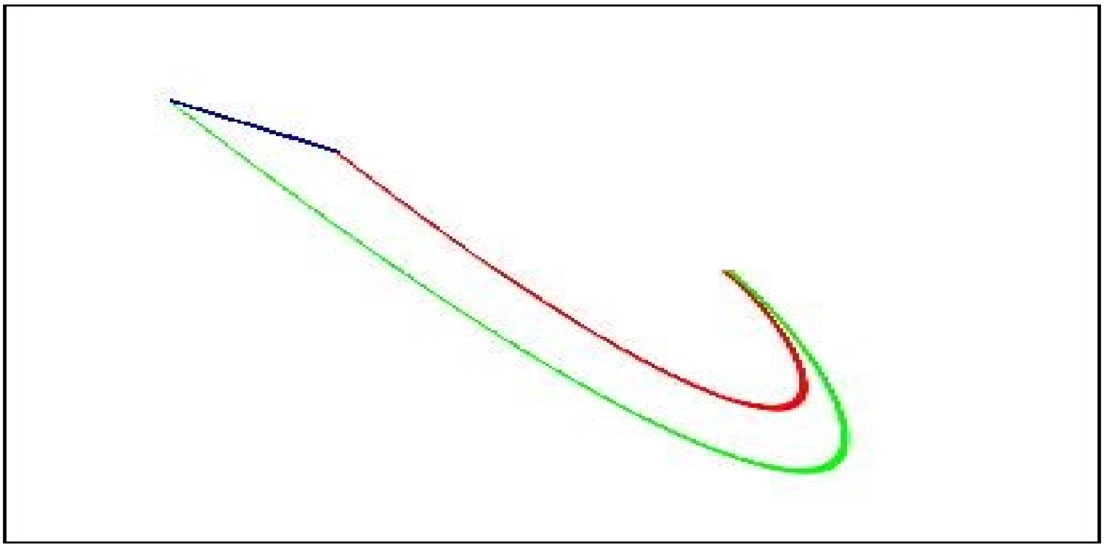

Figure 6.14: The image of $\mathbf{F_t}(H_k)$ on C_2.

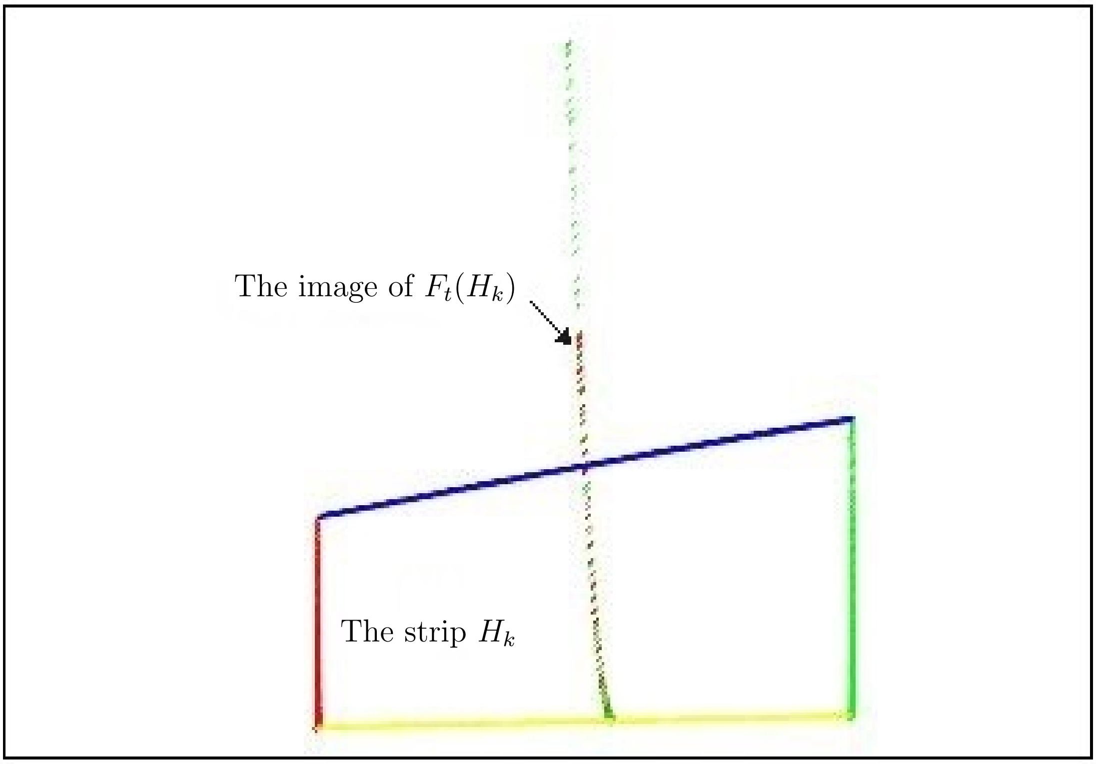

Figure 6.15: The image of the horizontal strip H_k and its image under $\mathbf{F}_t$ on the cross section C_1.

Chapter 7

The Integrability and the Zero-Hopf Bifurcation of the 3DLVS

This chapter focuses on examining the zero-Hopf bifurcation of the three dimensional Lotka-Volterra systems. First order averaging theory is used to study the possible periodic orbits bifurcating from a line of singularities, where every point on the line is of type zero-Hopf.

7.1 The Darboux Integrability of the 3DLVS

This section studies the integrability and the existence of a line of singularity for the three dimensional Lotka-Volterra systems. Some invariant plane conditions are found to construct the fourth invariant algebraic surface. In addition, sufficient conditions for the existence of a line of singularities with a zero eigenvalue are obtained. Under these conditions, a function of Darboux type produces two linearly independent first integrals.

Proposition 5. The three dimensional Lotka-Volterra system (1.1) always has three invariant algebraic surfaces $f_i(x_1, x_2, x_3) = x_i$ with cofactor $k_i = r_i + \sum_{j=1}^{3} a_{i,j}x_j,\ i = 1, 2, 3$. The surface $f_4(x_1, x_2, x_3) = 1 - x_1 - x_2 - x_3$ is also an invariant algebraic surface of the three dimensional system (1.1) with cofactor $k_4 = -(\sum_{i=1}^{3} r_i x_i)$ if and only if the following conditions hold:

$$a_{i,i} = -r_i \text{ and } a_{i,j} = -(r_i + r_j + a_{j,i}),\ (i, j = 1, 2, 3,\ j > i) \tag{7.1}$$

Proof. It is easy to check that $\mathcal{X}(f_i) = k_i f_i$ where f_i and $k_i,\ i = 1, 2, 3$ are defined above. Therefore, the $f_i = 0,\ i = 1, 2, 3$ are invariant algebraic surfaces of the three dimensional system (1.1).

To prove the second part, firstly we suppose that the surface $f_4(x_1, x_2, x_3) = 0$ is an invariant algebraic surface for the three dimensional system (1.1), then from the equation $\mathcal{X}(f_4) = k_4 f_4$ the conditions (7.1) are obtained.

Conversely, If the conditions (7.1) hold, then it is easy to show that $\mathcal{X}(f_4) = k_4 f_4$. Thus the surface $f_4(x_1, x_2, x_3) = 0$ is invariant algebraic surface for the three dimensional system (1.1). □

Theorem 6. Suppose $a \in S$, where

$$S = \left\{(r_1, r_2, r_3, a_{2,1}, a_{3,1}, a_{3,2}) \in \mathbb{R}^6 : r_1 r_3 + r_1 a_{3,2} + r_3 a_{2,1} - r_2 a_{3,1} = 0\right\}, \tag{7.2}$$

then for the three dimensional Lotka-Volterra system (1.1) satisfying (7.1) the following results are obtained:

1. The system has a line of singularities with a zero eigenvalue.

2. The system is integrable. More precisely, it has two independent first integrals.

Proof. A straight computation shows that in addition to the critical points $(1, 0, 0)$, $(0, 1, 0)$ and $(0, 0, 1)$ the system has a line of singularities, if

$$a_{2,1} = -\frac{r_1(r_3 + a_{3,2}) - r_2 a_{3,1}}{r_3}\ , \tag{7.3}$$

then the line of singularities will be defined by

$$L = \{(x_1, x_2, x_3) \in \mathbb{R}^3 : x_1 = -\frac{r_3 + (r_2 + a_{3,2})t}{r_1 + a_{3,1}},\ x_2 = t,\ x_3 = \frac{r_1 r_3 + (r_1 a_{3,2} - r_2 a_{3,1})t}{r_3(r_1 + a_{3,1})}\}. \tag{7.4}$$

To prove the second part of the theorem, we try to construct a Darboux first integral of the form

$$V = \Pi_{i=1}^{4} f_i^{\lambda_i}\ , \tag{7.5}$$

where f_i are invariant algebraic surfaces of the system and their cofactors K_i are defined in Proposition 5. From $\sum_{i=1}^{4} \lambda_i k_i = 0$, the following equation is obtained:

$$(-r_1\lambda_1 + a_{2,1}\lambda_2 + a_{3,1}\lambda_3 - r_1\lambda_4)x_1 + (-(r_1 + r_2 + a_{2,1})\lambda_1 - r_2\lambda_2 + a_{3,2}\lambda_3 - r_2\lambda_4)x_2 +$$
$$(-(r_1 + r_3 + a_{3,1})\lambda_1 - (r_2 + r_3 + a_{3,2})\lambda_2 - r_3\lambda_3 - r_3\lambda_4)x_3 + r_1\lambda_1 + r_2\lambda_2 + r_3\lambda_3 = 0.$$

This equation is equivalent to the following matrix equation:

$$\begin{bmatrix} -r_1 & a_{2,1} & a_{3,1} & -r_1 \\ -(r_1 + r_2 + a_{2,1}) & -r_2 & a_{3,2} & -r_2 \\ -(r_1 + r_3 + a_{3,1}) & -(r_2 + r_3 + a_{3,2}) & -r_3 & -r_3 \\ r_1 & r_2 & r_3 & 0 \end{bmatrix} \begin{bmatrix} \lambda_1 \\ \lambda_2 \\ \lambda_3 \\ \lambda_4 \end{bmatrix} = \begin{bmatrix} 0 \\ 0 \\ 0 \\ 0 \end{bmatrix}. \tag{7.6}$$

We note that the determinant of the matrix of this system is equal to $-(r_1 r_3 +$

$r_1a_{3,2}+r_3a_{2,1}-r_2a_{3,1})^2$. Therefore, if we take a point belonging to S, then there is a solution set with an infinite number of solutions, this means that $\exists\, \lambda_i \in \mathbb{R}$ not all zero such that $\sum_{i=1}^{n} \lambda_i\, k_i = 0$. Thus, the system has first integral of Darboux type.

Under the assumption $a_{2,1}$ satisfies equation (7.3) , the matrix equation (7.6) has the following non-trivial solutions

$$
\begin{aligned}
&(\lambda_1, \lambda_2, \lambda_3, \lambda_4) \longrightarrow (-r_3, 0, r_1, r_3 + a_{3,1}),\\
&(\lambda_1, \lambda_2, \lambda_3, \lambda_4) \longrightarrow (-r_2, r_1, 0, -\frac{r_1r_3 + r_1a_{3,2} - r_2r_3 - r_2a_{3,1}}{r_3}).
\end{aligned}
$$

Therefore the following functions are first integrals

$$
\begin{aligned}
\Phi_1 &= x_1^{-r_3}\ x_3^{r_1}\ (1 - x_1 - x_2 - x_3)^{(r_3+a_{3,1})},\\
\Phi_2 &= x_1^{-r2}\ x_2^{r_1}\ (1 - x_1 - x_2 - x_3)^{(-\frac{r_1r_3 + r_1a_{3,2} - r_2r_3 - r_2a_{3,1}}{r_3})}.
\end{aligned}
$$

It is easy to check that $\nabla\Phi_1$ and $\nabla\Phi_2$ are linearly independent, hence the above two first integrals are independent. Thus, the three dimensional Lotka-Volterra system (1.1) satisfying (7.1) is integrable. $\square$

7.2 Zero-Hopf Bifurcation

This section is devoted to the study of the zero-Hopf bifurcation of the three dimensional Lotka-Volterra systems. In the first subsection, we recall the averaging theory of the first order and some related concepts to it. The second subsection shows that there are three 3-parameter families of the system exhibiting a zero-Hopf equilibrium located at the line of singularities and the averaging theory is also applied to the system.

7.2.1 The First Order Averaging Method for Periodic Orbits

Averaging methods are useful tools for investigating the number of periodic orbits for some differential systems. Many researchers have devoted their effort to study the existence of periodic orbits via this method which has a long history as we see in the work of Marsden and McCracken (1976), Chow and Hale (1982), Sanders et al. (2007), Buică and Llibre (2004), Buică et al. (2007) and references therein.

We consider the system

$$\dot{x} = F_0(t, x), \tag{7.7}$$

with $F_0 : \mathbb{R} \times D \longrightarrow \mathbb{R}^n$ a C^2 function, $T-$periodic in t and D is an open subset of $\mathbb{R}^n$. We assume that all solutions of (7.7) are $T-$periodic *i.e.* the system has a submanifold of periodic solutions and also assume that the system is isochronous. The isochronous means that all closed orbits of the system have the same period. The linearization of (7.7) along the periodic solution $x(t, u)$ satisfying the initial condition $x(0, u) = u$ is denoted by

$$\dot{y} = D_x F_0(t, x(t, u))y, \tag{7.8}$$

where $D_x F_0$ is the Jacobian matrix of F_0 with respect to x. Here, we denote the fundamental matrix solution of (7.7) by $M_u(t)$ and also assume that there exists an open set V with $Cl(V) \subset D$ such that for each $u \in Cl(V)$, $x(t, u)$ is a $T-$periodic.

Consider the following perturbation of (7.7)

$$\dot{x} = F_0(t, x) + \epsilon F_1(t, x) + \epsilon^2 F_2(t, x, \epsilon), \tag{7.9}$$

where ϵ is a sufficiently small positive parameter (called the small perturbation parameter), $F_1 : \mathbb{R} \times D \longrightarrow \mathbb{R}^n$, $F_2 : \mathbb{R} \times D \times (-\epsilon_0, \epsilon_0) \longrightarrow \mathbb{R}^n$ are C^2 functions, $T-$periodic in the first variable. Averaging theory reduces the problem of finding $T-$periodic solutions of (7.9) to the problem of finding the simple zeros of a function which is called the *bifurcation function.*

In this section, we will recall the averaging theory that relates to the perturbing of isochronous systems. The averaging methods have different presentations, here, we present one of them which was obtained by Buica *et al.* in (Buică et al., 2007) which gives a sufficient condition of bifurcating periodic solutions from the $T-$periodic solutions $x(t, u)$.

Theorem 7 (Perturbations of an isochronous system)**.** We assume that there exists an open set V with $Cl(V) \subset D$ and such that for each $u \in Cl(V)$, $x(t, u)$ is a $T-$periodic. Consider the function $\mathcal{F} : Cl(V) \longrightarrow \mathbb{R}^n$ given by

$$\mathcal{F}(u) = \int_0^T M_u^{-1}(t) F_1(t, x(t, u)) dt. \tag{7.10}$$

If there exist $a \in V$ with $\mathcal{F}(a) = 0$ and $det(D_u \mathcal{F}(a)) \neq 0$, then there exists a $T-$periodic solution $\gamma(t, \epsilon)$ of system (7.9) such that $\gamma(t, \epsilon) \longrightarrow a$ as $\epsilon \longrightarrow 0$.

7.2.2 Periodic Orbits in the Zero-Hopf Bifurcation of the 3DLVS

The proposition below shows that there exist three 3-parameter families of the three dimensional Lotka-Volterra systems for which the equilibrium point at any point on the line of singularities defined in (7.4) is a zero-Hopf equilibrium point.

Proposition 6. The three dimensional Lotka-Volterra system (1.1) with conditions (7.1) and (7.3) has a zero-Hopf equilibrium point which is located at the line of singularities (7.4) if one of the following conditions is satisfied.

i. $r_2 = 0,\ a_{3,2} = 0$ and $\dfrac{r_1 r_3(r_3 + a_{3,1})}{r_1 + a_{3,1}} < 0.$

ii. $r_2 = r_3,\ a_{3,2} = -r_3$ and $\dfrac{r_1 r_3(r_3 + a_{3,1})}{r_1 + a_{3,1}} < 0.$

iii. $r_2 = r_1,\ a_{3,2} = a_{3,1}$ and $\dfrac{r_1 r_3(r_3 + a_{3,1})}{r_1 + a_{3,1}} < 0$.

Proof. The three dimensional Lotka-Volterra system (1.1) with conditions (7.1) and (7.3) is written as follows

$$\begin{aligned}
\dot{x_1} &= x_1(r_1 - r_1 x_1 + (\frac{r_1 a_{3,2} - r_2(r_3 + a_{3,1})}{r_3})x_2 - (r_1 + r_3 + a_{3,1})x_3), \\
\dot{x_2} &= x_2(r_2 + (\frac{r_2 a_{3,1} - r_1(r_3 + a_{3,2})}{r_3})x_1 - r_2 x_2 - (r_2 + r_3 + a_{3,2})x_3), \\
\dot{x_3} &= x_3(r_3 + a_{3,1}x_1 + a_{3,2}x_2 - r_3 x_3).
\end{aligned} \tag{7.11}$$

The characteristic polynomial $P(\lambda)$ of the linearization of system (7.11) at any point of the line (7.4) is given by

$$P(\lambda) = \lambda^3 - G\lambda,$$

where

$$\begin{aligned}
G =& \frac{(r_2 + a_{3,2})(r_1 a_{3,2} - r_2 a_{3,1})(r_1 r_3 + r_1 a_{3,2} - r_2 r_3 - r_2 a_{3,1} + r_3 a_{3,1} - r_3 a_{3,2})}{r_3^2(r_1 + a_{3,1})}t^2 + \\
& \frac{r_1 a_{3,2}(r_1 r_3 + r_1 a_{3,2} - 2r_2 r_3 - 2r_2 a_{3,1} + r_3^2 + 2r_3 a_{3,1} - r_3 a_{3,2}) + r_2 a_{3,1}(r_3 + a_{3,1})(r_2 - r_3)}{r_3(r_1 + a_{3,1})}t \\
& + \frac{r_1 r_3(r_3 + a_{3,1})}{r_1 + a_{3,1}}.
\end{aligned} \tag{7.12}$$

The eigenvalues associated at any point on line (7.4) will have pure imaginary eigenvalues if the value of G in equation (7.12) is negative and will not depend on the value of t. In that case, every point on the line of singularities becomes a zero-Hopf equilibrium point. By solving the coefficients of t in equation (7.12) with respect to r_2 and $a_{3,2}$, and choosing the value of G remains negative, then the set of conditions will be obtained. The line of singularities which satisfies the first set of the above conditions is shown in Figure 7.1. $\square$

Now, we apply the averaging theory described in Theorem 7 to the three dimensional Lotka-Volterra systems.

Theorem 8. Consider the three dimensional Lotka-Volterra system (1.1) with condition (7.1) and condition (i) in Proposition 6 where $a_{3,1} = -\dfrac{r_1(\omega^2 + r_3^2)}{\omega^2 + r_1 r_3}$, $\omega > 0$. Let

$$a_{2,1} = -r_1 + \epsilon\alpha,$$

where $\alpha \neq 0$ and ϵ be a sufficiently small positive parameter. Using First order averaging theory (Buică et al., 2007) , we can not find periodic orbits bifurcating from the zero-Hopf equilibrium point satisfying condition (i) in Proposition 6 and located on the interior equilibrium point of the system.

Proof. If $a_{2,1} = -r_1 + \epsilon\alpha$, then after transforming the interior equilibrium point to the origin, the 3DLVS satisfying the above conditions is written as follows

$$\begin{aligned}
\dot{x_1} &= \frac{-(A_1 x_1 + r_3(\omega^2 + r_1 r_3))}{(\omega^2 + r_1 r_3)A_1}(r_1(\omega^2 + r_1 r_3)x_1 + \alpha\epsilon(\omega^2 + r_1 r_3)x_2 + r_3(\omega^2 + r_1^2)x_3),\\
\dot{x_2} &= \frac{1}{A_1}(A_1 x_2 + \omega^2(r_1 - r_3))((\alpha\epsilon - r_1)x_1 - r_3 x_3), \qquad (7.13)\\
\dot{x_3} &= \frac{-(A_1 x_3 + \alpha(\omega^2 + r_1 r_3)\epsilon - (\omega^2 + r_1 r_3)r_1)}{(\omega^2 + r_1 r_3)A_1}(r_1(\omega^2 + r_3^2)x_1 + r_3(\omega^2 + r_1 r_3)x_3),
\end{aligned}$$

where $A_1 = \alpha\epsilon(\omega^2 + r_1 r_3) - r_1 r_3(r_1 - r_3)$. By rescaling the variables $(x_1, x_2, x_3) = (\epsilon X, \epsilon Y, \epsilon Z)$, system (7.13) becomes

$$\dot{X} = \frac{-(A_1\epsilon X + (\omega^2 + r_1 r_3)r_3)}{(\omega^2 + r_1 r_3)A_1}(r_1(\omega^2 + r_1 r_3)X + \alpha\epsilon(\omega^2 + r_1 r_3)Y + r_3(\omega^2 + r_1^2)Z),$$

$$\dot{Y} = \frac{1}{A_1}(A_1\epsilon Y + \omega^2(r_1 - r_3))((\alpha\epsilon - r_1)X - r_3 Z), \tag{7.14}$$
$$\dot{Z} = \frac{-(A_1\epsilon Z + \alpha\epsilon(\omega^2 + r_1 r_3) - r_1(\omega^2 + r_1 r_3))}{(\omega^2 + r_1 r_3)A_1}(r_1(\omega^2 + r_3^2)X + r_3(\omega^2 + r_1 r_3)Z).$$

When $\epsilon = 0$, the linearized system of (7.14) at the origin is not of the real Jordan form *i.e.* as

$$\begin{bmatrix} 0 & 0 & -\omega \\ 0 & 0 & 0 \\ \omega & 0 & 0 \end{bmatrix}.$$

For doing that, we consider the linear change of coordinates

$$\begin{bmatrix} X \\ Y \\ Z \end{bmatrix} = P \begin{bmatrix} y_1 \\ y_2 \\ y_3 \end{bmatrix}, \tag{7.15}$$

where

$$P = \begin{bmatrix} \frac{-r_3(\omega(\omega + r_1) - r_3(\omega - r_1))}{r_1(\omega^2 + r_3^2)} & 0 & \frac{-r_3(\omega(\omega - r_1) + r_3(\omega + r_1))}{r_1(\omega^2 + r_3^2)} \\ \frac{-\omega(\omega - r_3)(r_1 - r_3)}{r_1(\omega^2 + r_3^2)} & 1 & \frac{-\omega(\omega + r_3)(r_1 - r_3)}{r_1(\omega^2 + r_3^2)} \\ 1 & 0 & 1 \end{bmatrix}.$$

Then in the new variables (y_1, y_2, y_3), system (7.14) becomes

$$\begin{aligned} \dot{y_1} = {} & -\omega y_3 + \frac{\epsilon}{2r_1 r_3\omega(r_1 - r_3)^2(\omega^2 + r_1 r_3)(\omega^2 + r_3^2)}[\alpha\omega^2(r_1 - r_3)(\omega^2 + r_3^2)^2(\omega^2 + r_1 r_3)y_1 \\ & - \alpha r_1(\omega^2 + r_1 r_3)^2(\omega^2 + r_3^2)y_2 - \alpha\omega^2(r_1 - r_3)(\omega^2 + r_1 r_3)(\omega^2 + r_3^2)^2 y_3 \\ & + \omega r_1 r_3^2(r_1 - r_3)^3(\omega + r_3)(\omega^2 - \omega r_1 + \omega r_3 + r_1 r_3)y_1^2 - 4\omega^2 r_1 r_3^2(r_1 - r_3)^3(\omega^2 + r_1 r_3)y_1 y_3 \\ & - \omega r_1 r_3^2(r_1 - r_3)^3(\omega + r_3)(\omega^2 - \omega r_1 + \omega r_3 + r_1 r_3)y_3^2] + O(\epsilon^2), \end{aligned}$$

$$\dot{y_2} = 0 + \frac{\epsilon}{r_1(r_1-r_3)(\omega^2+r_3^2)}[\alpha(\omega^2+r_3^2)(\omega^2+r_1r_3)y_2 + r_1r_3(r_1-r_3)^2(\omega+r_3)y_1y_2$$
$$- r_1r_3(r_1-r_3)^2(\omega-r_3)y_2y_3] + O(\epsilon^2), \tag{7.16}$$
$$\dot{y_3} = \omega y_1 + \frac{\epsilon}{2r_1r_3\omega(r_1-r_3)^2(\omega^2+r_1r_3)(\omega^2+r_3^2)}[\alpha\omega^2(r_1-r_3)(\omega^2+r_3^2)^2(\omega^2+r_1r_3)y_1$$
$$+ \alpha r_1(\omega^2+r_1r_3)^2(\omega^2+r_3^2)y_2 - \alpha\omega^2(r_1-r_3)(\omega^2+r_1r_3)(\omega^2+r_3^2)^2y_3$$
$$+ \omega r_1r_3^2(r_1-r_3)^3(\omega-r_3)(\omega^2+\omega r_1-\omega r_3+r_1r_3)y_1^2 + 4\omega^2r_1r_3^2(r_1-r_3)^3(\omega^2+r_1r_3)y_1y_3$$
$$- \omega r_1r_3^2(r_1-r_3)^3(\omega-r_3)(\omega^2+\omega r_1-\omega r_3+r_1r_3)y_3^2] + O(\epsilon^2),$$

we note that the previous system is written as a differential system of the form (7.9). It is a normal form for applying the averaging theory described in Theorem 7. The first requirement is to find the solution of the unperturbed system of (7.16). The solution $x(t,u) = (y_1(t), y_2(t), y_3(t))$ of system

$$\begin{aligned} \dot{y_1} &= -\omega y_3, \\ \dot{y_2} &= 0, \\ \dot{y_3} &= \omega y_1, \end{aligned} \tag{7.17}$$

satisfying the initial condition $(y_1(0), y_2(0), y_3(0)) = (x_0, y_0, z_0) \in \mathbb{R}^3$ is written as

$$\begin{aligned} y_1(t) &= x_0 cos(\omega t) - z_0 sin(\omega t), \\ y_2(t) &= y_0, \\ y_3(t) &= x_0 sin(\omega t) + z_0 cos(\omega t). \end{aligned} \tag{7.18}$$

These solutions are periodic of period $\dfrac{2\pi}{\omega}$ when $(x_0, y_0, z_0) \neq (0,0,0)$. Therefore, the unperturbed system (7.17) of (7.16) is isochronous and we can apply Theorem 7. The fundamental matrix solution $M_u(t)$ of the unperturbed system (7.17) and its inverse $M_u^{-1}(t)$ is given by

$$M_u(t) = \begin{bmatrix} cos(\omega t) & 0 & -sin(\omega t) \\ 0 & 1 & 0 \\ sin(\omega t) & 0 & cos(\omega t) \end{bmatrix} \text{ and } M_u^{-1}(t) = \begin{bmatrix} cos(\omega t) & 0 & sin(\omega t) \\ 0 & 1 & 0 \\ -sin(\omega t) & 0 & cos(\omega t) \end{bmatrix}.$$

The bifurcating function (7.10) is given by

$$\mathcal{F}(u) = \int_0^{\frac{2\pi}{\omega}} M_u^{-1}(t) F_1(t, x(t,u)) dt$$

$$= \begin{bmatrix} \dfrac{-\pi\alpha(\omega^2 + r_3^2)}{r_1 r_3 (r_1 - r_3)} z_0 \\ \dfrac{2\pi\alpha(\omega^2 + r_1 r_3)}{\omega r_1 (r_1 - r_3)} y_0 \\ \dfrac{\pi\alpha(\omega^2 + r_3^2)}{r_1 r_3 (r_1 - r_3)} x_0 \end{bmatrix} \tag{7.19}$$

In system (7.19), $\mathcal{F}(u) = 0$ does not have any nontrivial solutions, therefore the averaging theory described in Theorem 7 does not provide any information about the possible periodic orbits bifurcating from the zero-Hopf equilibrium point.

□

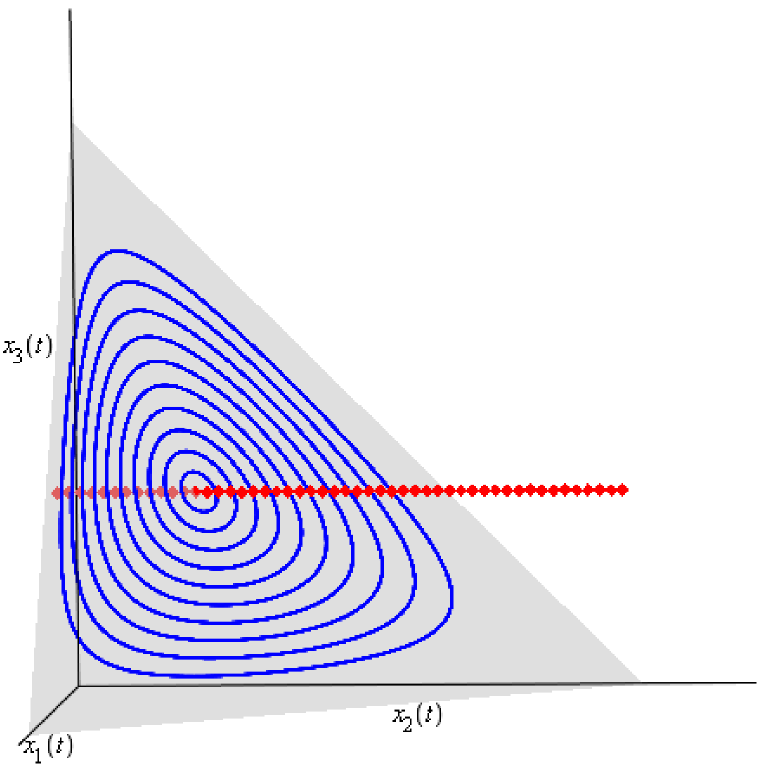

Figure 7.1: The red line depicts the line of singularities and blue cycles depict the periodic orbits a round one of the zero Hopf equilibrium points on the invariant plane $x_1 + x_2 + x_3 = 1$, where the parameters satisfy conditions (7.1), (7.3), condition (i) of Proposition 6, $r_1 = -2$, $r_3 = 1$ and $a_{3,1} = -\frac{10}{3}$.

References

Andronov, A. A., Leontovich, E., Gordon, I. I., and Maier, A. (1971). *Theory of bifurcations of dynamic systems on a plane*. Wiley.

Arneodo, A., Coullet, P., Peyraud, J., and Tresser, C. (1982). Strange Attractors in Volterra Equations for Species in Competition. *Journal of Mathematical Biology*, 14(2):153–157.

Aulbach, B. (1985). A classical approach to the analyticity problem of center manifolds. *Zeitschrift für angewandte Mathematik und Physik ZAMP*, 36(1):1–23.

Aziz, W. and Christopher, C. (2012). Local integrability and linearizability of three-dimensional Lotka-Volterra systems. *Applied Mathematics and Computation*, 219(8):4067 – 4081.

Baldomá, I. and Seara, T. M. (2006). Breakdown of Heteroclinic Orbits for Some Analytic Unfoldings of the Hopf-Zero Singularity. *Journal of Nonlinear Science*, 16(6):543–582.

Baldomá, I. and Seara, T. M. (2008). The inner equation for generic analytic unfoldings of the Hopf-zero singularity. *Discrete Contin. Dyn. Syst. Ser. B*, 10(2-3):323–347.

Bautin, N. N. (1952). On the number of limit cycles appearing with variation of the coefficients from an equilibrium state of the type of a focus or a center. *Matematicheskií Sbornik*, 72(1):181–196.

Berrone, L. R. and Giacomini, H. (2003). Inverse Jacobi multipliers. *Rendiconti del Circolo Matematico di Palermo*, 52(1):77–130.

Bibikov, Y. N. (1979). *Local Theory of Nonlinear Analytic Ordinary Differential Equations*. Lecture Notes in Mathematics. Springer-Verlag.

Broer, H. and Vegter, G. (1984). Subordinate Šil'nikov bifurcations near some singularities of vector fields having low codimension. *Ergodic Theory and Dynamical Systems*, 4(04):509–525.

Buică, A., Françoise, J.-P., and Llibre, J. (2007). Periodic solutions of nonlinear periodic differential systems with a small parameter. *Communications on Pure and Applied Analysis*, 6(1):103–111.

Buică, A., Garca, I. A., and Maza, S. (2012). Existence of inverse Jacobi multipliers around Hopf points in $\mathbb{R}^3$: Emphasis on the center problem. *Journal of Differential Equations*, 252(12):6324 – 6336.

Buică, A. and Llibre, J. (2004). Averaging methods for finding periodic orbits via Brouwer degree. *Bulletin des Sciences Mathmatiques*, 128(1):7–22.

Burchard, A., Deng, B., and Lu, K. (1992). Smooth conjugacy of centre manifolds. *Proceedings of the Royal Society of Edinburgh: Section A Mathematics*, 120(1-2):61–77.

Cairó, L. and Llibre, J. (2000). Darboux integrability for 3D Lotka-Volterra systems. *Journal of Physics A: Mathematical and General*, 33(12):2395–2406.

Carr, J. (1981). *Applications of centre manifold theory*, volume 35 of *Applied Mathematical Sciences*. Springer-Verlag, New York-Berlin.

Castellanos, V., Llibre, J., and Quilantan, I. (2013). Simultaneous Periodic Orbits Bifurcating from Two Zero-Hopf Equilibria in a Tritrophic Food Chain Model. *Journal of Applied Mathematics and Physics*, 1(7):31–38.

Champneys, A. and Kirk, V. (2004). The entwined wiggling of homoclinic curves emerging from saddle-node/Hopf instabilities. *Physica D: Nonlinear Phenomena*, 195(1-2):77–105.

Chow, S. N. and Hale, J. K. (1982). *Methods of bifurcation theory*, volume 251 of *Grundlehren der Mathematischen Wissenschaften [Fundamental Principles of Mathematical Science]*. Springer-Verlag, New York-Berlin.

Christie, J. R., Gopalsamy, K., and Li, J. (2001). Chaos in perturbed Lotka-Volterra systems. *The ANZIAM Journal*, 42(03):399–412.

Christodoulides, Y. T. and Damianou, P. A. (2009). Darboux polynomials for Lotka–Volterra systems in three dimensions. *Journal of Nonlinear Mathematical Physics*, 16(3):339–354.

Christopher, C. (1994). Invariant algebraic curves and conditions for a centre. *Proceedings of the Royal Society of Edinburgh: Section A Mathematics*, 124(06):1209–1229.

Christopher, C. (2005). Estimating Limit Cycle Bifurcations from Centers. In Wang, D. and Zheng, Z., editors, *Differential Equations with Symbolic Computation*, Trends in Mathematics, pages 23–35. Birkhäuser Basel.

Christopher, C. and Llibre, J. (1999). Algebraic aspects of integrability for polynomial systems. *Qualitative Theory of Dynamical Systems*, 1(1):71–95.

Coste, J., Peyraud, J., and Coullet, P. (1979). Asymptotic Behaviors in the Dynamics of Competing Species. *SIAM Journal on Applied Mathematics*, 36(3):516–543.

Darboux, G. (1878). Mémoire sur les équations différentielles algébriques du premier order et du premier degré. *Bulletin des Sciences Mathématiques et Astronomiques*, 2(1):151–200.

Devaney, R. (2003). *An Introduction to Chaotic Dynamical Systems*. Addison-Wesley studies in nonlinearity. Westview Press.

Euzébio, R. D., Llibre, J., and Vidal, C. (2014). Zero-Hopf bifurcation in the FitzHugh-Nagumo system. *Mathematical Methods in the Applied Sciences*, to appear.

Gao, P. and Liu, Z. (1998). An indirect method of finding integrals for three-dimensional quadratic homogeneous systems. *Physics Letters A*, 244(1-3):49–52.

García, I. A., Llibre, J., and Maza, S. (2014). On the periodic orbit bifurcating from a zero Hopf bifurcation in systems with two slow and one fast variables. *Applied Mathematics and Computation*, 232:84–90.

Gardini, L., Lupini, R., and Messia, M. (1989). Hopf bifurcation and transition to chaos in Lotka-Volterra equation. *Journal of Mathematical Biology*, 27(3):259–272.

Gilpin, M. E. (1979). Spiral Chaos in a Predator-Prey Model. *American Naturalist*, 113(2):306–308.

Glendinning, P. and Sparrow, C. (1984). Local and global behavior near homoclinic orbits. *Journal of Statistical Physics*, 35(5-6):645–696.

Guckenheimer, J. (1981). On a codimension two bifurcation. In *Dynamical Systems and Turbulence, Warwick 1980*, pages 99–142. Springer, Berlin.

Guckenheimer, J. and Holmes, P. (2013). *Nonlinear Oscillations, Dynamical Systems, and Bifurcations of Vector Fields*. Applied Mathematical Sciences. Springer New York.

Gyllenberg, M. and Yan, P. (2009a). Four limit cycles for a three-dimensional competitive Lotka-Volterra system with a heteroclinic cycle. *Computers and Mathematics with Applications*, 58(4):649–669.

Gyllenberg, M. and Yan, P. (2009b). On the number of limit cycles for three dimensional Lotka-Volterra systems. *Discrete and Continuous Dynamical Systems - Series B (DCDS-B)*, 11(2):347–352.

Gyllenberg, M., Yan, P., and Wang, Y. (2006). A 3D competitive Lotka-Volterra system with three limit cycles: A falsification of a conjecture by Hofbauer and So. *Applied Mathematics Letters*, 19(1):1–7.

Han, M. (1998). Existence of Periodic Orbits and Invariant Tori in Codimension Two Bifurcations of Three-Dimensional Systems. *Journal of Systems Science and Mathematical Sciences*, 18(4):403–409.

Hirsch, M., Smale, S., and Devaney, R. (2013). *Differential Equations, Dynamical Systems, and an Introduction to Chaos*. Academic Press.

Hofbauer, J. and Sigmund, K. (1998). *Evolutionary Games and Population Dynamics*. Cambridge University Press.

Hofbauer, J. and So, J.-H. (1994). Multiple limit cycles for three dimensional Lotka-Volterra equations. *Applied Mathematics Letters*, 7(6):59–63.

Hu, Z., Han, M., and Romanovski, V. G. (2013). Local integrability of a family of three-dimensional quadratic systems. *Physica D: Nonlinear Phenomena*, 265:78–86.

Jouanolou, J. (1979). Systemes de Pfaff algebriques. In *Equations de Pfaff algébriques*, volume 708 of *Lecture Notes in Mathematics*, pages 136–156. Springer Berlin Heidelberg.

Kozlov, V. and Vakulenko, S. (2013). On chaos in Lotka-Volterra systems: an analytical approach. *Nonlinearity*, 26(8):2299–2314.

Kuznetsov, Y. A. (2004). *Elements of applied bifurcation theory*, volume 112 of *Applied Mathematical Sciences*. Springer-Verlag, New York, third edition.

Kuznetsov, Y. A., Muratori, S., and Rinaldi, S. (1992). Bifurcations and Chaos in a Periodic Predator-Prey Model. *International Journal of Bifurcation and Chaos*, 02(01):117–128.

Li, T.-Y. and Yorke, J. A. (1975). Period Three Implies Chaos. *The American Mathematical Monthly*, 82(10):985–992.

Lins Neto, A. (1988). Algebraic solutions of polynomial differential equations and foliations in dimension two. In *Holomorphic dynamics (Mexico, 1986)*, volume 1345 of *Lecture Notes in Math.*, pages 192–232. Springer, Berlin.

Liu, Y. (2001). Theory of center-focus for a class of higher-degree critical points and infinite points. *Science in China Series A: Mathematics*, 44(3):365–377.

Llibre, J. (2014). Periodic Orbits in the Zero-Hopf Bifurcation of the Rössler System. *Romanian Astronomical Journal*, 24(1):49–60.

Llibre, J. and Euzebio, R. (2014). Zero-Hopf bifurcation in a Chua system. *arXiv preprint arXiv:1404.0613*.

Llibre, J., Makhlouf, A., and Badi, S. (2009). 3-dimensional Hopf bifurcation via averaging theory of second order. *Discrete and Continuous Dynamical Systems-Series A (DCDS-A)*, 25(4):1287–1295.

Llibre, J., Oliveira, R., and Valls, C. (2015). On the integrability and the zero-Hopf bifurcation of a Chen-Wang differential system. *Nonlinear Dynamics*, 80(1-2):353–361.

Llibre, J., Pantazi, C., and Walcher, S. (2012). First integrals of local analytic differential systems. *Bulletin des Sciences Mathématiques*, 136(3):342–359.

Llibre, J. and Pérez-Chavela, E. (2014). Zero-Hopf bifurcation for a class of Lorenz-type systems. *Discrete and Continuous Dynamical Systems - Series B*, 19(6):1731–1736.

Llibre, J. and Xiao, D. (2014). Limit cycles bifurcating from a non-isolated zero-Hopf equilibrium of three-dimensional differential systems. *Proceedings of the American Mathematical Society*, 142(6):2047–2062.

Llibre, J. and Zhang, X. (2009). Darboux theory of integrability in $\mathbb{C}^n$ taking into account the multiplicity. *Journal of Differential Equations*, 246(2):541–551.

Lotka, A. (1925). *Elements of Physical Biology.* Williams & Wilkins Company.

Lu, Z. and Luo, Y. (2002). Two limit cycles in three-dimensional Lotka-Volterra systems. *Computers and Mathematics with Applications*, 44(1-2):51–66.

Lu, Z. and Luo, Y. (2003). Three limit cycles for a three-dimensional Lotka-Volterra competitive system with a heteroclinic cycle. *Computers and Mathematics with Applications*, 46(2-3):231–238.

Marsden, J. E. and McCracken, M. (1976). *The Hopf Bifurcation and Its Applications*, volume 19 of *Applied Mathematical Sciences.* Springer New York.

Pan, Y. and Zhang, X. (2013). Algebraic aspects of integrability for polynomial differential systems. *Journal of Applied Analysis and Computation*, 3(1):51–69.

Polácik, P. (2002). Parabolic Equations: Asymptotic Behavior and Dynamics on Invariant Manifolds. *Handbook On Dynamical Systems*, 2:835–883.

Rinaldi, S., Muratori, S., and Kuznetsov, Y. (1993). Multiple attractors, catastrophes and chaos in seasonally perturbed predator-prey communities. *Bulletin of Mathematical Biology*, 55(1):15–35.

Robinson, C. (1995). *Dynamical systems: stability, symbolic dynamics, and chaos.* Studies in advanced mathematics. CRC Press.

Sabin, G. C. and Summers, D. (1993). Chaos in a periodically forced predator-prey ecosystem model. *Mathematical Biosciences*, 113(1):91–113.

Sanders, J. A., Verhulst, F., and Murdock, J. (2007). *Averaging methods in nonlinear dynamical systems*, volume 59 of *Applied Mathematical Sciences*. Springer, New York, second edition.

Schaffer, W. M. (1985). Order and Chaos in Ecological Systems. *Ecology*, 66(1):93–106.

Scheurle, J. and Marsden, J. (1984). Bifurcation to Quasi-Periodic Tori in the Interaction of Steady State and Hopf Bifurcations. *SIAM Journal on Mathematical Analysis*, 15(6):1055–1074.

Shilnikov, L. P. (1963). Some cases of generation of period motions from singular trajectories. *Matematicheskií Sbornik*, 103(4):443–466.

Shilnikov, L. P., Shilnikov, A. L., Turaev, D., and Chua, L. O. (2001). *Methods of Qualitative Theory in Nonlinear Dynamics, Part II. World Scientific Series on Nonlinear Science, Series A.* World Scientific.

Sijbrand, J. (1985). Properties of Center Manifolds. *Transactions of the American Mathematical Society*, 289(2):431–469.

Takeuchi, Y. (1996). *Global Dynamical Properties of Lotka-Volterra Systems.* World Scientific.

Ushiki, S. (1982). Central difference scheme and chaos. *Physica D: Nonlinear Phenomena*, 4(3):407–424.

Vano, J. A., Wildenberg, J. C., Anderson, M. B., Noel, J. K., and Sprott, J. C. (2006). Chaos in low-dimensional Lotka-Volterra models of competition. *Nonlinearity*, 19(10):2391–2404.

Volterra, V. (1926). *Variazioni e fluttuazioni del numero d'individui in specie animali conviventi.* Città di Castello.

Wang, D. (1991). Mechanical manipulation for a class of differential systems. *Journal of symbolic computation*, 12(2):233–254.

Wang, Q. and Huang, W. (2012). The equivalence between singular point quantities and Liapunov constants on center manifold. *Advances in Difference Equations*, 2012(1):78.

Wang, Q., Huang, W., and Li, B.-L. (2011a). Limit cycles and singular point quantities for a 3D Lotka-Volterra system. *Applied Mathematics and Computation*, 217(21):8856–8859.

Wang, Q., Huang, W., and Wu, H. (2011b). Bifurcation of Limit Cycles for 3D Lotka-Volterra Competitive Systems. *Acta Applicandae Mathematicae*, 114(3):207–218.

Wang, Q., Liu, Y., and Haibo, C. (2010). Hopf bifurcation for a class of three-dimensional nonlinear dynamic systems. *Bulletin des Sciences Mathmatiques*, 134(7):786–798.

Wiggins, S. (1992). *Chaotic transport in dynamical systems*, volume 2 of *Interdisciplinary Applied Mathematics*. Springer-Verlag, New York.

Wiggins, S. (2003). *Introduction to applied nonlinear dynamical systems and chaos*, volume 2 of *Texts in Applied Mathematics*. Springer-Verlag, New York, second edition.

Wiggins, S. and Shaw, S. W. (1988). Chaos and Three-Dimensional Horseshoes in Slowly Varying Oscillators. *Journal of Applied Mechanics*, 55(4):959–968.

Xiao, D. and Li, W. (2000). Limit Cycles for the Competitive Three Dimensional Lotka-Volterra System. *Journal of Differential Equations*, 164(1):1–15.

Yu, P. and Han, M. (2004). Twelve limit cycles in a cubic order planar system with Z2 symmetry. *Communications on Pure and Applied Analysis*, 3(3):515–525.

Zeeman, M. L. (1993). Hopf bifurcations in competitive three-dimensional Lotka-Volterra systems. *Dynamics and Stability of Systems*, 8(3):189–216.

Zeeman, M. L. and van den Driessche, P. (1998). Three-Dimensional Competitive Lotka–Volterra Systems with no Periodic Orbits. *SIAM Journal on Applied Mathematics*, 58(1):227–234.

Zhang, W.-B. (2005). *Differential equations, bifurcations, and chaos in economics*, volume 68 of *Series on Advances in Mathematics for Applied Sciences*. World Scientific Publishing Co. Pte. Ltd., Hackensack, NJ.

Zhang, X. (2008). Analytic normalization of analytic integrable systems and the embedding flows. *Journal of Differential Equations*, 244(5):1080–1092.